Influence of Adiponectin on the Rodent Cementoblasts Hemeostasis and Signaling Pathway Interaction under Compressive Force

Inaugural Dissertation

submitted to the

Faculty of Medicine

in partial fulfillment of the requirements

for the Ph.D. degree

of the Faculties of Veterinary Medicine and Medicine

of the Justus Liebig University Giessen

by

Jiawen Yong

of

Shandong, China

Giessen 2021

From the Medical Center for Dentistry and Oro-Maxillofacial Medicine,
Department of Orthodontics
Director: Univ. - Prof. Dr. Sabine Ruf
of the Faculty of Medicine of the Justus Liebig University Giessen

First Supervisor and Committee Member: Prof. Dr. Sabine Ruf
Co-Supervisor: Dr. Sabine Groeger, Dr. Dr. Gisela Ruiz-Heiland
Second Supervisor and Committee Member: Prof. Dr. Monika Kressin
Committee Member (Chair): Prof. Dr. Klaus-Dieter Schlüter
Committee Member: Prof. Dr. Klaus-Dieter Schlüter, Prof. Dr. Monika Kressin,
Prof. Dr. Sabine Ruf, Prof. Andreas Jäger

Date of Doctoral Defense: 05.07.2022

List of Contents

1. List of Tables

2. List of Figures

3. Abbreviations

AAC	Acellular Afibrillar Cementum
Acrp30	Adipocyte complement-related protein of 30 kDa
AdipoR1	Adiponectin Receptor 1
AdipoR2	Adiponectin Receptor 2
AdipoRs	Adiponectin Receptors
AEFC	Acellular Extrinsic Fiber Cementum
AMPK	AMP-Activated Protein Kinase
AP	Alkaline Phosphatase
BCA	Bicinchoninic Acid
BMI	Body Mass Index
BSP	Bone Sialoprotein
cDNA	Complementary DNA
CIFC	Cellular Intrinsic Fiber Cementum
CMSC	Cellular Mixed Stratified Cementum
CO_2	Carbon Dioxide
Cq	Quantification Cycles
DAPI	4’,6-Diamidino-2-Phenylindole
DMSO	Dimethyl Sulfoxide
DNA	Deoxyribonucleic Acid
DNase	Deoxyribonuclease
ELISA	Enzyme-Linked Immunosorbent Assay
ERK1/2	Extracellular Signal-Regulated Kinase
FBS	Fetal Bovine Serum
g	Gram
GAPDH	Glyceraldehyde 3-Phosphate Dehydrogenase
GSK-3β	Glycogen Synthase Kinase-3beta
h	Hour

HMW	High-molecular weight
JNK	Jun N-Terminal Kinase
kDa	Kilodalton
L	Liter
LAL	Limulus Amebocyte Lysate
LMW	Low-molecular weight
m	Meter
M	Molar
MAPK	Mitogen-Activated Protein Kinase
MC3T3-E1	Osteoblasts
MEKK2	Mitogen-activated protein kinase kinase kinase 2
min	Minute
mL	Milliliter
MTS	3-(4,5-dimethylthiazol-2-yl)-5-(3-carboxymethoxyphenyl)-2-(4-sulfophenyl)-2H-tetrazolium
MWM	Medium-molecular weight
ng	Nanogram
NIDCR	National Institute of Dental and Craniofacial Research
NIH	National Institutes of Health
N	Newton
ObR	Leptin Receptors
OCCM-30	Cementoblasts
OCN	Osteocalcin
OIIRR	Orthodontically Induced inflammatory Root Resorption
OPG	Osteoprotegerin
OPN	Osteopontin
OTM	Orthodontic Tooth Movement
P38	P38 Mitogen-Activated Protein Kinases
PBS	Phosphate-Buffered Saline

PDL	Periodontal Ligament
PPAR-α	Peroxisome Proliferator-Activated Receptorα
qRT-PCR	Quantitative Reverse Transcription Polymerase Chain Reaction
RAW24	Macrophage cell line
RNA	Ribonucleic Acid
RNase	Ribonuclease
RT	Room Temperature
Runx-2	Runt-Related Transcription Factor-2
s	Seconds
SD	Standard Deviation
SDS-PAGE	Sodium Dodecyl-Sulfate Polyacrylamide Gel Electrophoresis
sg-gAd	Single-chain globular domain adiponectin
siRNA	Small-interfering RNA
TBST	Tris Buffered Saline with Tween-20
TBS-T	Tris-Buffered Saline, Tween-20
WAT	White Adipose Tissue
α-MEM	A-Minimum Essential Medium
β-Catenin	Beta-Catenin
µg	Microgram
µL	Microliter

4. Introduction

4.1 Obesity and orthodontics

4.1.1 Obesity and adipokines

Obesity is defined as a chronic disease due to the excessive adipose tissue and has become a major global threat for adults as well as children affecting both developed and developing countries [1]. Since leptin was discovered in 1994 [2], the white adipose tissue (WAT) has been recognized as a dynamic endocrine organ to produce and secrete several bioactive polypeptides named adipokines [3].

Adipokines comprise of approximately leptin, adiponectin, resistin, visfatin, apelin, chemerin, perinol binding protein-4, serum amyloid A, plasminogen activator inhibitor-1, angiotensinogen, vaspin, omentin, chemerin and zinc-alpha2-glycoprotein (**Figures 1A-B**). Two pro-inflammatory cytokines known as tumor necrosis factor-alpha (TNF-α) and interleukin-6 (IL-6) which are produced by macrophages infiltrating WAT are also considered as adipokines [4]. These soluble adipokines bind to their specific receptors on target tissue and cells to active intracellular signaling. Due to their involvement in physiological processes of disease in human, adipokines have been intensively studied in all diseases related to obesity [5].

It was demonstrated, that obesity that is concomitant with an increased body mass index (BMI) appears to be a risk factor for less appliance wear during orthodontic treatment with removable appliances [6], less cooperation, a longer treatment duration, and more oral health-related problems during multibracket appliance orthodontic treatment [7]. Obesity could play a role in bone metabolism via adipocyte-derived adipokines directly or indirectly through leptin and adiponectin [8]. Moreover, increased serum leptin levels and decreased serum adiponectin levels in obese patients may influence the process of orthodontic treatment and probably acts via several molecular mechanism in periodontal cells [9].

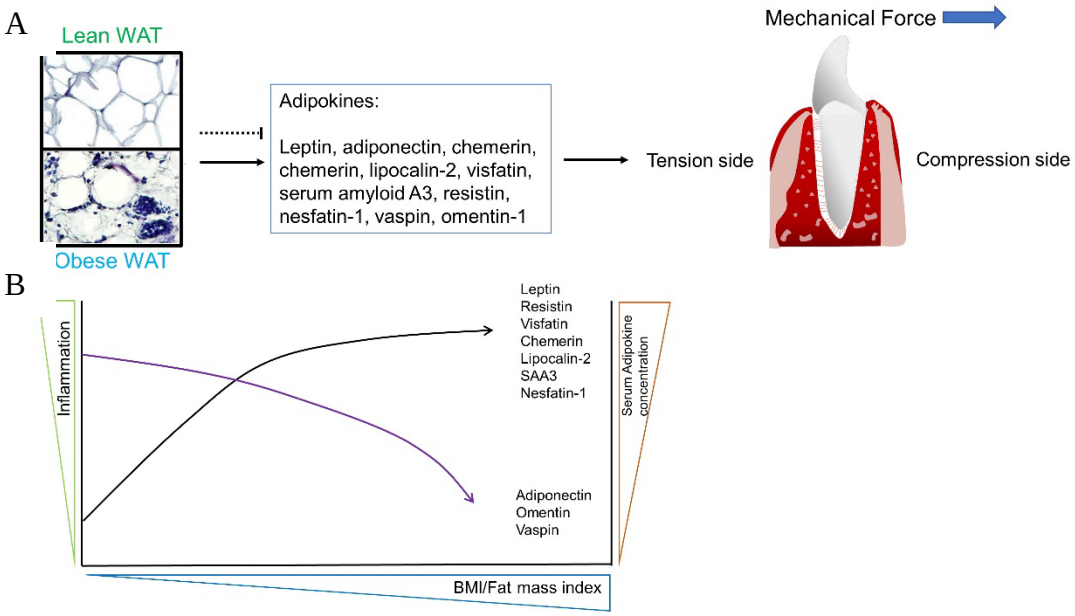

Figure 1. Hypothetical model showing the relationship between obesity, adipokines and orthodontic tooth movement.

(A) Soluble adipokines synthesized by WAT of lean/obese individuals. Altered levels of adipokines may be the critical underlying pathomechanism during OTM. Adipocyte-derived adipokines are linked to the regulation for negative side effects of OTM. WAT: White Adipose Tissue. (Adapted from Azamar-Llamas et al. [10])

(B) Serum concentration of adipokines is related to the BMI in obese patients. OTM: Orthodontic Tooth Movement; BMI: Body Mass Index. (Adapted from Azamar-Llamas et al. [10])

4.1.2 Adipokines and orthodontics

When it comes to orthodontic tooth movement (OTM), multiple cell types in the periodontium are involved: cementoblasts, periodontal ligament (PDL) cells, PDL fibroblasts, osteoblasts and osteoclasts. Adipokines could significantly affect orthodontic treatment through their impact on bone/cementum metabolism [11].

Saloom et al. (2017) conducted a cohort study showing that adipokines show different kinetics during OTM [12]. Without orthodontic treatment, the concentration of adiponectin in gingival crevicular fluid (GCF) are reduced in obese patients, which is in agreement with Kadowaki et al. (2005) who reported lower plasma adiponectin levels and its receptors in obese individuals [13, 14]. Another study reported that patients undergoing orthodontic treatment showed that the concentration of leptin increased in both GCF and serum of the obese group. Conversely, other researchers reported that leptin

concentrations in GCF are reduced during orthodontic treatment [15]. These findings indicate that adipokines and orthodontic treatment influence each other during OTM.

Li et al. (2014) reported that leptin and its receptor are widely expressed and commonly distributed in dental and periodontal tissues of primates such as gingiva and dental pulp [16]. Notably, the expression of leptin receptors (ObR) in cementoblasts has been identified in a previous study [17]. Moreover, adiponectin receptor 1 and 2 (AdipoR1 and AdipoR2) were reported to ubiquitously expressed in the mouse oral tissues including bone-forming osteoblasts [18], human gingival fibroblasts as well as in a murine macrophage-like cell line [19]. These finding indicate the possible roles of adipokines in periodontal disease and their involvement in OTM.

4.2 Obesity and adiponectin

4.2.1 Adiponectin cleavage

It has been demonstrated, that adipocytokines (mainly but not exclusively secreted by adipose tissue) and adipokines (only produced by the adipose tissue) can influence bone metabolism [20] and tooth movement [21]. Adiponectin (also referred to as Acrp30 [22], AdipoQ [23], apM1 [24] and GBP28 [25] in initial reports), encoded by the AdipoQ gene in humans [26] and produced by mature adipocytes but also in the salivary gland epithelial cells, has been shown to modulate metabolic and immune functions of salivary gland epithelial cell [27].

Structure features of single-chain globular domain adiponectin (sg-gAd) are shown in **Figures 2A, B**. The primary sequence of full-length human adiponectin comprises 244 amino acid residues including 4 regions: a short NH_2-terminal signal sequence, a short region that varies between species, a collagenous-like domain and a COOH-terminal globular domain [28, 29]. This cleavage is mediated by a leukocyte elastase, secreted by activated monocytes and/or neutrophils [30]. In contrast to humans, mouse adiponectin is a 247 amino acid long protein having huge structural similarity with C1q [31]. In the blood stream, adiponectin is found in three forms of oligomeric complexes including low-

molecular weight (LMW) trimer, medium-molecular weight (MMW) hexamer and high molecular weight (HMW) multimer [32] (**Figure 2C**). Moreover, the globular adiponectin results from the cleavage of the full-length monomer [33], is the most biologically active form of the different oligomers [29]. These oligomers are in turn related to the regulation of bone metabolism and thus acts as indispensable diagnostic marker in clinical practice [34].

4.2.2 Adiponectin receptors

Two major adiponectin receptors (AdipoRs) subtypes exist, adiponectin receptor 1 and 2 (AdipoR1 and AdipoR2). They are expressed in various tissues and cells such as human gingival fibroblasts and PDL cells [35] and mediate the biological effects of adiponectin. AdipoRs are surface membrane proteins with structurally related seven transmembrane domains including a cytoplasmic NH_2-terminus and an extracellular COOH-terminal domain [31] (**Figure 2C**). AdipoR1 acts as a high-affinity receptor for globular adiponectin and a low-affinity receptor for full-length adiponectin in skeletal muscle [36]. On the other hand, AdipoR2 is an intermediate-affinity receptor for both globular and full-length HMW adiponectin forms in liver [36]. Yamaguchi et al. (2012) showed that the AdipoRs were abundantly expressed in the oral tissues of mice such as tongue, gingiva, buccal and labial mucosa, as well as in macrophage (RAW24) cell line [37]. Besides AdipoRs, Hug et al. (2004) isolated a third adiponectin receptor known as T-cadherin receptor which has an affinitive relationship with hexameric and HMW forms of adiponectin [38]. The underlying mechanism by which T-cadherin receptor interacts with signaling pathways still needs to be investigated. However, Denzel et al. (2010) reported that T-cadherin-deficient mice have elevated serum adiponectin levels, especially of the HMW form [39].

It has been reported, that adiponectin and its two major receptors are expressed in primary human osteoblasts [40] which act as an important signaling link between fat and body weight to bone density [18]. However, some studies reveal that adiponectin has emerged as a key intracellular mediator having anti-inflammatory and anti-apoptotic effects during

biological activities in various experimental animal models [41, 42].

Both AdipoRs play similar effects on the activation of intracellular signaling but have individual signaling preferences. Phosphorylation of Extracellular Regulated Kinase 1/2 (ERK1/2) may depend on both receptors. AdipoR1 is more prominent in AMP-activated protein kinase (AMPK), P38 MAPK, c-Jun N-terminal Kinase (JNK), peroxisome proliferator-activated receptor-α (PPAR-α) and nuclear factor-*k*B (NF-*k*B) pathways, while AdipoR2 is more tightly linked to PPAR pathways activation in muscle cells [43]. AdipoR1 and AdipoR2 have been identified in the plasma membrane [44] as well as in the cytoplasm (cytoplasmic puncta) [45].

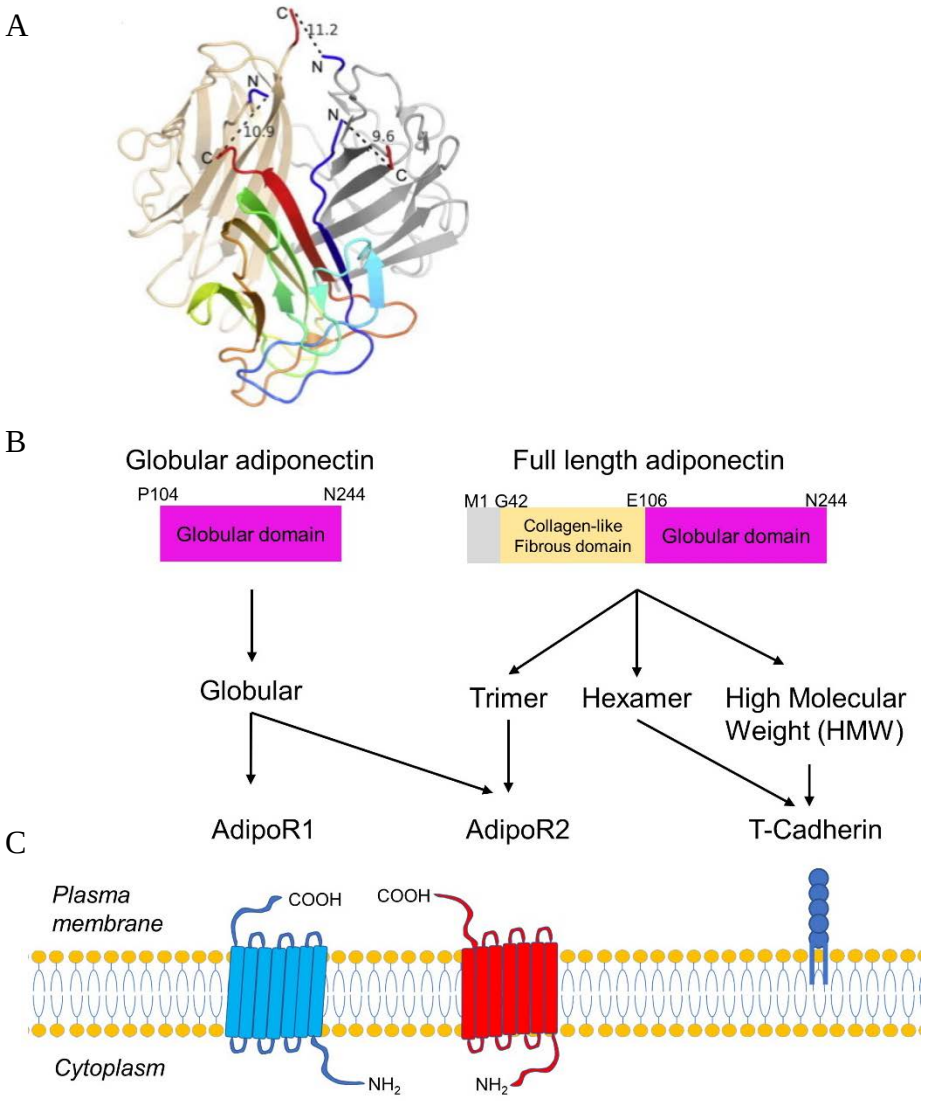

Figure 2. Adiponectin and adiponectin receptors.

(A) Structure of single-chain globular domain human adiponectin (sc-gAd). Base region of mouse gAd structure showing in spectrum color scheme where light blue arrow represents the N-terminus and red arrow represents the C-terminus of the sequence. (Adapted from Min et al. [28])

(B) Domain features of adiponectin. Schematic post translational modification of adiponectin. A full-length adiponectin (~30 kDa) consists of 244 amino acids including a globular domain at the C-terminus, a collagenous-like fibrous domain at the N-terminus, a species-specific domain and a signal peptide. Circulating adiponectin forms low-molecular weight (LMW) homotrimers, hexamers and high-molecular weight (HMW) multimers. (Adapted from Achari et al. [32])

(C) Proposed structure of adiponectin receptors. AdipoR1 has a greater affinity for the globular form, whereas AdipoR2 has a moderate affinity for both globular and full-length forms. (Adapted from Khoramipour et al. [36])

4.2.3 Correlation of adiponectin concentration with obesity

Previous studies stated that human salivary adiponectin concentration is low (0.37-6.42 ng/mL) in comparison to that of circulating adiponectin in plasma (5-30 µg/mL) [46, 47]. The relation between obesity and concentration of adipokines has been studied extensively. Unlike leptin, the concentration of circulating adiponectin in obese human individuals is significantly lower than in non-obese [48] (**Figure 1B**). *In vivo*, adiponectin secretion is regulated by the amount of adipose tissue [49, 50] and is inversely correlated to the degree of obesity [46, 51, 52]. Cao et al. (2015) reported that patients with obesity have lower serum levels of adiponectin than normal weight individuals [53].

Obesity may cause lower adiponectin- and AdipoRs-levels in healthy subjects than in patients with severe periodontitis [19, 54], thus in turn deteriorates periodontal disease. Furthermore, since adiponectin and AdipoRs are expressed in osteoblast cells, it is suggested to be involved in the anti-inflammatory functions and bone metabolism [18]. It may influence the function of PDL cells in another way than osteoblasts and cementoblasts [55].

4.3 Cementoblasts and orthodontics

4.3.1 Biology of cementum and cementoblasts

The periodontium consists of the soft tissues gingiva and periodontal ligament as well as of the hard tissues root cementum and alveolar bone [56]. Cementum, a heterogeneous mineralized layer covering the entire root dentin surface, anchors with the bony alveolus by Sharpey's fibers and with the dentin surfaces by collagen fibers [57]. As a special mineralized tissue, cementum has a similar composition to alveolar bone, consisting of approximately 61% mineralized as well as 27% organic matrix, and 12% water [58].

Cementoblasts, the cells comprising the cellular component of cementum, are highly differentiated mesenchymal cells of the periodontal ligament with the capacity to build up cementum [59]. The cementum matrix is composed of collagenous proteins and non-collagenous proteins such as Alkaline phosphatase (AP), Bone Sialoprotein (BSP),

Osteopontin (OPN), Osteocalcin (OCN), Osteoprotegerin (OPG) [60] and F-Spondin [61], while cementoblasts have a similar gene expression pattern as osteoblasts, including glycogen synthase kinase-3β (GSK-3β), β-Catenin, OCN and OPG [60, 62].

Arzate et al. (2015) classified three types of cementum: intermediate cementum, cellular and acellular cementum, according to the presence or absence of cementocytes which are cementoblasts that become trapped in the lacunae within the matrix [59]. The intermediate cementum is found in the area of the cemento-enamel junction. The acellular cementum is attaching to the tooth dentin and covers the coronal and mid-portion of the tooth. The cellular cementum presents in the apical and interradicular portions of the root and contains cementoblasts [63] (**Figure 3A**).

The formation of root cementum is considered to be determined by the extent and quality of the cementogenesis and mineralization process of cementoblasts [64]. Briefly, during the initial stages of cementogenesis, the cementoblasts lay down organic matrix with fibers and synthesize the pre-cementum onto the dentin matrix. After implantation, the pre-cementum proceeds to mineralize [65]. It was demonstrated that Hertwig's epithelial root sheath (HERS) produces acellular cementum in the initial stage of cementogenesis following with cellular and reparative cementum secreted by the cementoblasts [66].

4.3.2 Cementoblasts and orthodontic tooth movement

OTM depends on coordinated remodeling activities such as resorption and formation of the surrounding bone and tissue of the periodontium [67]. In the course of OTM, the periodontium is subjected to different magnitudes of mechanical forces which is one of the numerous conditions that have impact on the periodontium during orthodontic treatment [68]. Mechanical force, including compressive and tensile forces, are considered as main factors in regulating the homeostasis of cementum during OTM [69]. In the present study, I used sterilized glass discs to mimic hydrostatic pressure on adherent mouse cementoblasts (OCCM-30) to simulate pressure conditions as close as possible to the *in vivo* condition during orthodontic force loading (**Figures 3A, B**).

Orthodontically induced inflammatory root resorption (OIIRR) is a deleterious iatrogenic

side-effects of orthodontic therapy which has been subject of many research projects around the world [70]. OIIRR was defined as the pathologic removal of cementum and dentin [71]. Once it is evoked, clinician cannot predict its actual clinical outcome. The extent of the inflammatory process depends upon many factors such as genetics, the root morphology involved, the virulence or aggressiveness of the different resorbing cells, as well as the repairing cells. Thus, the mechanism of OIIRR remains beyond our understanding. Clinician are therefore unable to predict the incidence and extent of OIIRR after force application [72]. While the vitality of teeth with OIIRR is not compromised, the periodontal support is. The reduced total PDL area will severity-dependent result in an increased tooth mobility. This can lead to premature tooth loss especially in case of periodontal disease comorbidity or initiate a vicious circle triggering root resorption progression, periodontal breakdown and tooth hypermobility.

Orthodontic forces initiate the cellular process of periodontal cells. Cementum and PDL cells (mainly cementoblasts) are the one responsible for OIIRR repair [73]. One major goal of orthodontic treatment is to avoid OIIRR and promote new cementum formation if OIIRR has occurred. The latter process requires cementoblasts to start cementogenesis and the molecular factors regulating their recruitment and mineralization [59]. On the pressure side, the cementum is constantly compressed through the compressive force application, thus, cementoblasts become mechanically deformed and start repairing the cellular cementum by replenishing it with cellular mineralized cementum [74]. Research into the biologic regulation of cementum repair has revealed that β-Catenin signaling is critical for normal cementum formation under constant mechanical loading [75, 76].

During orthodontic force application, compressive forces induce human mandibular-derived osteoblast differentiation via β-Catenin signaling [76]. It has been highlighted that β-Catenin signaling regulates cementum homeostasis and a down-regulation of WNT causes root resorptions [75]. WNT/β-Catenin signaling was reported to inhibit cementoblasts differentiation and promote their proliferation [77]. Also, multiple signaling pathways participate in this process [78]. Recent advances suggest a possible intersection cross-reacting network in which β-Catenin signaling is mediated by mitogen-

activated protein kinase (MAPK) signaling pathways [79, 80]. The P38 MAPK pathway is known to regulate cementoblast differentiation [81]. Bikkavilli et al. (2008) demonstrated that P38 MAPK inactivates GSK-3β by direct phosphorylation at its C terminus, leading to activation of β-Catenin signaling [79].

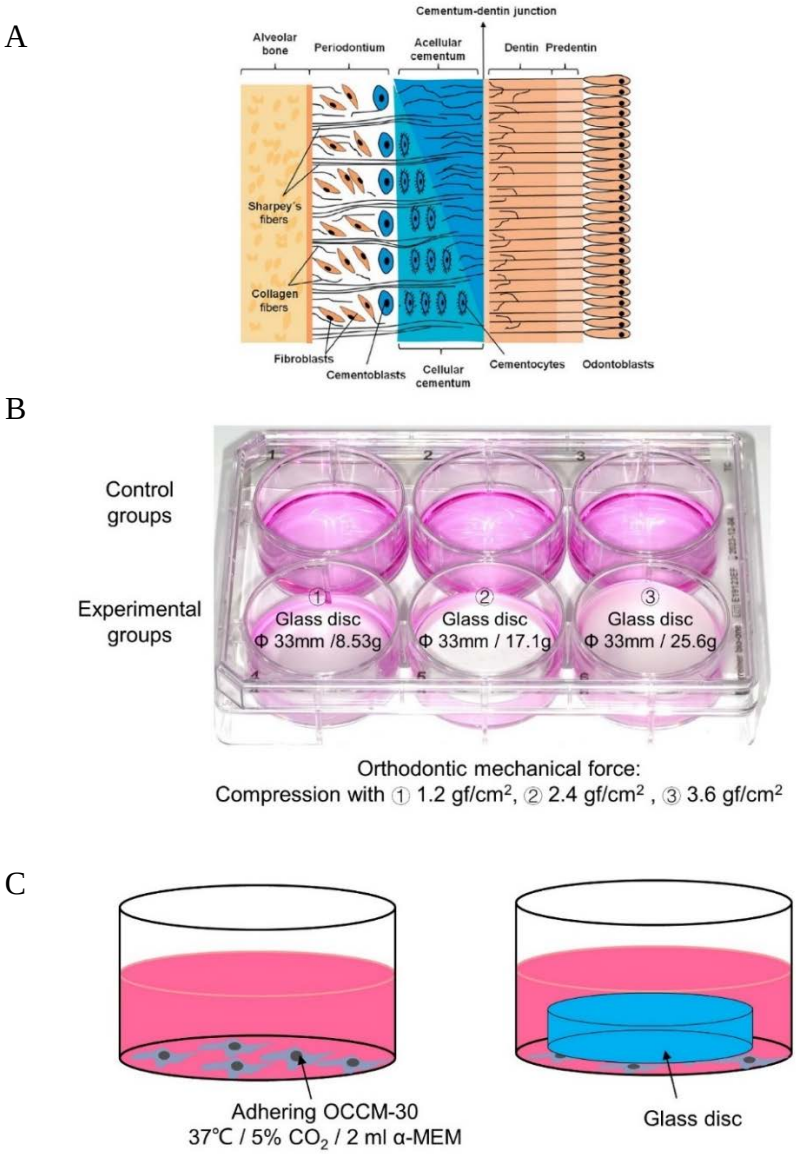

Figure 3. Cementoblast location and in vitro model used to mimic the stimulation of orthodontic mechanical compression.

(A) Distribution of cementoblasts and cementum. Acellular cementum is located around the root neck and cellular cementum is covering the root up to the apex. (Adapted from Matalová et al. [63])

(B) The OCCM-30 cells cultivated in 6-well plate with 3 control wells and 3 wells stimulated with different magnitudes of compressive force (1.2 gf/cm^2; 2.4 gf/cm^2; 3.6 gf/cm^2).

(C) Schematic model of the physiological cell culture conditions and the cells stimulated by compressive force.

5. Aim of the study

Given that a recent study revealed that local submucosal injection of adiponectin prevented experimental orthodontic tooth movement in rats [21], demonstrating that adiponectin is involved in the homeostasis of periodontal tissues and thus might influence orthodontic treatment.

It has also been reported, that adiponectin and its receptors are expressed in bone marrow-derived osteoblasts and adipocytes [55], suggesting that adiponectin may play a role in bone metabolism [82]. Considering the multifunctional role of adiponectin, it seems possible that it may have functional characteristics in cementoblasts similar to that in other mineralized tissue-forming cells such as osteoblasts [55].

Taken together, I hypothesized that adiponectin may be one of the critical factors during OTM and OIIRR. The decreased levels of adiponectin, as found in obese individuals, might be a critical pathomechanistic link.

To date, the physiological effect of adiponectin on cementoblasts has not been elucidated. It is also unknown how the interaction between the MAPK pathway and β-Catenin signaling occurs in cementoblasts. Additionally, the mechanism of compression-adiponectin regulation in cementoblasts remains unclear.

Therefore, the present study was undertaken to investigate:

1) The effect of adiponectin on OCCM-30 cells homeostasis *in vitro*.
2) The effect that compressive forces exerted on OCCM-30 especially in the presence of adiponectin.
3) The effect of adiponectin on the intracellular signaling molecules of MAPK pathway.
4) Furthermore, it was aimed to identify the molecular mechanism how β-Catenin signaling modulation is regulated via the activation of MAPK signaling.

6. Materials and methods

6.1 Materials

6.1.1 Chemicals/Reagents

All the chemicals listed in **Table 1** were purchased from the named companies. The application of assays listed below are described in the corresponding methods part.

Table 1. Chemicals/Reagents

Item	Supplier
Cell Culture Medium	α-MEM Medium (ThermoFisher Scientific)
Serum-Free Medium	Opti-MEM™ Reduced Serum Medium (ThermoFisher Scientific)
FBS	Fetal Bovine Serum (FBS) with low Endotoxin (Sigma-Aldrich)
PBS Buffer	Phosphate Buffered Saline (PBS) Dulbecco without Ca^{2+} w/o Mg^{2+} (Gibco)
Antibiotics	Penicillin/Streptomycin 10,000 U/mL (Gibco)
Cell Detachment Solution	StemPro@ Accutase@ (Gibco)
Protein Lysis Buffer	RIPA buffer (ThermoFisher Scientific)
Cementogenesis Induction	β-Glycerophosphate (Calbiochem) Ascorbic Acid (Roth)
Protease Inhibitor	Protease Inhibitor Cocktail (ThermoFisher Scientific)
Cell Counting Staining	0.4% Trypan Blue Solution (Sigma-Aldrich)
SDS-PAGE	Mini-PROTEAN@ TGX™ Gels (Bio-Rad)
Protein Molecular Weight Marker	PageRuler™ Prestained Protein Ladder, 10 to 180 kDa (ThermoFisher Scientific)
Western Blot Transfer	Transfer-blot@ Turbo™ Transfer Pack (Bio-Rad)

	Nitrocellulose Membrane (Bio-Rad)
Blocking Buffer	5% Non-Fat Milk (Carl Roth)
Washing Buffer	1× Tris-Buffered Saline, 0.1% Tween@-20 Detergent (TBS-T) (Sigma-Aldrich)
Western Blot Stripping Buffer	Restore™ PLUS Western Blot Stripping Buffer (ThermoFisher Scientific)
ECL Reagent	ECL Western Blotting Detection Reagent (GE Healthcare)
β-Mercaptoethanol	Purity ≥ 99.0% (Sigma-Aldrich)
RT-PCR Supermix	SsoAdvanced™ Universal SYBR@ Green Supermix (Bio-Rad)
PCR Primers	Synthesis by Bio-Rad: Lumican and Fibromodulin
PCR DNase/RNase-Free Water	Invitrogen Distilled Nuclease-Free Water (ThermoFisher Scientific)
Ethanol	70% denatured Ethanol (Carl Roth)
Tween-20	Tween@-20 (Sigma-Aldrich)
Tween X-100	0.5% Triton™ X-100 Surfact-Amps™ Detergent Solution (ThermoFisher Scientific) 0.1% Triton™ X-100 (Sigma-Aldrich)
Alizarin Red S Staining	1% Alizarin Red S Solution (Sigma-Aldrich)
Calcium Assay	Cetylpyridinium Chloride (Sigma-Aldrich)
DMSO	Dimethyl Sulfoxide for Molecular Biology, Purity ≥99.9% (Sigma-Aldrich)

6.1.2 Instruments/Apparatus

All instruments/apparatus used in the study are listed in **Table 2**.

Table 2. Technical Apparatus

Item	Supplier
Sterilization	Systec™ Laboratory Autoclaves V-75 (Linden, Germany)
Air-Flow Cell Culture Hoods	Laminar Flow Hood (ThermoFisher Scientific, Germany)
Ultra-pure Water Purification Machine	Elix@ Reference Water Purification System ZRX0010WW (Billerica, American)
Dishwasher	Miele™ Professional Dishwasher G7883 CD (Gütersloh, Germany)
Precision Balance	Denver Instrument SI-234A (Wertheim, Germany)
CO_2 Cell Culture Incubator	HERAcell 150i CO_2 Incubator (ThermoScientific)
Water Bath	GFL@ Water Bath (GB Technik, Germany)
Centrifuge	Centrifuge Mikro 200R (Hettich, Germany) Centrifuge 5810 (Eppendorf, Germany) Galaxy MiniStar (VWR, Germany)
ELISA Reader	Mithras LB 940 Multimode Microplate Reader (Berthold Technologies, Germany) 96-Well Micro-Plate Reader (BioTek, Winooski, VT, USA)
Light Microscope	Eclipse LV150N (Nikon, Japan)
Fluorescent Microscope	Leica Microscopy System (Leica, Germany)
Pipetboy	Eppendorf Easypet (Eppendorf, Germany)
Pipettes	Ergonomic High-Permance (VWR, Germany) Eppendorf Xplorer (Eppendorf, Germany)

	Multipette Eppendorf Research Pro (Eppendorf, Germany)
Refrigerator	1-4°C Refrigerator (Liebherr, Germany) -20°C Refrigerator (Liebherr, Germany) -80°C Refrigerator (ThermoFisher Scientific, Germany)
Shaker	Vortex-2 Genie (Scientific Industries, Germany)
Roller	Roller Mixer SRT6 (Stuart, United Kingdom) MAXI HP 1P VARIOMAC@ (Germany)
Spectrophotometer	Nanodrop 2000 (ThermoScientific, Germany)
Electrophoresis Chambers	Mini-PROTEAN Tetra Vertical Electrophoresis Cell (Bio-Rad, Germany)
Western Blot Transfer System	Trans-Blot@ Turbo™ Transfer System (Bio-Rad, Germany)
Western Blot Cassettes	Trans-Blot Turbo™ Cassette (Bio-Rad, Germany)
Film Detection Device	OPTIMAX X-Ray Processor (PROTEC GmbH, Germany)

6.1.3 Consumables

All consumables used in this study are listed in **Table 3**.

Table 3. Consumables

Item	Supplier
Tips	Eppendorf Biosphere@ Filter Tip: 10 µL, 100 µL, 1,000 µL (Sarstedt, Germany)
Cell Counting Chamber	Manual Counting Chamber (Marienfeld, Germany)
Cell Culture Plate	35 mm 6-Well Cell Culture Plate (Greiner Bio-One, Germany) 9 mm 96-Well Cell Culture Plate (Greiner Bio-One,

	Germany)
Reaction Tubes	1.5 mL Micro Tube (Sarstedt, Germany) 15/50 mL Falcon type centrifuge tube (Sarstedt, Germany)
Syringe	Sterile Injekt@ 10 mL Luer Solo (Braun, Germany)
Syringe Filter	Sterile Syringe Filter 0.45 µm Cellulose Acetate Membrane (VWR, Germany)
Cell Scraper	STERILE CELL SCRAPER 28 CM LONG (Greiner Bio-One, Germany)
cDNA Tube	Multiply@-µStripPro Low Profile (Sarstedt, Germany)
PCR Plate	0.2 mL non-Skirted 96-Well PCR Plate (Scientific Industries, Germany)
Western Blot Film	X-Ray Amersham Hyperfilm (GE Healthcare, Germany)

6.1.4 Kit

All Kits used in this study are listed in **Table 4**.

Table 4. Kits

Kits	Supplier
Protein Assay Kit	Pierce™ BCA Protein Assay Kit (ThermoFisher Scientific)
RNA Isolation Kit	NucleoSpin@ RNA Kit (MACHEREY-NAGEL)
cDNA Synthesis Kit	InnuSCRIPT@ Reverse Transcriptase Kit (Analytik Jena)
MTS Kit	CellTiter 96@ Aqueous One Solution (Promega)
Film Detection Kit	Amersham ECL Western Blotting Detection Reagents (GE Healthcare)

Western Blot Membrane	Trans-Blot Turbo RTA Mini 0.2 µm Nitrocellulose Transfer Kit (Bio-Rad)
β-Catenin Transcription Detection	TCF/LEF Reporter Kit (BPS Bioscience)

6.1.5 Software

All digital software applications used in this study are listed in **Table 5**.

Table 5. Software

Application	Software and Company
Statistical Analysis	Graphpad Prism 8.0 (San Diego, California)
Data Analysis	Microsoft Office 365 (Microsoft, USA)
Image Analysis System	Leica Application Suite LASV4.8 (Leica, Germany) Image J Software (NIH, USA)
References Management	EndNote X9 (Thomson Reuters, USA)
Western Blot Film Management	Adobe Photoshop CC 2019 (Adobe, USA)
Figure Management	Adobe Illustrator CC 2019 (Adobe, USA)

6.1.6 RT-PCR Primers

All primers used for RT-PCR in this study are listed in **Table 6**.

Table 6. RT-PCR Primers

Primers (Bio-Rad Inc.)	Catalog number
AdipoR1	qMmuCID0023619
AdipoR2	qMmuCID0010157
AP	qMmuCED0003797
BSP	qMmuCID0006396

OCN	qMmuCED0041364
OPG	qMmuCID0005205
Runx-2	qMmuCID0005205
F-spondin (Spondin-1)	qMmuCED0049433
MAPK3 (ERK1)	qMmuCED0025043
GAPDH	qMmuCED0027497
β-actin	qMmuCED0027505
Primers (Eurofins Genomics Inc.)	Sequence (5’ - 3’)
MAPK1 (ERK2) _forward	TCT CCC GCA CAA AAA TAA GG
MAPK1 (ERK2) _reverse	TCG TCC AAC TCC ATG TCA AA
MAPK8 (JNK1) _forward	AGA AAC TGT TCC CCG ATG TG
MAPK8 (JNK1) _reverse	TGA TGT ATG GGT GCT GGA GA
MAPK14 (P38α MAPK) _forward	ATC ATT CAC GCC AAA AGG AC
MAPK14 (P38α MAPK) _reverse	AGC TTC TGG CAC TTC ACG AT
GSK-3β_forward	CAG TGG TGT GGA TCA GTT GG
GSK-3β_reverse	ATG TGC ACA AGC TTC CAG TG
β-Catenin_forward	GTG CAA TTC CTG AGC TGA CA
β-Catenin_reverse	CTT AAA GAT GGC CAG CAA GC

6.1.7 Antibodies

All antibodies used in this study are listed in **Table 7**.

Table 7. Antibodies

Primary Antibody	Dilution	Company
ERK1/2	1:1,000 (WB)	BIOZOL
phospho-ERK1/2	1:1,000 (WB)	ThermoFisher
p54/p56 JNK	1:1,000 (WB)	Cell Signaling Technology
phospho-JNK	1:1,000 (WB)	ThermoFisher

P38 MAPK	1:1,000 (WB)	Cell Signaling Technology
phospho-P38 MAPK Alpha	1:1,000 (WB)	Cell Signaling Technology
STAT1	1:1,000 (WB)	Bio-Rad
phospho-STAT1 Tyr701	1:1,000 (WB)	ThermoFisher
STAT3	1:1,000 (WB)	ThermoFisher
phospho-STAT3 S727	1:1,000 (WB)	ThermoFisher
AdipoR1	1:1,000 (WB)	Abcam
	1:250 (IF)	
AdipoR2	1:1,000 (WB)	Abcam
	1:250 (IF)	
GSK-3β	1:1,000 (WB)	Cell Signaling Technology
	1:250 (IF)	
phospho-GSK-3β (Ser9)	1:1,000 (WB)	Cell Signaling Technology
β-Catenin	1:1,000 (WB)	Cell Signaling Technology
	1:250 (IF)	
phospho-β-Catenin (Ser33/37/Thr41)	1:1,000 (WB)	Cell Signaling Technology
β-actin	1:2,000 (WB)	Abcam
Secondary Antibody	Dilution	Company
Peroxidase-conjugated Polyclonal Goat Anti-Rabbit	1:2,000 (WB)	Dako
Peroxidase-conjugated Polyclonal Rabbit Anti-Goat	1:2,000 (WB)	Dako
Peroxidase-conjugated Polyclonal Goat Anti-Rabbit	1:2,000 (WB)	Dako
DyLight 488 polyclonal goat anti-rabbit	1:500 (IF)	Abcam
Alexa Fluor 647donkey anti-goat	1:500 (IF)	Abcam

6.2 Cell line

6.2.1 Cell culture conditions

OCCM-30 cell line, a clonal population of immortalized murine cementoblasts, was kindly provided by Prof. M. Somerman (NIH, NIDCR, Bethesda, Maryland) and cultured as explant culture techniques according to previous description [83]. Briefly, cells were obtained from the root surface of the first mandibular molars of osteocalcin-transgenic mice. These mice contain the simian virus 40 (SV40) large T-antigen under the control of the osteocalcin promoter, and thus, only cells that express osteocalcin also express T-antigen in accordance with an immortalized cell line [83]. OCCM-30 cells were maintained in α-MEM (11095-080, Gibco, Invitrogen, Paisley, UK) growing medium containing 10% Fetal Bovine Serum (FBS) (10270-106, Gibco) and 1% Penicillin/Streptomycin (15140-122, Gibco) and incubated in a humidified atmosphere of 5% CO_2 at 37℃. The cells were seeded into 6-well plates (657160, Greiner Bio-One, Frickenhausen, Germany) in a density of 3×10^5 cells/well and the medium was changed twice a week. Upon reaching confluence, they were passaged and detached in the StemPro@ Accutase@ (A11105-01, Gibco) solution and passage 3 to 7 were used for processing the experiments.

For freezing the cells, the cells were washed twice with 1×phosphate-buffered saline (PBS) and treated with pre-warmed StemPro@ Accutase@ (A11105-01, Gibco). After 5 minutes incubation at 37℃, detached cells were diluted with warm growing medium, centrifuged at 1,000 rpm/min for 3 minutes and the supernatant was removed carefully. The concentrated cell suspension was diluted with freshly prepared freezing medium [(50% FBS and 50% DMSO (D8418-50ML, Sigma-Aldrich)] and keep at -20℃ for 2 hours followed by -80℃ freezing. To thaw the frozen cells, a vial was transferred to a 37℃-water bath as soon as possible and incubated for 1 minute. Cells were further suspended directly in fresh pre-warmed medium for centrifugation, after removing the supernatant containing DMSO cells were plated with fresh growing medium to grow.

6.2.2 Cell counting

When cells reached confluence, they were detached using StemPro@ Accutase@ (A11105-01, Gibco) at 5% CO_2 and 37°C for 5 minutes. The process was stopped using α-MEM (11095-080, Gibco) containing 10% FBS (10270-106, Gibco) and 1% Penicillin/Streptomycin (15140-122, Gibco). Cell counting was done using a single-use Neubauer-improved counting chamber (0640011, Marienfeld, Lauda-Königshofen, Germany) and an inverted light microscope (Leica, Wetzlar, Germany). 50 µL of cell suspension was mixed with 50 µL of 0.4% trypan blue solution (T8154, Sigma-Aldrich, Munich, Germany) by gently pipetting, and then 10 µL of the mixture was loaded into the side of the counting chamber. Counts were performed by triplicate by one analyst under a 40× objective according to the standard Algorithm [84]. Briefly, cells at four corner quadrants e and those that are over the top and right sides of the square are counted. If I have counted N cells in four large squares, the concentration of our sample will be: $N \times 10^4 \times 2$ cell/mL (2 means concentration-dilution factor).

6.3 Mechanical stimulation: a static compressive force application

The OCCM-30 cells were seeded into 6-well plates (657160, Greiner Bio-One). After reaching 60-70% confluence, compressive force application was applied as described by Kanzaki et al. [85] and Proff et al. [86]. Briefly, 33 mm diameter glass cylinders with pulled surfaces were made by Reichmann Feinoptik Inc. (Brokdorf, Germany). Cylinders of different volumes were fabricated in order to reach pressure forces of 1.2, 2.4, and 3.6 gf/cm^2, respectively. The cells were covered with the glass cylinders as soon as 60-70% confluence had been grown [17].

6.4 Reagent

Cells were stimulated using different concentrations of mouse Adiponectin/Acrp30/ADIPOQ protein (His Tag) from Sino Biological Inc. (Cat. N°: 50636-M08H). Purity > 95% (Determined by SDS-PAGE). Endotoxin < 1.0 EU/µg (Determined by the LAL method). Protein construction: The DNA sequence encoding

mouse ADIPOQ (NP_033735.3) (Met 1-Asn 247) was expressed with a C-terminal polyhistidine tag. Expression Host: HEK 293 cells. Formulation: Lyophilized from sterile PBS, pH 7.4, 5% Trehalose, 5% Mannitol, 0.01% Tween-80. The protein was reconstituted following manufacturer indications to a stock solution of 0.25 mg/mL in sterile water and stored at - 20°C.

6.5 Pharmacological inhibitors

The MAPK inhibitor for P38 (SB203580) (#tlrl-sb20, InvivoGen, California, USA), the ERK1/2 inhibitor (FR180204) (#328007, Calbiochem, Darmstadt, Germany) and the JNK inhibitor (SP600125) (#tlrl-sp60, InvivoGen, California, US) were used.

6.6 Quantitative Reverse Transcription Polymerase Chain Reaction (qRT-PCR)

6.6.1 RNA isolation

Cells were grown to 60-70% confluence and kept overnight in starvation medium [α-MEM (11095-080, Gibco) containing 0.5% FBS (10270-106, Gibco) and 1% Penicillin/Streptomycin (15140-122, Gibco)]. Afterwards, cells were either stimulated with adiponectin (100 ng/mL) (Cat. N°: 50636-M08H, Sino Biological Inc., Germany) or cultivated under compression (1.2 gf/cm^2, 2.4 gf/cm^2, 3.6 gf/cm^2). Total RNA was extracted from sample using NucleoSpin$^@$ RNA Kit (740955.50, MACHEREY-NAGEL, Düren, Germany) according to the manufacturer's instructions. For this purpose, stimulated cells were lysed by 350 µL RA1 buffer containing 1% β-Mercaptoethanol. The lysis solution was collected with a rubber policeman and then transferred into the NucleoSpin Filter and centrifuged for 1 minute at 14,000 rpm/min. The flow-through was mixed with 350 µL Ethanol (70%) by pipetting up and down for at least 5 times. After this step, total around 700 µL of the homogenized lysate was transferred into another NucleoSpin RNA Column followed by centrifugation for 30 seconds at 14,000 rpm/min. Next, 350 µL of MDB buffer was added into the column followed by the same centrifugation. To eliminate and genomic DNA contamination, the RNA sample was

thereafter intubated with 100 µL of DNase Reaction Mixture for 15 minutes at room temperature (RT). The sample was then washed by adding 200 µL of RAW2 buffer, 600 µL of RA3 buffer and 250 µL of RA3 buffer followed by the same centrifugation, respectively. At this stage the spin column was placed into a fresh collection tube, then 40 µL of RNase-free water was added followed by 1 minutes at 13,000 rpm/min. The purified RNA remaining in the collection tube was stored at -20°C until further processing.

6.6.2 Quality and quantification of total RNA

To prevent potential contamination, the standard precautions were carefully taken for all steps and devices. For example, the working area was cleaned with RNaseZap$^{@}$ RNase Decontamination Wipes (AM9786, Life Technologies). The RNAse/DNAse free tubes and RNAse/DNAse free water were used.

Using a spectrophotometer (Nanodrop 2000, ThermoFisher scientific), RNA concentrations (ng/µL) were measured and the quality and quantity of RNA was evaluated. The spectrophotometric values of A260/280 varied from a range of 2.0-2.2 and A260/230 values yield a ratio around 2.0 suggested that the isolated RNA was free of polyphenols, polysaccharides, and protein contaminants.

6.6.3 Complementary DNA (cDNA) synthesis

For synthesis of cDNA, 1.0 µg RNA was transcribed using commercial InnuSCRIPT Reverse Transcriptase kit (845-RT-6000100, Analytik Jena, Jena, Germany). The mRNA sample was mixed with 3 µL of Oligo primer, Rnase-free water to achieve 14.2 µL and incubate the reaction mix at 65°C for 5 minutes. Next, 2 µL of 10× RT-buffer, 0.8 µL of 25 mM dNTP mix, 2 µL of 100 mM DTT and 1 µL of RT-enzyme were added to each reaction mix and the resulting final volume of 20 µL solution was incubated at 25°C for 10 minutes, 42°C for 60 minutes and 70°C for 15 minutes. Further 1.0 µL of the synthesized cDNA was used for qRT-PCR.

6.6.4 qRT-PCR

RT-PCR amplification was carried out using the SsoAdvanced^{TM} Universal SYBR$^{@}$ Green Supermix (1723271, Bio-Rad). The primers used were purchased from Bio-Rad (**Table. 6**). The primers for MAPK1, MAPK8, MAPK14, GSK-3β, β-Catenin were designed from Eurofins Genomics Inc. and their sequences are summarized in **Table 6**. Reaction conditions comprised 40 cycles repeat and were denatured initially for 15 seconds at 95°C, subsequently, each cycling stage was performed at 95°C for 15 seconds and 1 minute of amplification at 60°C.

6.6.5 qRT-PCR data analysis

The expression of each gene was measured in triplicate for each sample and expression was normalized to that of the housekeeping gene glycerinaldehyde-3-phosphate dehydrogenase (GAPDH) (qMmuCED0027497, Bio-Rad). The cycle threshold value (C_q) for each individual PCR product was calculated by the Bio-Rad CFX Manager 3.1 software. Relative levels of transcript expression were quantified using the $2^{\Delta\Delta Ct}$ method [87].

6.7 Protein extraction and Western blot (WB)

6.7.1 Protein extraction

The stimulated OCCM-30 cells were washed with cold 1×PBS and then lysed using 200 μL of RIPA buffer (89901, ThermoFisher Scientific, Waltham, USA) supplemented with 3% protease inhibitor (78442, ThermoFisher Scientific) on ice for 30 minutes. By using cell scrapers (Greiner Bio-One, Germany), the lysate underwent disruption and homogenization was collected. The insoluble material was removed from the protein lysates by centrifugation at 14,000 rpm/min for 15 minutes at 4°C.

6.7.2 Measurement of protein concentration

The total cell extract contained in the supernatants were collected and protein

concentrations were measured using Pierce™ BCA Protein Assay Kit (23225, Thermo Scientific) on a DR/2000 Spectrophotometer (#4480000, HACH, Manchester, UK) following the instrument [88]. Briefly, working solutions of BCA were prepared freshly by mixing 50 parts of reagent A (23228, BCA, sodium carbonate, sodium bicarbonate, bicinchoninic acid and sodium tartrate in 0.1 M sodium hydroxide) with 1 part of reagent B (1859078, $CuSO_4$, 4%), as indicated by the manufacturer. 30 µL of lysate protein samples were pipetted onto the 1.5 mL Biosphere@ SafeSeal Tube, and 570 µL of BCA working solutions were added, giving a BCA working solution: sample ratio of 20:1. The tubes were quickly shaken for 30 seconds by Vortex-2 Genie (Scientific Industries, Germany) before reading and plates incubated for 30 minutes at 37°C. The absorbance at 562 nm of the microplates was followed in a direct reading DR/2000 spectrophotometer (HACH).

6.7.3 Gel electrophoresis

For separating proteins by different molecular size, 20 µg lysate/lane was diluted in sample loading buffer (#G031, abm) and separated by 4-15% gradient Mini-PROTEAN@ TGX™ Gels (Bio-Rad) for the electrophoresis at 120 V for 90 minutes. Then, the resolved proteins were transferred electrophoretically to nitrocellulose membranes using Transfer-blot@ Turbo™ Transfer Pack (1704271, Bio-Rad) on Transfer-blot@ Turbo™ Transfer system (1704150, Bio-Rad). Protein loading was verified by Ponceau S staining (6226-79-5, Sigma). Membranes were blocked with 5% non-fat milk (m/v) (T145.1, ROTH) for 1 hour at RT and further incubated with the primary antibodies for ERK1/2 (1:1,000, MBS8241746, BIOZOL, Eching, Germany); phospho-ERK1/2 (p44/42, Thr202/Tyr204) (1:1,000, #4370, Cell Signaling Technology, Frankfurt am Main, Germany); p54/p56 JNK (1:1,000, #9252, Cell Signaling Technology), phosphor-SAPK/JNK (Thr183/Tyr185) (1:1,000, #4668, Cell Signaling Technology); P38 MAPK (1:1,000, #9212, Cell Signaling Technology); phospho-P38 MAPK Alpha (1:1,000, #4511, Cell Signaling Technology), GSK-3β (1:1,000, #12456, Cell Signaling Technology); phospho-GSK-3β (Ser9) (1:1,000, #9323, Cell Signaling Technology); β-

Catenin (1:1,000, #8480, Cell Signaling Technology); phospho-β-Catenin (Ser33/37/Thr41) (1:1,000, #9561, Cell Signaling Technology) and β-actin (1:2,000, ab8227, Abcam) followed by peroxidase-conjugated secondary antibodies included Polyclonal Goat Anti-Rabbit (1:2,000, P0448, Dako, Frankfurt am Main, Germany); Rabbit Anti-Goat (1:2,000, P0160, Dako) and Polyclonal Goat Anti-Mouse (1:2,000, P0447, Dako) in 2.5% non-fat milk (T145.1, ROTH) for 1 hour at RT. The antibodies used are listed in **Table 5**. The band signal detection was then performed with X-ray Amersham Hyperfilm (28906836, GE Healthcare, Hamburg, Germany) utilizing Amersham ECL Western blotting Detection Reagents (9838243, GE Healthcare) and detected with on OPTIMAX X-Ray Film Processor (11701-9806-3716, PROTEC GmbH, Oberstenfeld, Germany) in a dark room.

6.8 Cell migration assay

OCCM-30 cells were plated at a density of 8×10^3 cells/well in 6-well plates (657160, Greiner Bio-one) in α-MEM (11095-080, Gibco) containing 10% FBS (10270-106, Gibco) and 1% Penicillin/Streptomycin (15140-122, Gibco) and cultured until confluence. Cells were preincubated for 12 hours in starvation medium and wounded by scratching using a 100 µL tip. Through this way, a cell-free area was created in the center of the cell layer. Afterwards, all non-adherent cells were washed with 1×PBS (10010023, ThermoFisher). The wounded cell monolayers were incubated in the presence and absence of different concentration of adiponectin (50636-M08H, Sino Biological Inc.) for 24 hours. Wounded-area images were taken immediately after wounding and 24 hours after scratching. The wounded cell layers were photographed at 10× magnification (Leica Microsystems, Wetzlar, Germany) and the percentages of wound closure area between cell layer borders were analyzed and calculated over time using the Image J software (National Institutes of Health and University of Wisconsin, USA).

For the MAPK inhibition experiment, OCCM-30 cells were pretreated with the P38 inhibitor SB203580 (InvivoGen), the ERK1/2 inhibitor FR180204 (Calbiochem) or the JNK inhibitor SP600125 (InvivoGen) at a concentration of 1.0 µg/mL as well as with

DMSO (D8418-50ML, Sigma-Aldrich) at 0.1% (v/v) (Control group) for 1 hour before adiponectin addition. Afterwards, the pretreated OCCM-30 cells were wounded and cultivated in the presence or absence of adiponectin (50636-M08H, Sino Biological Inc.).

6.9 *In vitro* mineralization assay

OCCM-30 cells at passages 5 to 7 were seeded to 6-well plates (657160, Greiner Bio-one) at a density of 3×10^4 cells/well using α-MEM (11095-080, Gibco) containing 10% FBS (10270-106, Gibco) and 1% Penicillin/Streptomycin (15140-122, Gibco). After the cell reached confluence, to induce cementogenesis the culture medium was supplemented with 50 μg/mL Ascorbic Acid (6288.1, Roth, Karlsruhe, Germany) and 10 mM β-Glycerophosphate disodium salt hydrate (#35675, Calbiochem, Darmstadt, Germany) with different concentrations of adiponectin (50636-M08H, Sino Biological Inc.).

Mineralization of extracellular matrix was determined on days 7 and 14 by Alizarin Red S staining. Briefly, mineralized monolayer cell cultures were washed with 1×PBS (10010023, ThermoFisher) three times and stained using 1% Alizarin Red S solution (A5533, Sigma-Aldrich) during 5 minutes at RT after being fixed with 70% Ethanol (64-17-5, Sigma-Aldrich) for 1 hour at 4°C. Mineralized nodule formation was assessed by inverted phase contrast microscopy (Leica Microsystems, Wetzlar, Germany) using the LASV4.8 software (Leica, Wetzler, Germany).

To quantify the degree of calcium accumulation in the mineralized extracellular matrix, Alizarin Red S-stained cultures were dissolved using 100 mM Cetylpyridinium chloride (6004-24-6, Sigma-Aldrich) for 1 hour to release calcium-bound dye into the solution. The absorbance of the released dye was measured at 570 nm using a spectrophotometer (xMarkTM, Microplate Absorbance Spectrophotometer, 1681150, Bio-Rad, Germany).

To measure the effect of MAP kinase in adiponectin-induced cementogenesis, cells were incubated with the inhibitors: SB203580 (InvivoGen), FR180204 (Calbiochem) and SP600125 (InvivoGen) at a concentration of 1.0 μg/mL as well as with DMSO (D8418-50ML, Sigma-Aldrich) at 0.1% (v/v) for 7 and 14 days, respectively.

6.10 MTS cell proliferation assay

Cell viability and proliferation was examined using 3-(4,5-dimethylthiazol-2-yl)-5-(3-carboxymethoxyphenyl)-2-(4-sulfophenyl)-2H-tetrazolium (MTS) assay (CellTiter 96$^{@}$ Aqueous One Solution Cell Proliferation Assay, Promega, Walldorf, Germany) according to manufacturer's instructions. Briefly, OCCM-30 cells at a passage 3-5 were seeded at a density of 5×10^3 cells/well in a 96-well plate (655180, Greiner Bio-one). Cells were cultured in α-MEM containing 5% FBS overnight to allow adherence. Then, cells were washed twice with 1×PBS (10010023, ThermoFisher) and treated with various concentrations of adiponectin (50636-M08H, Sino Biological Inc.) in α-MEM containing 0.5% FBS over a period of 24 hours.

To assess the involvement of the MAP kinase cascade in adiponectin-induced proliferation, cells were pretreated 1 hour with the inhibitors: SB203580 (InvivoGen), FR180204 (Calbiochem) and SP600125 (InvivoGen) at a concentration of 1.0 μg/mL as well as with DMSO (D8418-50ML, Sigma-Aldrich) at 0.1% (v/v), respectively. Thereafter, 20 μL of the MTS reagent was added into each well and the cells were incubated during 2 hours at 37°C in a 5% CO_2 atmosphere. Plates were read by 490 nm using a 96-well micro-plate reader (BioTek, Winooski, VT, USA) to measure the amount of formazan by cellular reduction of MTS.

6.11 Immunofluorescence staining

Cementoblasts were cultured on sterile Falco^{TM} Chambered Cell Culture Slides (354108, Fisher Scientific) until 50% confluence and afterwards fixed with 4% paraformaldehyde (158127, Sigma-Aldrich) dissolved in 1×PBS (1401683, Gibco) and adjusted to pH 7.4, for 10 minutes at RT and permeabilized with 0.5% Triton^{TM} X-100 Surfact-Amps^{TM} Detergent Solution (28313, ThermoFisher) for 20 minutes at RT. Then, cells were kept in blocking buffer containing 10% goat serum, 0.3 M glycine, 1% BSA (071M8410, Sigma-Aldrich) and 0.1% tween-20 (P1319, Sigma-Aldrich) for 30 minutes at RT and incubated with primary antibodies for AdipoR1 (1:250, ab70362, Abcam), AdipoR2 (1:250, ab77612, Abcam), GSK-3β (1:500, #12456, Cell Signaling Technology) and β-

Catenin (1:500, #8480, Cell Signaling Technology) at 4°C overnight. After washing three times with 1×PBS (1401683, Gibco) - 0.1% TRITON X-100 (T-9284, Sigma-Aldrich) for 5 minutes, the cells were incubated with secondary antibodies: DyLight 488 goat anti-rabbit polyclonal (1:500, ab96899, Abcam) or Alexa Fluor 647 donkey anti-goat (1:500, ab150131, Abcam) which conjugated to fluorescein isothiocyanate for 1 hour at RT. After washing with 1×PBS-Tween-20, DNA was stained using a fluorescent Mounting Medium with 4',6-diamidino-2-phenylindole (DAPI) (ab104139, Abcam) for 15 minutes. Staining was analyzed using a high-resolution fluorescence microscope (Leica Microsystems, Wetzlar, Germany) and photographed.

6.12 Small-interfering RNAs transfection

The small-interfering RNAs (siRNA) targeting the mouse AdipoR1 (SI00890295), AdipoR2 (SI00890323), MAPK1 (SI02672117), MAPK3 (SI01300579), MAPK8 (SI1300691), MAPK14 (SI01300523), negative control (1027280) and cell death control (SI04939025) were purchased from QIAGEN (Germany). siRNAs were incubated with 12 µL HiPerFect$^{@}$ Transfection Reagent (301705, QIAGEN) in 100 µL Opti-MEM medium (31985-062, Gibco) at RT for 10 minutes, and then each transfection mixture was added into 2.3 ml growth medium in the 6-well plate in which OCCM-30 cells were cultured at 60-70% confluence. After siRNA transfection for 24 hours, the cells were kept in starvation medium for 2 hours and afterwards 100 ng/mL adiponectin (Cat. N°: 50636-M08H, Sino Biological Inc.) was added.

6.13 Enzyme-Linked Immunosorbent Assay (ELISA)

6.13.1 Alkaline phosphatase (AP) enzymatic activity assay

After cementogenesis induction during 14 days, OCCM-30 cells were lysed in distilled deionized water and sonicated for 15 seconds (SONIFIER 150, BRANSON, G. HEIHEMANA, Germany). The lysate was incubated at 37°C for 30 minutes with p-Nitrophenyl phosphate (p-NPP; Alkaline Phosphatase Substrate, Sigma-Aldrich) in an

alkaline phosphatase buffer solution (1.5 mM). The reaction was stopped by adding NaOH, and absorbance was read at 405 nm (xMarkTM, Microplate Absorbance Spectrophotometer, 1681150, Bio-Rad).

6.13.2 Dual luciferase (TCF/LEF reporter) assay

OCCM-30 cells were seeded into 96-well plate at a density of 3×10^4 cells/well in 100 µL growth medium [α-MEM (11095-080, Gibco) containing 10% FBS (10270-106, Gibco) and 1% Penicillin/Streptomycin (15140-122, Gibco)] overnight. The reverse transfection of OCCM-30 cells with silencing RNA was performed with specific siRNAs to knock-down AdipoR1, AdipoR2, MAPK1, MAPK3, MAPK8 and MAPK14. Briefly, cells were incubated with 24.25 µL Opti-MEM antibiotic-free medium (31985-062, Gibco), 0.75 µL HiPerFect@ Transfection Reagent (301705, QIAGEN) supplement with 12.5 ng specific siRNA for incubation for 24 hours.

The cells were then simultaneously transfected with TCF/LEF Reporter Kit (#60500, BPS Bioscience). For control transfection, cells were transfected with DNA mixture by 1 µL of TCF/LEF luciferase reporter vector (#60500, BPS Bioscience) plus negative control siRNA (1027280, Qiagen); 1 µL of non-inducible luciferase vector (#60500, BPS Bioscience) plus negative control siRNA (1027280, Qiagen); 1 µL of non-inducible luciferase vector (#60500, BPS Bioscience) plus specific siRNA in 15 µL Opti-MEM antibiotic-free medium (31985-062, Gibco). For experimental transfection, the DNA mixture of 1 µL TCF/LEF luciferase reporter vector (#60500, BPS Bioscience) plus specific siRNA was incubated in 15 µL Opti-MEM antibiotic-free medium (31985-062, Gibco). All DNA mixtures were then mixed with 0.35 µL Lipofectamine™ 2000 Transfection Reagent (11668030, ThermoFisher) in 15 µL Opti-MEM antibiotic-free medium (31985-062, Gibco) at RT for 25 minutes. After 24 hours of transfection, medium was changed to fresh growth medium. Following incubation for another 23 hours, adiponectin (100 ng/mL) was added to stimulate cells for 1 hour. I set up each treatment in triplicate.

After 48 hours of transfection, the firefly luciferase activities were performed using BPS

Dual Luciferase (Firefly/Renilla) Assay system (#60683-1, BPS Bioscience) using a Mithras LB 940 Luminometer (38099, BERTHOLD TECHNOLOGIES) and analyzed by MikroWin 2000 (Mikrotek Laborsysteme GmbH, Germany), which was normalized to the Renilla luciferase activities.

6.14 Statistical analysis

Experiments were performed in triplicate successfully. The most convincing result was used for further evaluation. Statistical analyses were plotted using GraphPad Prism 8.0 software (GraphPad Prism Inc., San Diego, CA, USA). Quantitative values are expressed as means ± standard deviation (SD) and analyzed using independent one-way t-test followed by a Tukey's post-hoc test for unpaired samples to determine the statistically significant differences for multiple comparisons. Differences were considered statistically significant at a p-value of < 0.05. All p-values are shown with respect to controls unless otherwise indicated. Correlations between the expression of AP, BSP, OCN, OPG, Runx-2 and F-spondin were analyzed using Pearson's correlation coefficient analysis. In the figures, asterisks denote statistical significance (*$p < 0.05$; **$p < 0.01$; ***$p < 0.001$; ****$p < 0.0001$). Figures were assembled using Adobe Illustrator CC 2019 software.

7. Results

7.1 Adiponectin interacts *in vitro* with cementoblasts influencing cell migration, proliferation and mineralization partially through the MAPK signaling pathway.

7.1.1 Expression of adiponectin receptor 1 and 2 in cementoblasts.

To investigate whether OCCM-30 cementoblasts express adiponectin receptors (AdipoRs) and their relative expression level, the expression of AdipoRs were verified by Western blot (WB), RT-PCR and immunofluorescence (IF) analysis. The WB results could establish that AdipoR1 as well as AdipoR2 are markedly expressed on this cell line (**Figure 4A**). The mRNA expression of AdipoRs demonstrated that by RT-PCR analysis interestingly AdipoR1 had about 67% higher expression levels than its counterpart AdipoR2 (**Figure 4B**). IF staining showed that AdipoR1 was mostly expressed in the cytoplasm, cytomembrane and nucleus, while AdipoR2 was expressed around the nucleus (**Figure 4C**).

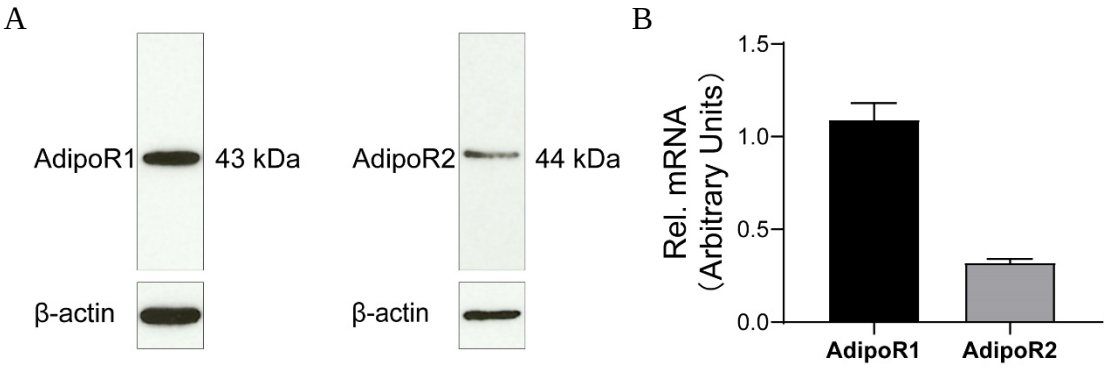

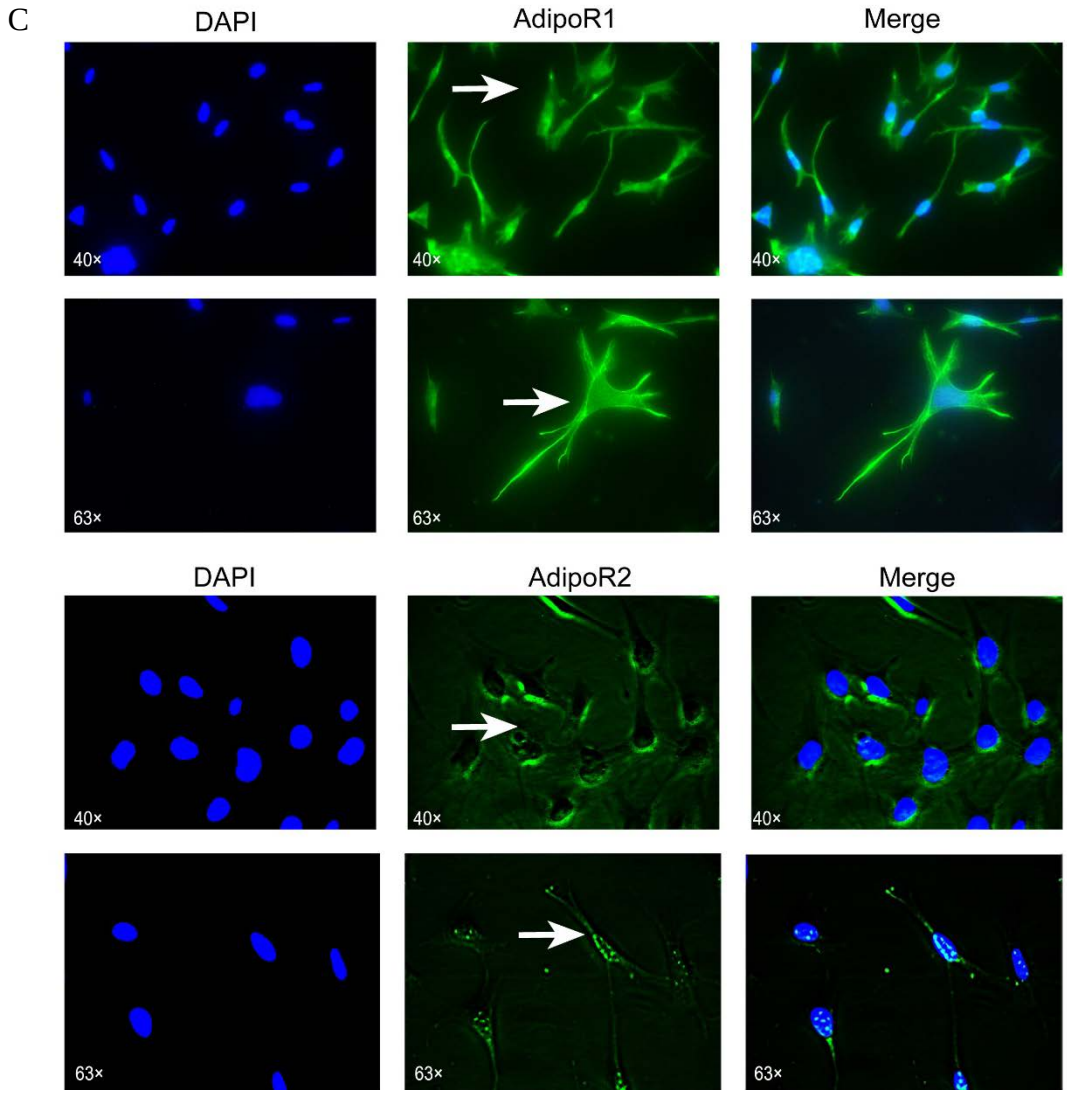

Figure 4. Cementoblasts express adiponectin receptors.

(A) Expression of AdipoR1 and AdipoR2 in OCCM-30 mouse cementoblasts examined by Western blot, β-actin is shown as reference protein.

(B) RT-PCR analysis indicates that the mRNA expression of AdipoR1 is significantly higher than the expression of AdipoR2.

(C) Distribution of AdipoRs in OCCM-30 cells were visualized by IF staining (Green color). DAPI staining was used for nuclei detection. Arrows show cellular receptor localization. AdipoR1 is located in the cytoplasm, cytomembrane and nucleus, while AdipoR2 is distributed mostly around the nucleus and in the cytoplasm of the OCCM-30 cells. DAPI: 4',6-diamidino-2-phenylindole; IF: immunofluorescence.

Values are shown as means ± standard deviation (SD). Asterisks indicate significant differences compared to control cells (***$p < 0.001$, **$p < 0.01$, and *$p < 0.05$, ns = not significant).

7.1. 2 Adiponectin promotes *in vitro* cementoblasts mineralization as well as the cementogenesis-related biomarker expression.

Next, I aimed to analyze the possible effect that exogenous adiponectin exerts on cementoblasts mineralization. Alizarin Red S staining was used to visualize and quantify the biological effect of adiponectin on OCCM-30 cell mineralization.

The microscopic view of this method revealed that adiponectin significantly increased mineralized nodule formation in a dose-dependent manner over a period of fourteen days during cementogenesis induction (**Figure 5A**). Colorimetric analysis revealed that adiponectin-stimulated OCCM-30 cells had higher levels of mineralized matrix production in comparison to unstimulated cells (**$p < 0.01$) (**Figures 5B, C**).

The analysis of the AP enzymatic activity over a period of 48 hours of cells stimulated with different concentrations of adiponectin showed increased AP activity in time- and dose-dependent manner, reaching statistical significance (**$p < 0.01$) after 24 hours in the group stimulated with 80 ng/mL adiponectin (**Figure 5D**).

OCCM-30 cells cultivated for a period of 3 days in a mineralization-inducing medium, were afterwards stimulated over a period of three hours with adiponectin (100 ng/mL). The kinetic analysis of the relative mRNA expression of AP, Runx-2, BSP, OPG, OCN and F-Spondin increased notably, reaching statistical significance after 45 minutes of stimulation in comparison to timepoint 0 minute. These stimulatory effects were sustained over the entire period of three hours (*$p < 0.05$) (**Figure 6**).

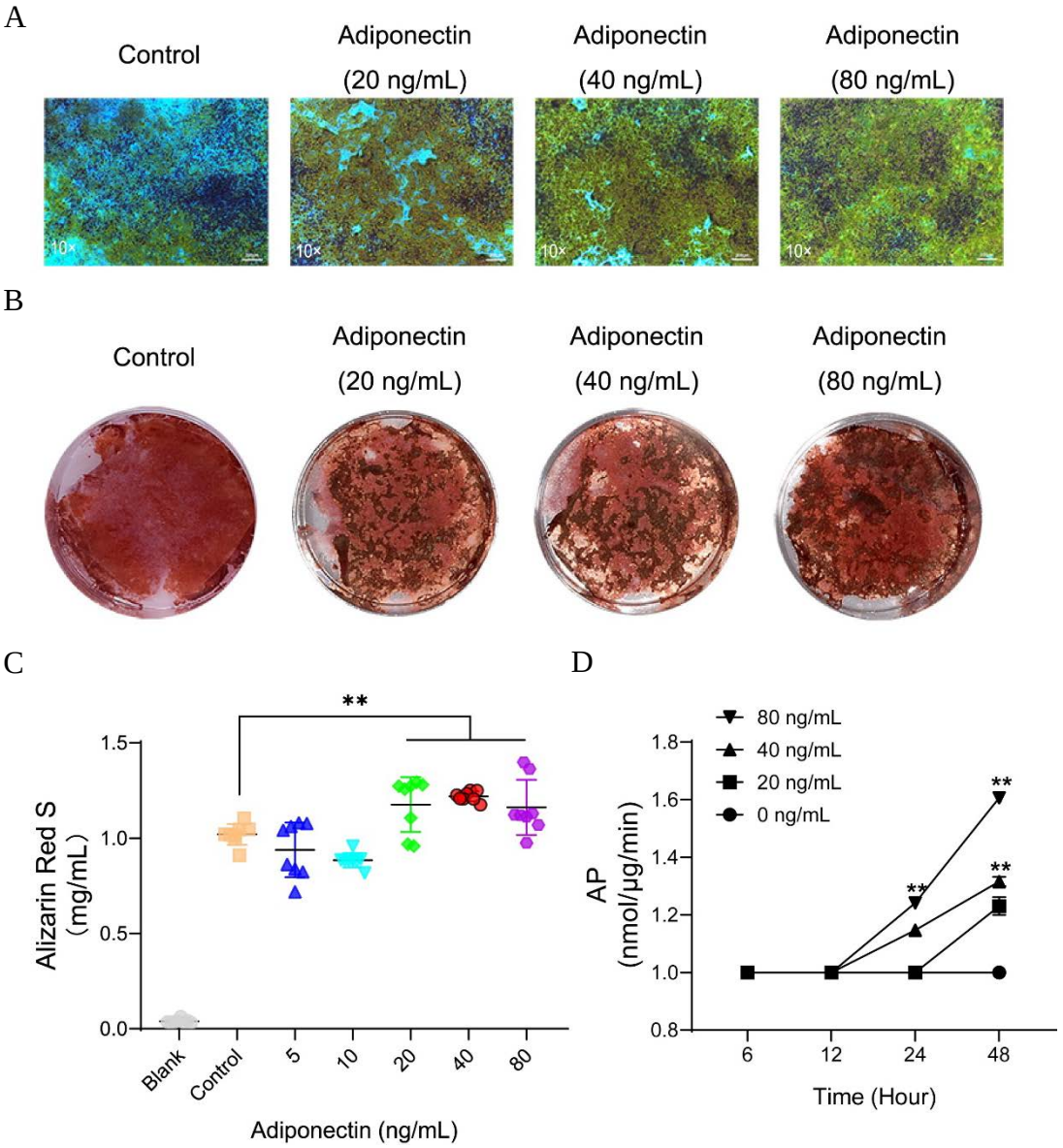

Figure 5. Adiponectin promotes mineralization in vitro.

(A) Microscopic view of OCCM-30 cells after 14 days of stimulation with different concentrations of adiponectin (Staining: Alizarin Red S).

(B, C) Cells were cultivated with 0 (Control), 20, 40 and 80 ng/mL recombinant mice adiponectin for 14 days. Mineralization grade was visualized and quantified using Alizarin red S staining and by further dilution with Cetylpiridiumchlorid. Results are expressed as mg/mL of Alizarin Red S.

(D) Adiponectin added to OCCM-30 cells increases the alkaline phosphatase enzymatic activity dose-dependently, reaching statistical significance after 24 hours in comparison with the untreated group (Data are normalized to 1).

Values are shown as means ± SD. Asterisks indicate significant differences compared to control cells (***$p < 0.001$, **$p < 0.01$, and *$p < 0.05$, ns = not significant).

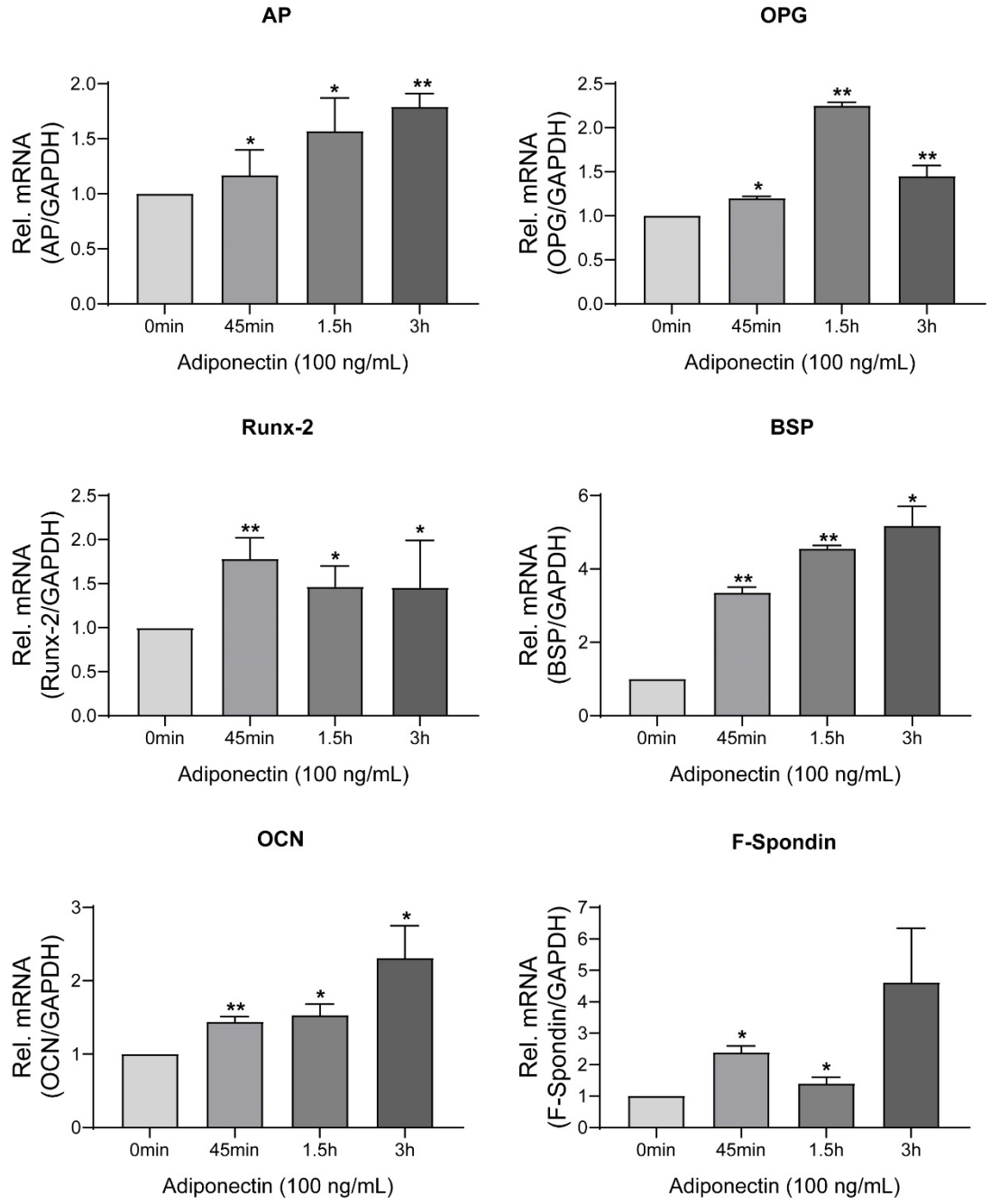

Figure 6. Adiponectin up-regulates cementogenesis marker expression in cementoblasts.

Kinetic analysis of mRNA expression of Alkaline Phosphatase (AP), Bone Sialoprotein (BSP), Osteoprotegerin (OPG), Osteocalcin (OCN), Runx2 and F-spondin in cementoblasts after adiponectin stimulation. Values are expressed as means ± SD and data are normalized to GAPDH which was used as housekeeping gene. Asterisks indicate significant differences compared to control cells (***$p < 0.001$, **$p < 0.01$, and *$p < 0.05$, ns = not significant).

7.1.3 Adiponectin facilitates *in vitro* cementoblasts migration and proliferation.

The effects of the adiponectin exert on cell proliferation and migration were analyzed by a standard scratching method and MTS assay, respectively. Cells were grown to 100% confluency and were then scratched using a 100 µL pipet tip. Immediately thereafter, cells were stimulated with different concentrations of adiponectin (0, 0.1, 0.5, 1 and 2 µg/mL) during 24 hours.

The cell migration ability was visualized and measured using microscopic photography of the cell-free areas (**Figure 7A**). The calculation of the recovered area indicates that adiponectin at concentrations of 1 and 2 µg/mL significantly facilitates wound closure at migration rate of 24.35 ± 2.38% and 30.3 ± 2.68%, respectively (**Figure 7B**). Furthermore, I observed that cells stimulated with adiponectin over a period of 24 hours have increased mitogenic activity. The proliferation assay showed that the groups stimulated with 0.4, 0.8 and 1.6 µg/mL adiponectin showed a significantly increased proliferation rate in comparison to unstimulated cells (**Figure 7C**).

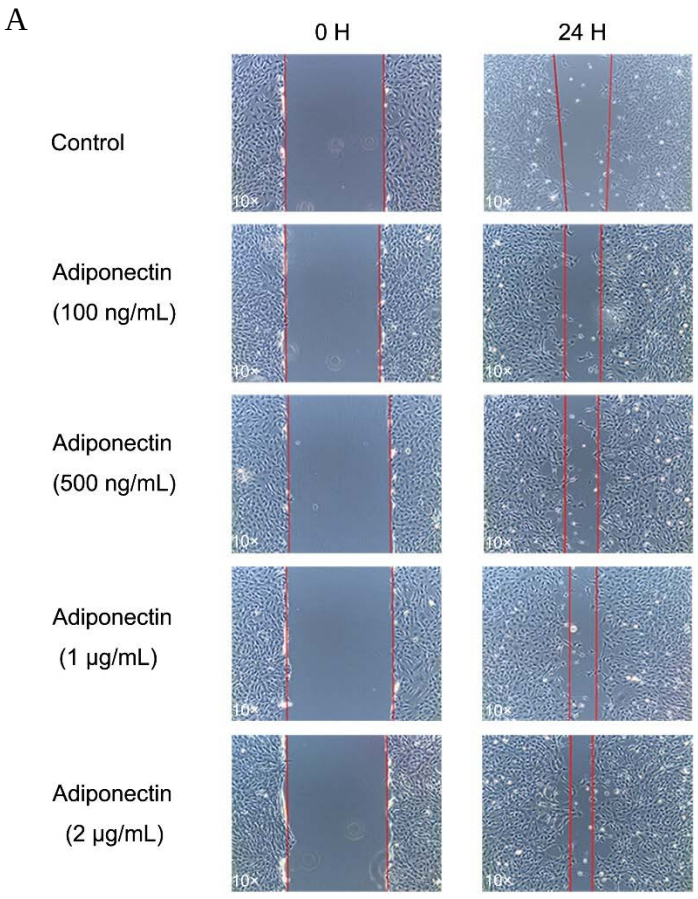

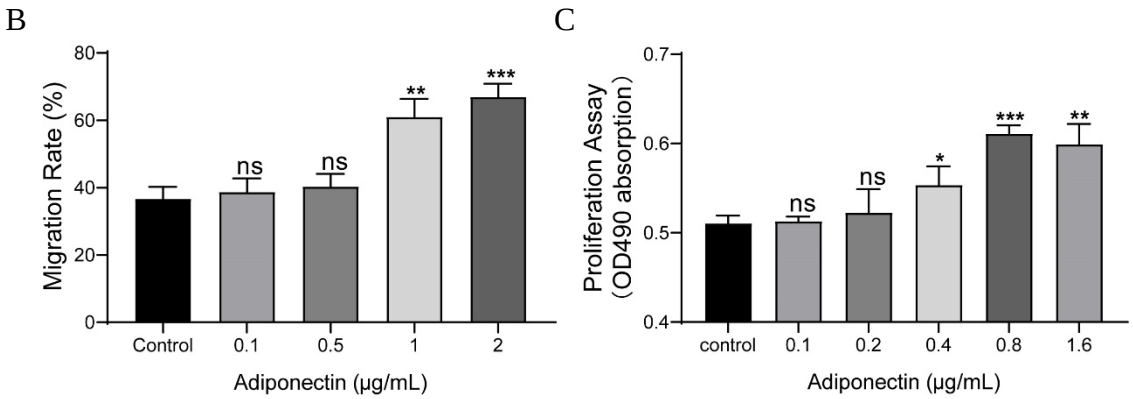

Figure 7. Increased migration and proliferation rates of OCCM-30 cells treated with adiponectin.

(A, B) Images show the migration effect that adiponectin exerts on OCCM-30 cells wounded monolayers at 0 and 24 hours after standard scratching using a 100 µL pipet tip. The red lines indicate the wound edge at the beginning and at the end of the experiment. The migration rates were measured over a period of 24 hours. Data are presented as percentage of wound recovery.

(C) The proliferation assay showed that adiponectin-treated cells during 24 hours have an increased proliferation rate in comparison to untreated cells. This effect occurred dose-dependently, reaching statistical significance at a concentration of 0.4 µg/mL adiponectin. Values are shown as means ± SD. Asterisks indicate significant differences compared to control cells (***$p < 0.001$, **$p < 0.01$, and *$p < 0.05$, ns = not significant).

7.1.4 Adiponectin induces P38, ERK1/2 and JNK phosphorylation in OCCM-30 cells.

To elucidate if adiponectin can activate the MAPK pathway, I performed a kinetic analysis of P38, ERK1/2 and JNK protein phosphorylation by WB (**Figures 8A, B**).

WB revealed that P38 phosphorylation occurs 5 minutes after adiponectin (20 ng/mL) stimulation. The phosphorylated-state of P38 was sustained over a period of 4 hours, reaching a peak at time point 10 minutes (**$p < 0.01$). The phosphorylation of ERK1/2 as well as P54/P46 JNK reached a peak after 5 minutes' adiponectin addition, being the WB's bands detectable during 30 minutes in both cases (**Figures 8A, B**).

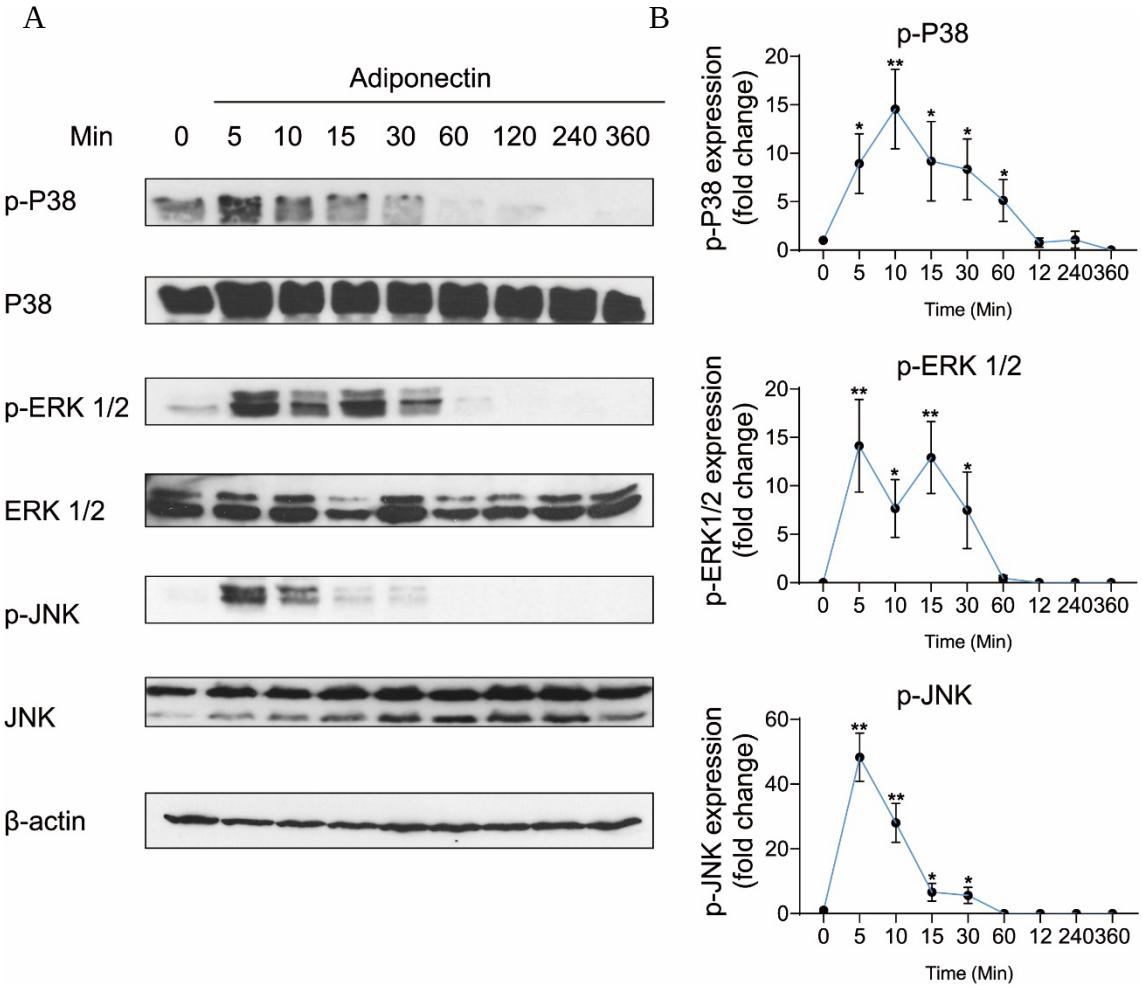

Figure 8. Adiponectin promotes JNK, ERK1/2 and P38 phosphorylation on cementoblasts.

(A) The expression of JNK (46 and 54 kDa), ERK1/2 (42 and 44 kDa) and P38 (42 kDa) as well as their phosphorylated forms stimulated by adiponectin were detected by Western blot, β-actin served as a loading control.

(B) Graphics show the relative expression of p-JNK, p-ERK1/2 and p-P38 compared to cells at time point 0 minute.

Values are shown as means ± SD. Asterisks indicate significant differences compared to control cells (***$p < 0.001$, **$p < 0.01$, and *$p < 0.05$, ns = not significant).

7.1.5 Blockade of MAPK attenuates *in vitro* adiponectin-induced cementoblast migration and proliferation.

Since the previous results showed that adiponectin increased phosphorylation of P38, ERK1/2 and JNK in OCCM-30. In order to evaluate whether the activation of MAP kinases is essential for adiponectin-stimulated cell migration and proliferation, OCCM-30 cementoblasts were preincubated with the pharmacological inhibitors: 1 μM of

SB203580 (P38), 1 μM of FR180204 (ERK1/2) and 1 μM of SP600125 (JNK) as well as with 1 μM of DMSO (Control group) for 1 hour and afterwards stimulated with adiponectin.

The MTS assay indicated that MAPK blockade reduced the cell proliferation in unstimulated and stimulated cells (**Figure 9A**). However, this suppression effect was partially counteracted by adiponectin (100 ng/mL) (**Figure 9B**).

As shown in the **Figures 9C, D**, the scratched areas were measured after 24 hours, which is represented by a front-end yellow edge line (**Figure 9C**). The migratory capacity of OCCM-30 cells treated with MAPK inhibitors was examined in the presence or absence of adiponectin (100 ng/mL). As result, the migration rate of cells was significantly attenuated after ERK1/2 as well as JNK blockade despite adiponectin (100 ng/mL) co-stimulation, whereas this effect was not observed in the group pretreated with the P38 inhibitor (**Figure 9D**).

A

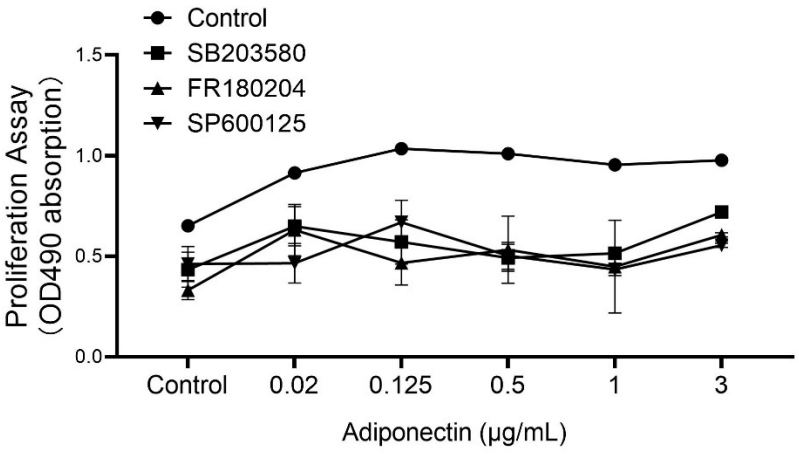

B

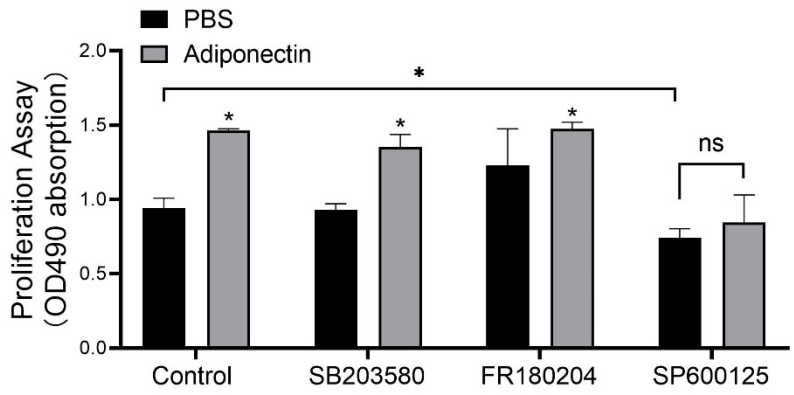

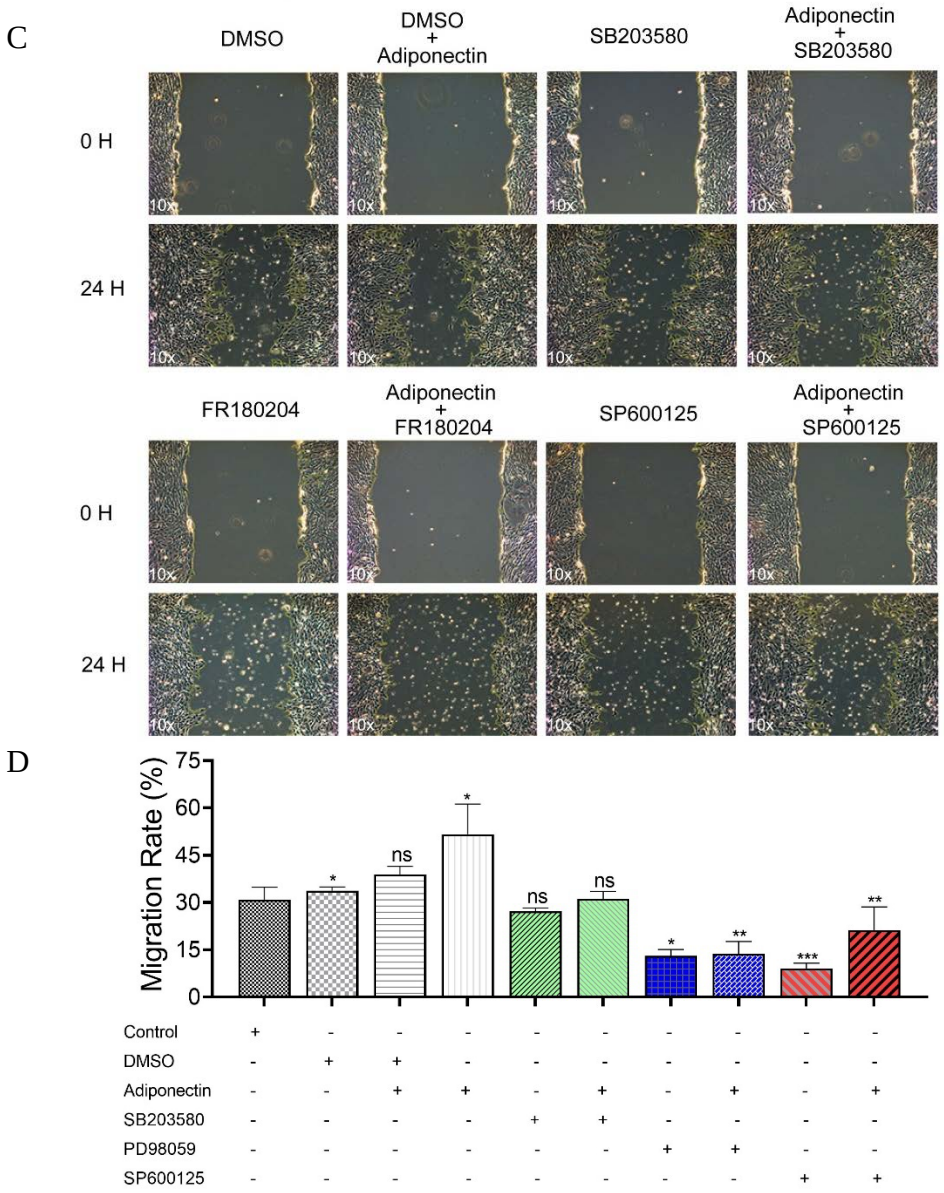

Figure 9. The MAPK pathway is involved in adiponectin-induced proliferation and migration of cementoblasts.

(A, B) Cells were pretreated with MAPK inhibitors for 1 hour and afterwards stimulated with adiponectin for 24 hours. As result, MAP kinase inhibition impairs cell proliferation (MTS Assay) despite adiponectin stimulation.

(C) Images of cell migratory properties were captured prior to stimulation (0 hour) and after 24 hours. The area of the migrated cell was measured by the starting and ending edge of cells which was represented by front-end yellow line.

(D) The migrated area (24 hours) was calculated using Image J software by comparing the relative area of the starting and ending edges. Blockade of ERK 1/2 (PD98059) and JNK (SP600125) over a period of 24 hours significantly decreased cell migration whereas P38 inhibition did not significantly influence the migration rate.

Values are shown as means ± SD. Asterisks indicate significant differences compared to control cells (***$p < 0.001$, **$p < 0.01$, and *$p < 0.05$, ns = not significant).

7.1.6 Inhibition of MAPK alters adiponectin-induced mineralization.

The colorimetric analysis performed after dilution of Alizarin Red S staining for a period of 3 days' mineralization induction, did not show significant differences among groups despite adiponectin treatment (**Figures 10A, B**).

After 14 days' induction, cells treated with MAPK inhibitors microscopically exhibited increased mineralization in the absence of adiponectin. In the presence of adiponectin, such effect was slightly but significantly decreased. On the contrary, adiponectin did not alter the mineralized matrix production of OCCM-30 cells after sustained blockade of JNK (**Figures 10A, B**).

A

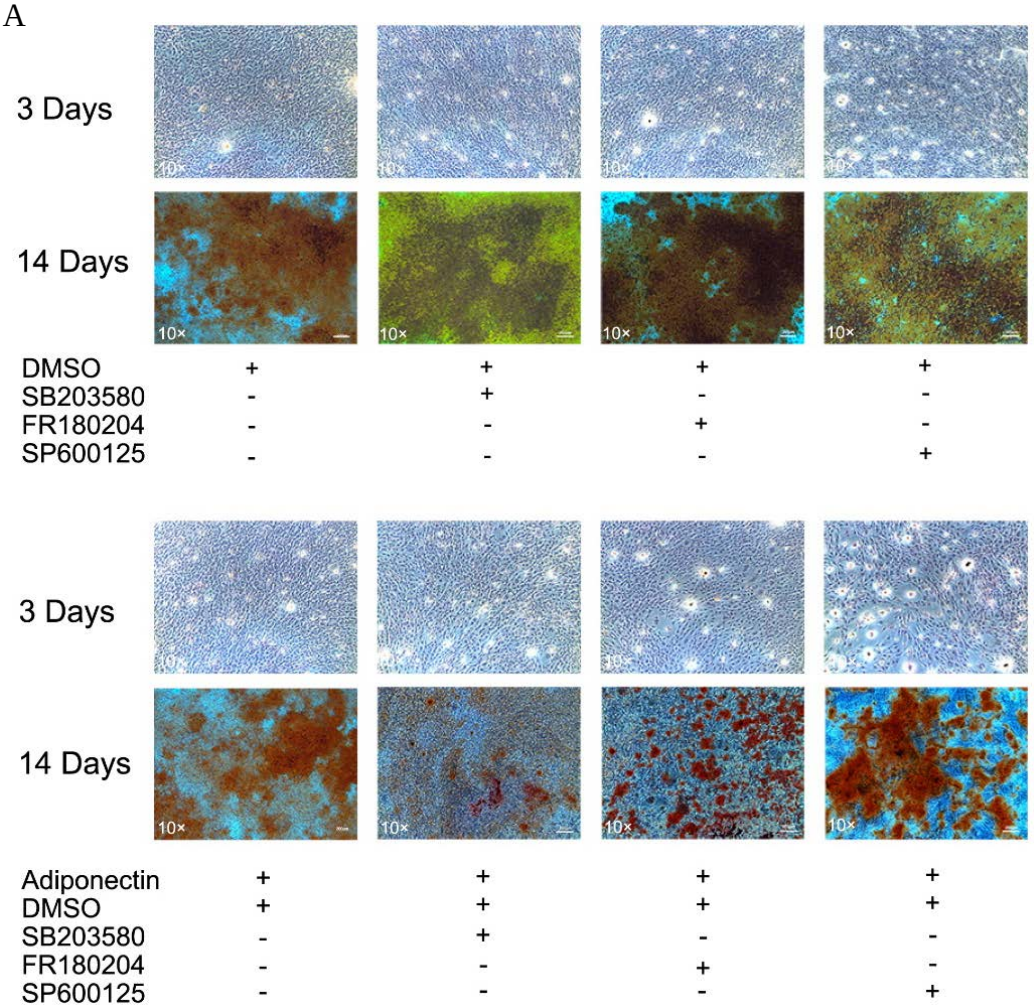

B

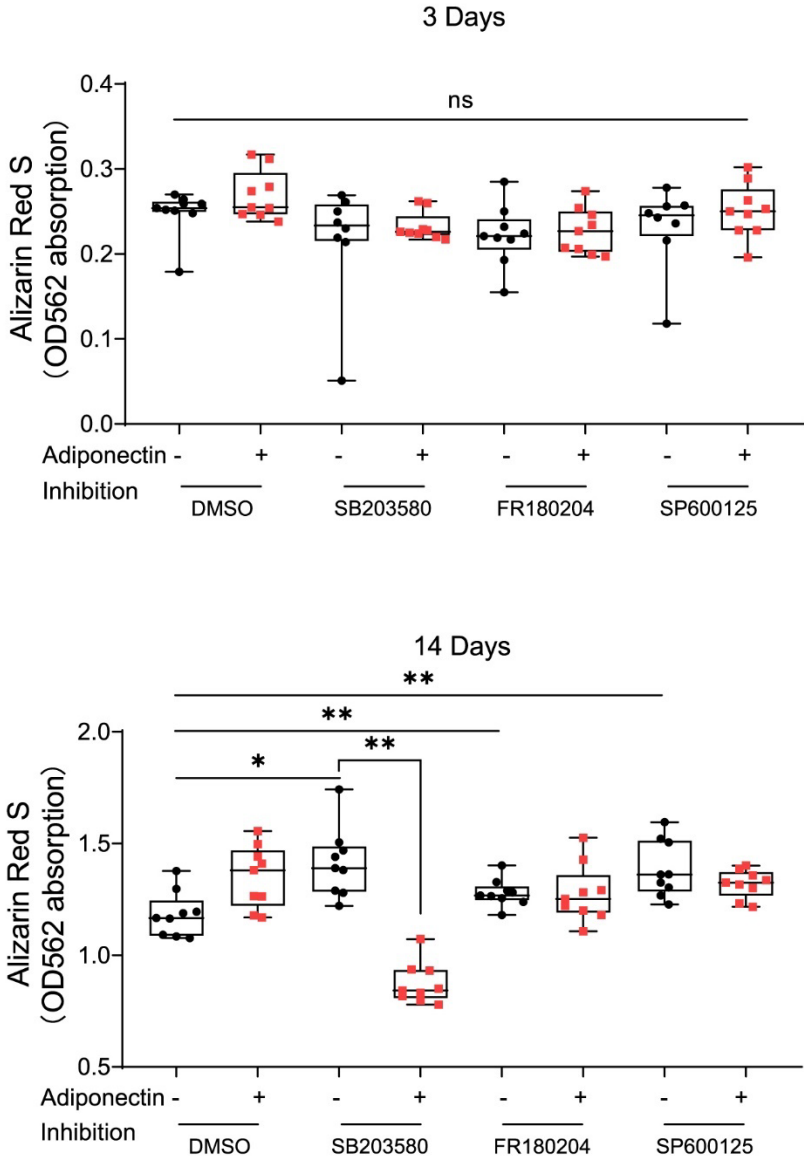

Figure 10. MAPK pathway was involved in adiponectin-induced cell mineralization in cementoblasts.

(A) Cells were treated with MAPK inhibitors in the presence or absence of 100 ng/mL adiponectin for 3 and 14 days, respectively.

(B) Graphic shows the absorbance (OD_{562}) of Alizarin Red S liquefaction after induction of mineralization after 3 and 14 days. The mineralization process did not differ significantly among the groups after 3 days induction. However, after 14 days induction, the MAPK inhibitors promoted the degree of Alizarin Red S staining.

Values are shown as means ± SD. Asterisks indicate significant differences compared to control cells (***$p < 0.001$, **$p < 0.01$, and *$p < 0.05$, ns = not significant).

7.2 Adiponectin and compressive forces regulate *in vitro* β-Catenin expression on cementoblasts via MAPK signaling activation.

7.2.1 Compressive forces up-regulate the expression of AdipoRs.

In order to evaluate the interaction between adiponectin and compressive forces exert *in vitro* on cementoblasts, the gene and protein analysis of AdipoRs expression were performed by cultivating the cells in the presence of exogenous adiponectin and different compressive forces (1.2 gf/cm^2, 2.4 gf/cm^2 and 3.6 gf/cm^2).

The RT-PCR analysis revealed that the addition of adiponectin did not significantly influence AdipoRs mRNA expression ($p > 0.05$), while the application of compressive forces of 2.4 gf/cm^2 or 3.6 gf/cm^2 significantly increased its expression ($*p < 0.05$) (**Figures 11A, B**). Consistent with the RT-PCR results, WB revealed that compression up-regulated the protein expression of AdipoRs at different degrees (**Figure 11A, B**).

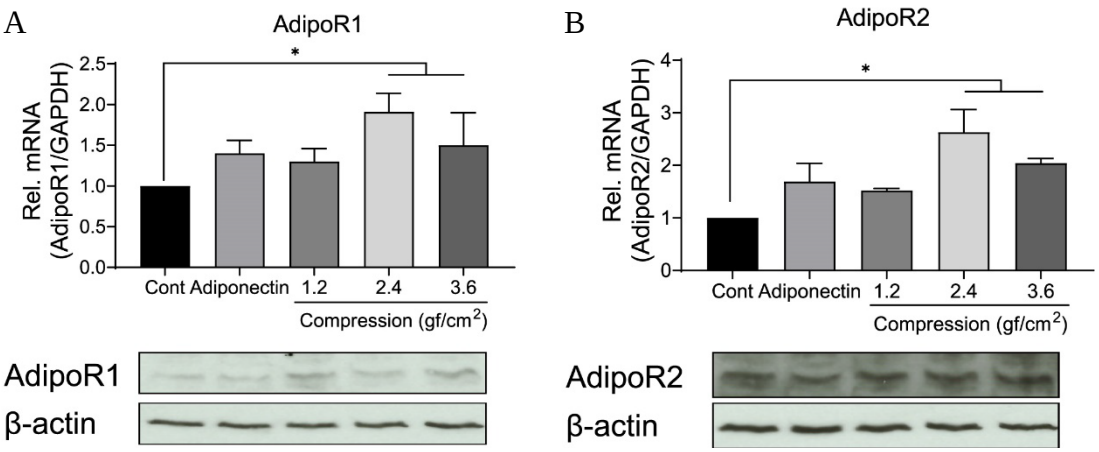

Figure 11. Compression increases the expression of AdipoRs.

(A, B) Representative Western blot showing the expression changes of AdipoR1 (A) and AdipoR2 (B) in the presence of adiponectin (100 ng/mL) or compression (1.2 gf/cm^2, 2.4 gf/cm^2, 3.6 gf/cm^2). RT-PCR and Western blot analysis showed that 2.4 or 3.6 gf/cm^2 compressive forces significantly increased mRNA and protein expression of adiponectin receptors in mouse OCCM-30 cells.

Values are shown as means ± SD. Asterisks indicate significant differences compared to control cells (***$p < 0.001$, **$p < 0.01$, and *$p < 0.05$, ns = not significant).

7.2.2 Adiponectin or compressions up-regulates the expression of MAPKs and β-Catenin.

Furthermore, I analyzed the relative mRNA expression of P38, JNK and ERK after cells were additionally stimulated by adiponectin or compressive forces. RT-PCR results show that the expression of P38α and JNK1 was strongly up-regulated by adiponectin (*p < 0.05) or compression (*p < 0.05) (**Figure 12A**), whereas cells showed slight up-regulation (*p < 0.05) of ERK1 and ERK2 in the presence of adiponectin or compressive forces (**Figure 12B**).

Adiponectin exerted a negative effect on the GSK-3β mRNA expression (*p < 0.05), while it positively upregulated β-Catenin expression (**p < 0.01) after 1 hour of stimulation (**Figure 12C**). Compressive forces alone decreased the mRNA expression of both GSK-3β (3.6 gf/cm^2, *p < 0.05) and increased β-Catenin expression (1.2 gf/cm^2, **p < 0.01; 2.4 gf/cm^2 and 3.6 gf/cm^2, *p < 0.05) (**Figure 12C**).

WB assays show increased protein expression of p-P38, p-ERK1/2 and p-JNK as a reaction to adiponectin or compression (**Figures 12A, B**). These observations prompted me to examine the possibility that adiponectin and compression regulate MAP kinase and β-Catenin on OCCM-30 cells.

A

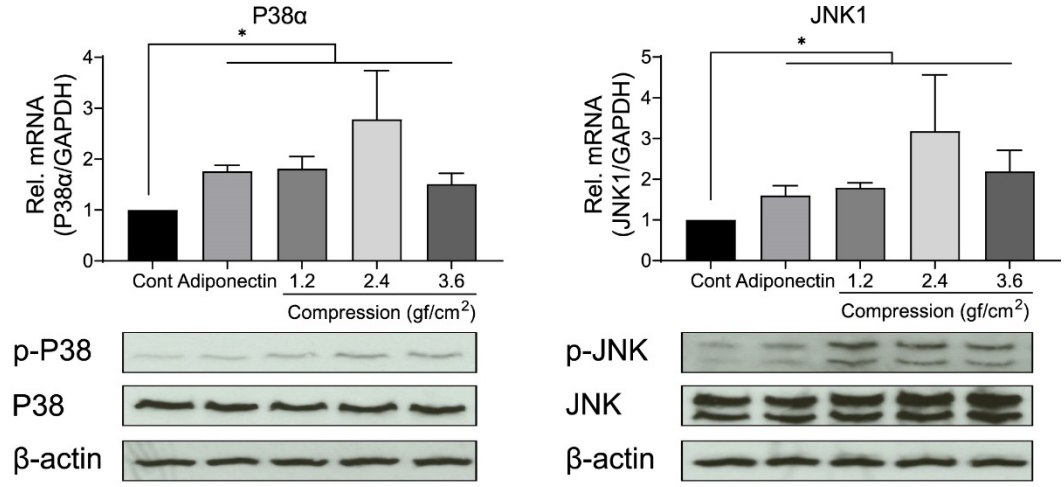

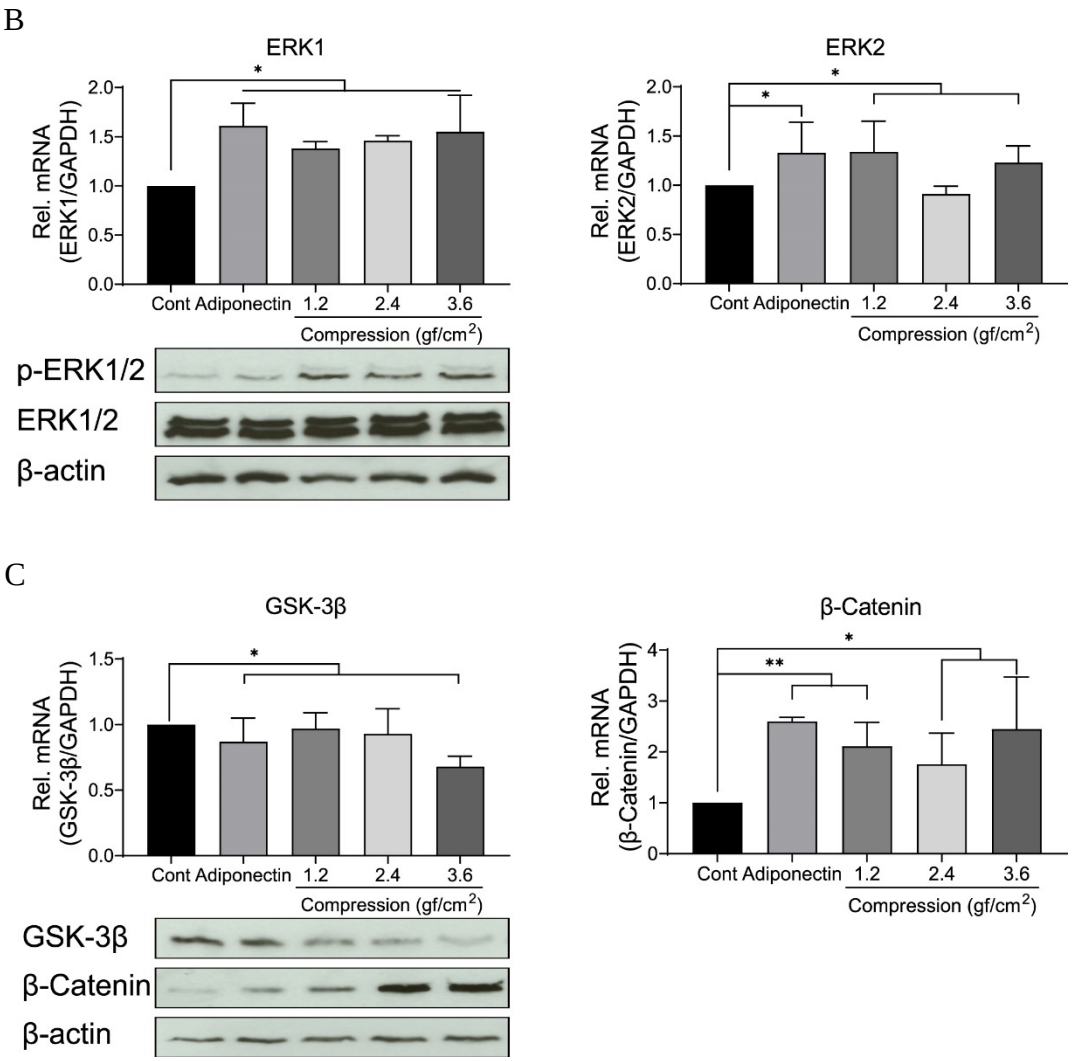

Figure 12. Adiponectin as well as compression regulates the expression MAPK and β-Catenin.

(A-C) Graphics show mRNA expression levels of P38α (A), JNK1 (A), ERK1 (B), ERK2 (B), GSK-3β (C) and β-Catenin (C) after 60 minutes stimulation with adiponectin or compression. Western blot shows the expression of p-P38 (A), p-JNK (A) and p-ERK1/2 (B) induced by adiponectin or compression. The OCCM-30 cells showed down-regulated mRNA expression of GSK-3β when exposed to adiponectin (100 ng/mL) or compression (3.6 gf/cm^2), whereas up-regulated mRNA expression of β-Catenin was demonstrated (**$p < 0.01$). β-Catenin protein expression was increased after stimulation with compression (*$p < 0.05$).

Data is normalized to non-stimulated control and values are expressed as means ± SD. Asterisks indicate significant differences compared to control cells (***$p < 0.001$, **$p < 0.01$, and *$p < 0.05$, ns = not significant).

7.2.3 Adiponectin in combination with compression promotes MAPK signaling activation.

Compressive forces of 2.4 gf/cm^2 alone caused the phosphorylation of P38 and ERK1/2 after 30 minutes of cell exposure, whereas the phosphorylation of JNK occurred 1 hour after stimulation (**Figures 13A, B**).

The co-cultivation of cementoblasts with adiponectin (100 ng/mL) under compressive forces (2.4 gf/cm^2) resulted in an increased and sustained phosphorylation stage of P38, ERK1/2 and JNK. WBs revealed that the phosphorylation of P38 and ERK1/2 was detectable from 0.5 hour to 24 hours, reaching a peaking during 2 - 6 hours stimulation. The phosphorylation of JNK occurred after 4 hours, reaching a peak at 6 hours (**Figures 13C, D**).

Further, I found that adiponectin combined with compressive force enhanced the protein expression of p-P38, p-ERK1/2 and p-JNK on cementoblasts, at different degrees (**Figures 14A, B, C**).

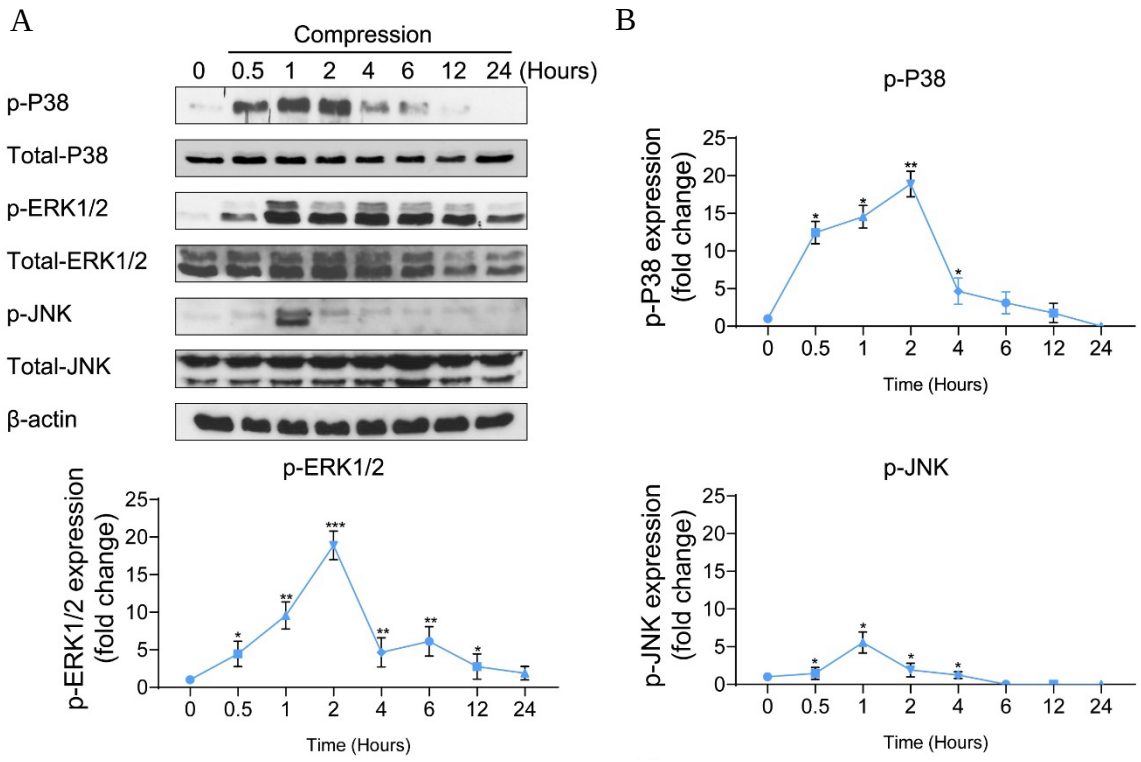

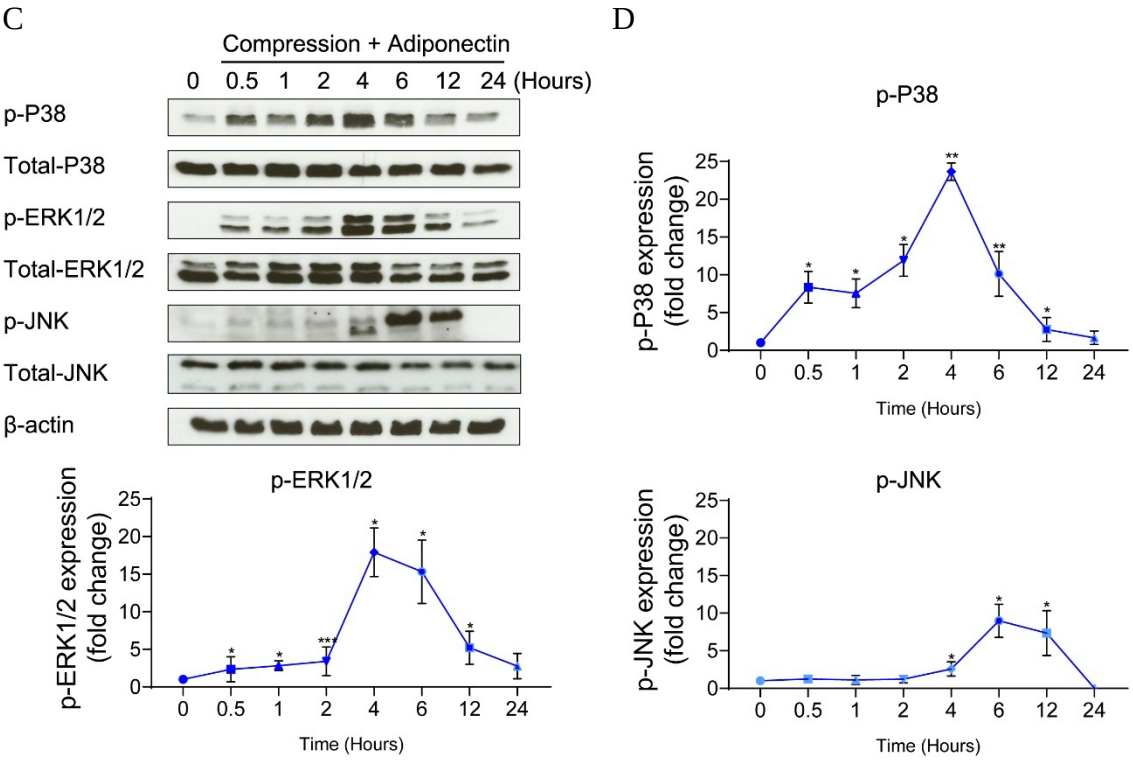

Figure 13. Compression activates the expression of MAPK signaling.

(A, B) Compression promotes P38, ERK1/2 and JNK phosphorylation on OCCM-30 cells. The kinetic protein expression of P38, ERK1/2 and JNK as well as their phosphorylated forms in response to compressive forces of 2.4 gf/cm^2 were analyzed by Western blots, β-actin served as a loading control.

(C, D) After stimulation with 2.4 gf/cm^2 compression and adiponectin (100 ng/mL), phosphorylated forms of P38, ERK1/2 and JNK were up-regulated at different time points. Graphics represent the relative expression values of p-P38, p-ERK1/2 and p-JNK normalized to control cells at time point 0 as protein fold changes, respectively.

Values are shown as means ± SD. Asterisks indicate significant differences compared to control cells (***$p < 0.001$, **$p < 0.01$, and *$p < 0.05$, ns = not significant).

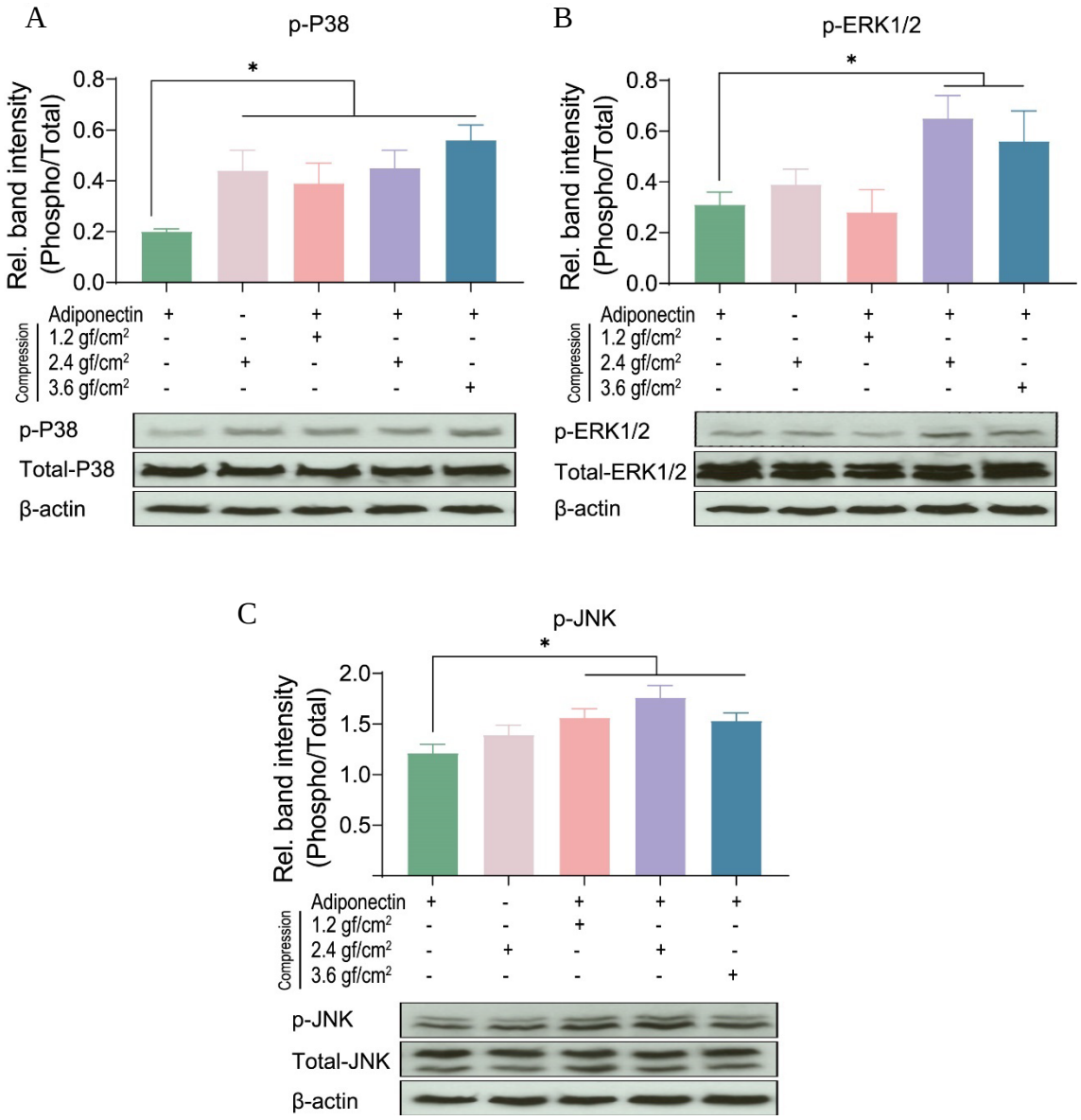

Figure 14. Adiponectin in combination with compression enhances MAPK signaling activation.

(A-C) Western blot shows the expression changes of MAPK protein induced by adiponectin (100 ng/mL), compression (2.4 gf/cm^2) or adiponectin combined with compression (1.2 gf/cm^2, 2.4 gf/cm^2, 3.6 gf/cm^2). The quantification ratio of p-P38, p-ERK1/2 and p-JNK were shown as phosphorylated state unit/total unphosphorylated protein (Phospho/Total).

Values are shown as means ± SD. Asterisks indicate significant differences compared to control cells (***p < 0.001, **p < 0.01, and *p < 0.05, ns = not significant).

7.2.4 The co-stimuli of adiponectin with compressive forces enhances β-Catenin expression on cementoblasts.

IF staining revealed that adiponectin-mediated GSK-3β expression was almost fully

inhibited and β-Catenin showed an increasing expression 30 minutes after stimulation (**Figures 15A, B**).

WB analysis show attenuated activity of GSK-3β phosphorylation and decreased GSK-3β expression in response to adiponectin (100 ng/mL) over a time period from 30 minutes to 3 hours (**Figures 15C, D**). Adiponectin also enhanced β-Catenin phosphorylation after 1-hour stimulation, but increased β-Catenin accumulation concurrently from 5 minutes to 2 hours (**Figures 15C, D**). Surprisingly I found that adiponectin administration caused a constant increase in the β-Catenin expression, over a time frame that was coincident with the acute and transient increase of β-Catenin phosphorylation in OCCM-30 cells (**Figures 15C, D**).

Next, I performed WBs to verify the effect that compressive forces (2.4 gf/cm^2) alone had on the cellular accumulation of β-Catenin. The time-kinetics experiments showed that the activation of β-Catenin protein was transiently increased during 10 minutes to 2 hours during compression expose (**Figures 15E, F**), which indicates that the application of compressive forces initially promotes WNT-independent accumulation of β-Catenin in OCCM-30 cell cultures.

Additionally, it was observed that adiponectin (100 ng/mL) in combination with compressive forces (2.4 gf/cm^2) upregulated the expression of dephosphorylated β-Catenin 10 minutes after exposure. This effect was sustained over a period of three hours (**Figures 15G, H**).

Furthermore, OCCM-30 cultivated with adiponectin and compression showed a decreasing expression of GSK-3β and increasing expression of β-Catenin (**Figures 16B, D**).

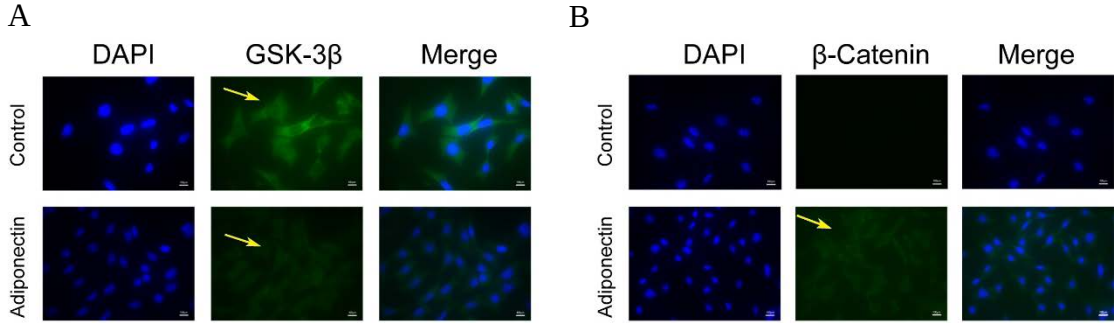

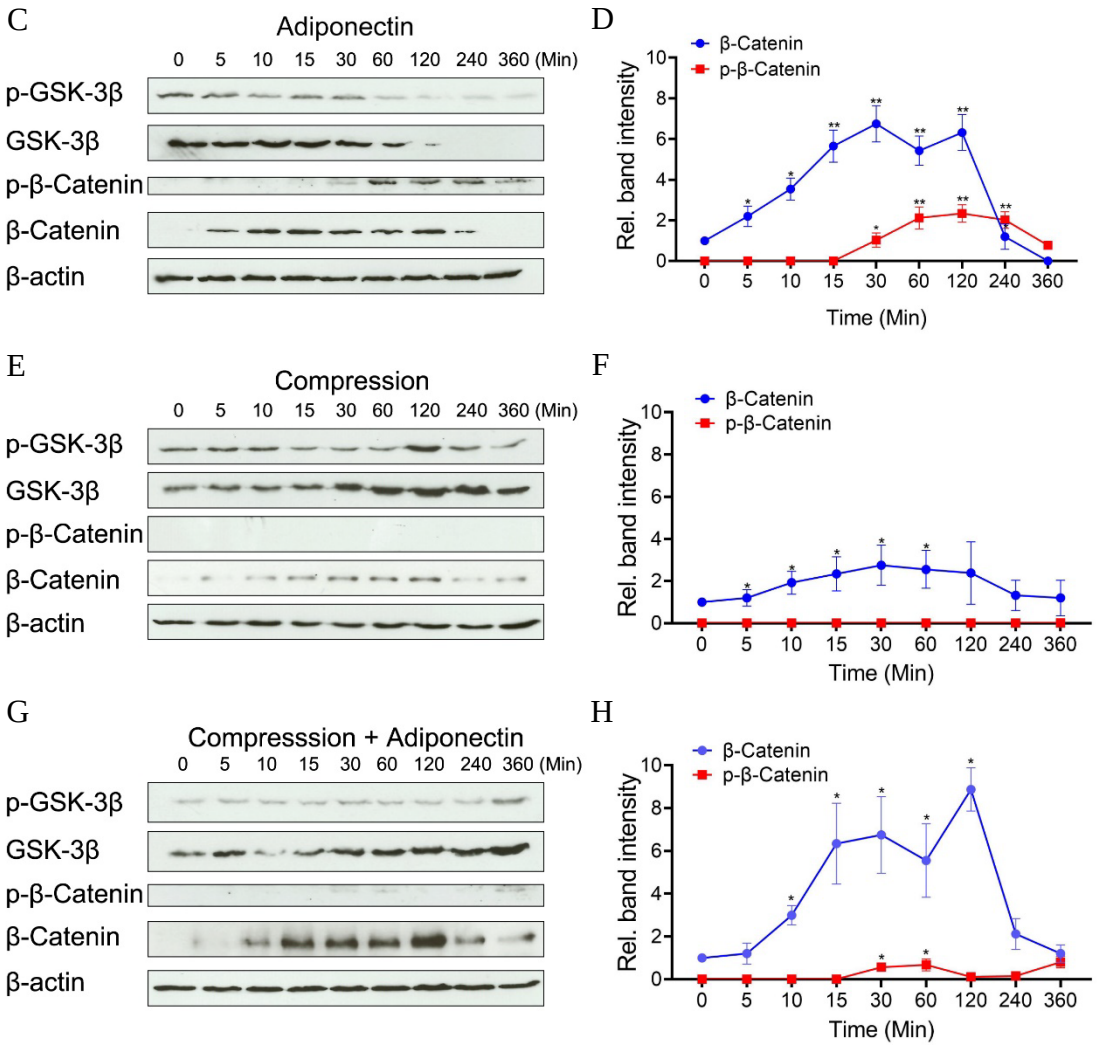

Figure 15. Compression and/or adiponectin regulates β-Catenin expression on cementoblasts.

(A, B) IF staining showed that adiponectin (100 ng/mL) induced decreased expression of cytoplasmic GSK-3β in OCCM-30 cells and the cellular β-Catenin expression was increased after addition of adiponectin (100 ng/mL).

(C, D) Western blots indicate that after addition of adiponectin (100 ng/mL) to OCCM-30 cells, phosphorylated and total GSK-3β protein expression decreased after one hour, whereas the expression of total β-Catenin increased from 5 minutes to 2 hours due to adipokine stimulation.

(E, F) Compressive forces exert a dual effect on OCCM-30 cells. The expression of GSK-3β was increased as well as the levels of total β-Catenin. Western blots indicate that the expression of phosphorylated and total GSK-3β as well as total β-Catenin is increased after exposure to 2.4 gf/cm^2 compression for 0 - 6 hours.

(G, H) Compression in combination with adiponectin (100 ng/mL) enhanced the expression of β-Catenin: The kinetic analysis performed on OCCM-30 cells cultivated under 2.4 gf/cm^2 compression combined with adiponectin (100 ng/mL) showed that total β-Catenin was significantly up-regulated after 10 minutes stimulation over a period of 4 hours.

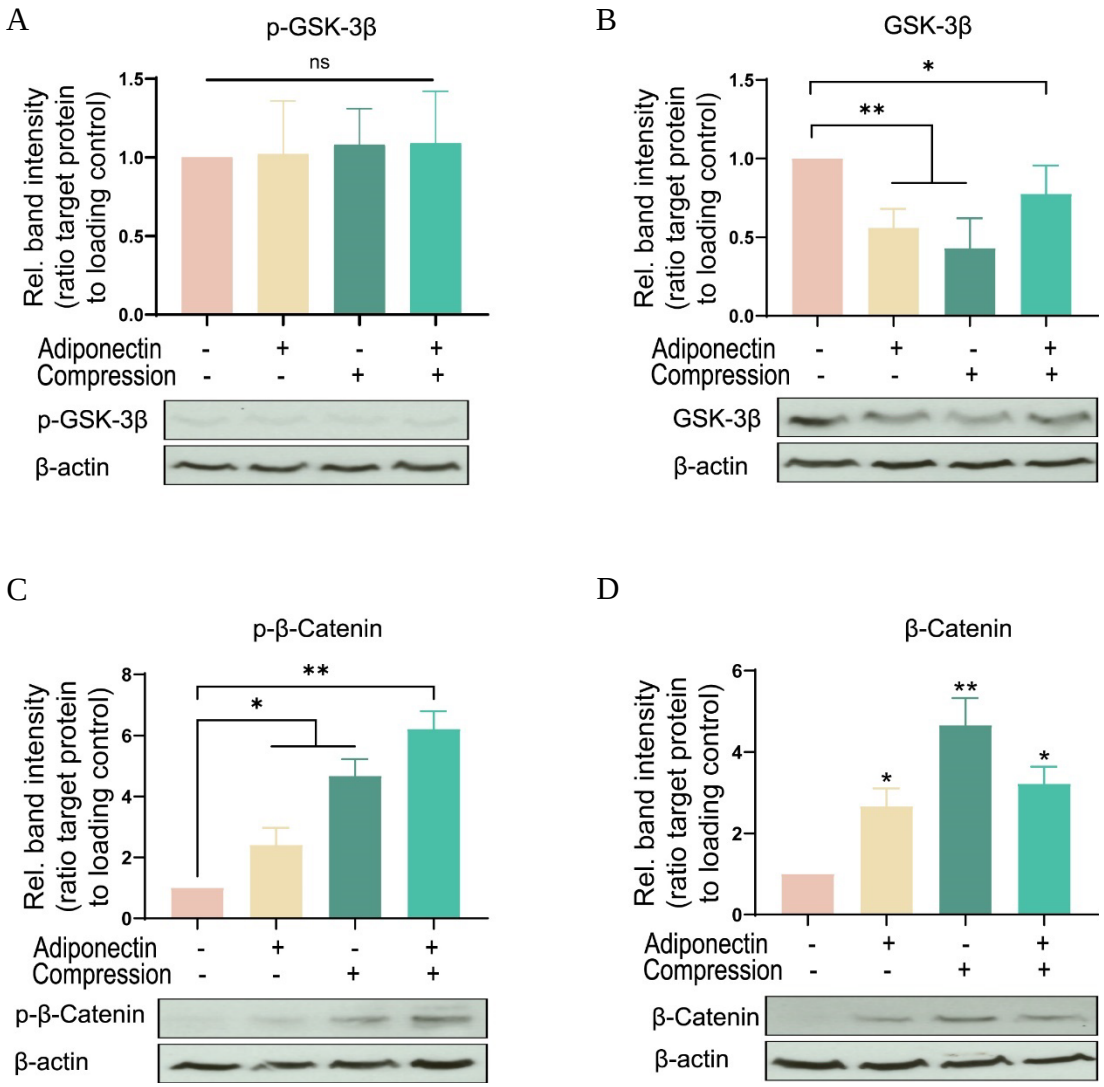

Figure 16. Co-stimulation of adiponectin with compression enhance β-Catenin expression on cementoblasts.

(A-D) Representative Western blot showing the expression changes of GSK-3β and β-Catenin induced by adiponectin (100 ng/mL) in the presence or absence of compression (2.4 gf/cm^2). Graphic represents the protein intensity which was quantified as ratio to loading control to show the protein expression of p-GSK-3β (A), GSK-3β (B), p-β-Catenin (C) and β-Catenin (D).

Values are shown as means ± SD. Asterisks indicate significant differences compared to control cells (***p < 0.001, **p < 0.01, and *p < 0.05, ns = not significant).

7.2.5 Blockade of MAPKs alter the adiponectin- and compression-induced activation of β-Catenin on OCCM-30 cells.

Then, I examined if adiponectin-mediated MAPK signaling activation may cross react with GSK-3β or β-Catenin activity.

In the absence of exogenous adiponectin, the blockade of ERK1/2 caused the total GSK-

3β expression to decrease significantly, whereas by co-stimulation with adiponectin (100 ng/mL) this effect was reversed (**Figure 17A**). In the presence of adiponectin, blockade of P38 and JNK decreased the total GSK-3β expression (**Figure 17A**), indicating that adiponectin modulates GSK-3β via P38 and JNK signaling. The expression of total β-Catenin was down-regulated in the presence of P38 or ERK1/2 inhibitor, but rescued by adiponectin (100 ng/mL) addition, which suggests that P38, ERK1/2 and JNK modulate GSK-3β and in turn subsequent cellular events such as the cytoplasmic accumulation of β-Catenin (**Figures 17A, B**).

In order to investigate if the MAPK pathway influences β-Catenin signaling during compression, the cells were cultivated under compressive forces of 2.4 gf/cm² during 60 minutes. Afterwards, I examined by means of WB the expression of GSK-3β and β-Catenin. The results showed that the suppression of MAPK pathway has a significant blocking effect on β-Catenin expression. This effect was restored when cells were exposed to compression for 1-hour stimulation (**Figures 17C, D**). In contrast, MAPK inhibition facilitated GSK-3β expression at varying degrees. These effects were reversed by the application of compressive forces (**Figures 17C, D**).

Furthermore, to determine if activation of P38, ERK1/2 and JNK is involved in the stimulation of β-Catenin by adiponectin or compression, the cells were preincubated with the pharmacological MAPK inhibitors SB203580 (P38), FR180204 (ERK1/2), SP600125 (JNK) for 1-hour and then cultivated under compressive forces of 2.4 gf/cm² and co-stimulated with adiponectin (100 ng/mL) for another 1 hour.

As result it was observed that ERK1/2 inhibition as well as JNK inhibition in combination with compression inhibited GSK-3β expression, whereas the total GSK-3β expression was promoted in the group treated with P38 inhibitor in the presence of compression and adiponectin (**Figures 17E, F**). The total expression of β-Catenin was slightly reduced in all groups treated with MAPK inhibitors and compression in the presence or absence of adiponectin in comparison to controls (**Figures 17E, F**), indicating that adiponectin modulates compression-induced GSK-3β and β-Catenin expression partly throughout P38 MAPK signaling.

A

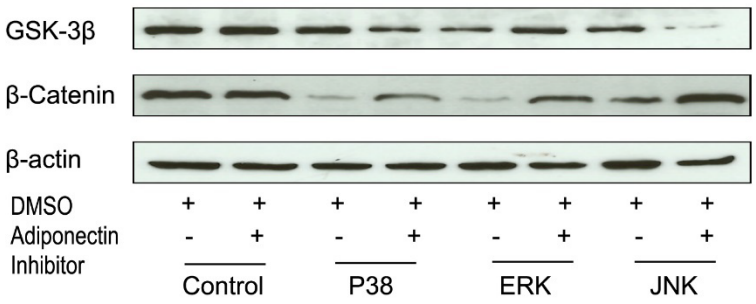
GSK-3β
β-Catenin
β-actin
DMSO
Adiponectin
Inhibitor
Control
P38
ERK
JNK

B

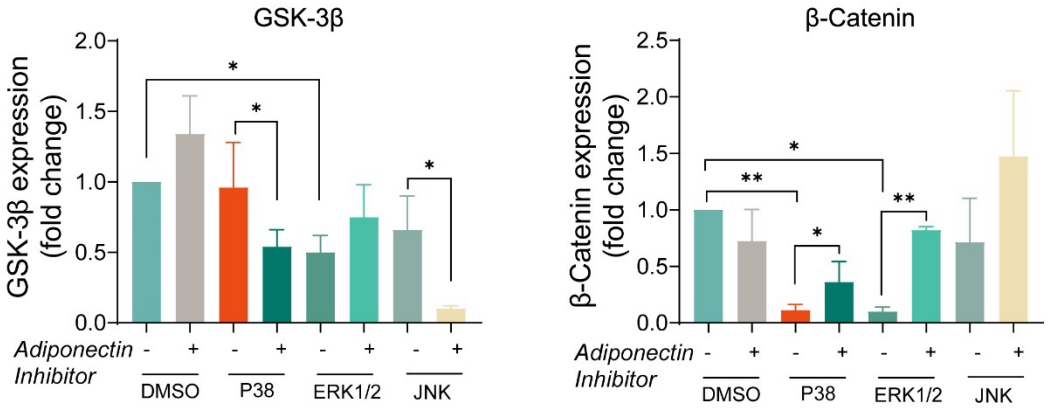
GSK-3β
GSK-3β expression (fold change)
Adiponectin
Inhibitor
DMSO
P38
ERK1/2
JNK
β-Catenin
β-Catenin expression (fold change)

C

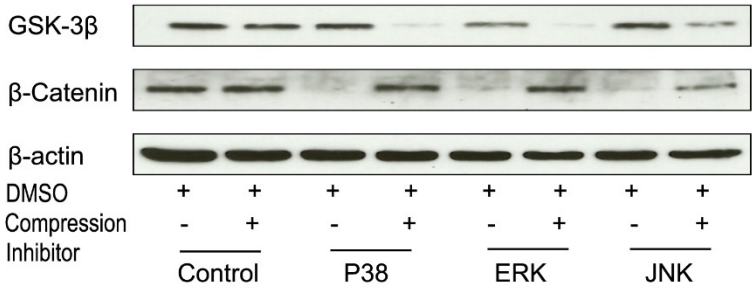
GSK-3β
β-Catenin
β-actin
DMSO
Compression
Inhibitor
Control
P38
ERK
JNK

D

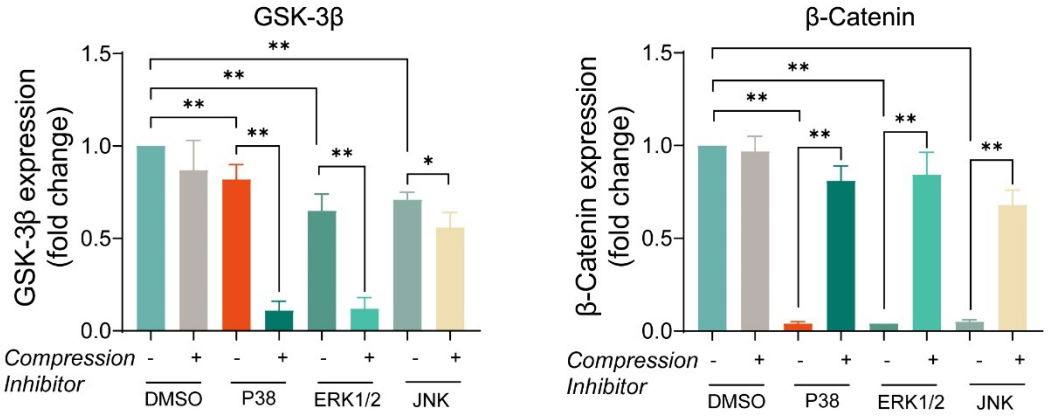
GSK-3β
GSK-3β expression (fold change)
Compression
Inhibitor
DMSO
P38
ERK1/2
JNK
β-Catenin
β-Catenin expression (fold change)

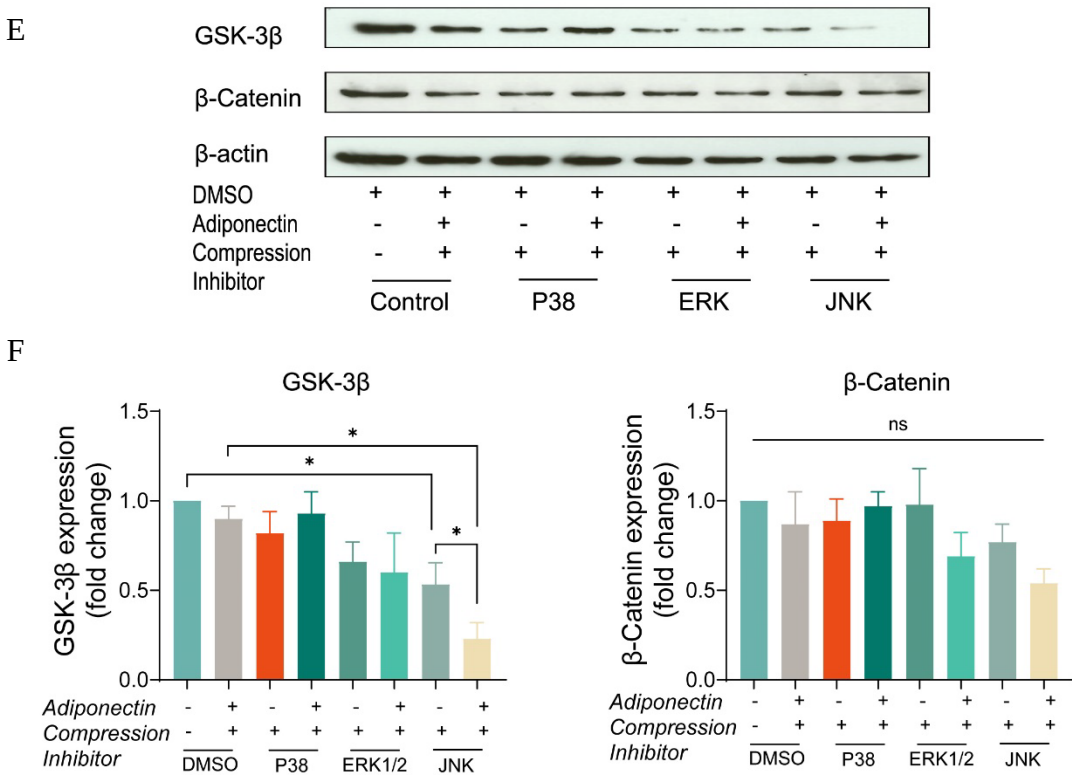

Figure 17. MAPK inhibition blocks β-Catenin, whereas adiponectin/compression addition effectively rescues its expression.

(A, B) Western blot indicated that GSK-3β expression was influenced by MAPK inhibitors for 1 hour after adiponectin addition: SB203580 (P38) and SP600125 (JNK) inhibitors addition to OCCM-30 cells up-regulated GSK-3β protein expression. The expression of β-Catenin was reduced after P38 and ERK1/2 inhibition. The suppressed β-Catenin signaling could be rescued by adiponectin in different degrees.

(C, D) Compressive forces of 2.4 gf/cm^2 induced decreased expression of total GSK-3β protein in cells pretreated with SB203580 (P38), SP600125 (JNK) and FR180204 (ERK1/2) inhibitors and increased expression of cellular β-Catenin. Single suppression of P38, ERK and JNK blocked the β-Catenin expression but this effect was reversed by compression stimulation.

(E, F) The negative effect that ERK1/2 and JNK inhibition exerted on the expression of total GSK-3β protein on OCCM-30 cells upon compression was not altered by additional adiponectin co-stimulation for 1 hour. P38 inhibitor combined with compression decreased the GSK-3β expression. This effect was enhanced by addition of adiponectin. The expression of β-Catenin was not significantly modified in the presence of MAPK inhibitors and compression despite adiponectin.

Graphics show the variations of GSK-3β and β-Catenin protein expression as fold change when cells were exposed to MAPK inhibitors in cells cultivated under compressive forces (2.4 gf/cm^2) and/or adiponectin (100 ng/mL) compared to controls. Values are shown as means ± SD. Asterisks indicate significant differences compared to control cells (***$p < 0.001$, **$p < 0.01$, and *$p < 0.05$, ns = not significant).

7.2.6 Adiponectin/AdipoRs/P38α/JNK1 regulates TCF/LEF transcription.

I then tested the effects of knocking down of AdipoR1, AdipoR2, P38α, ERK1, ERK2 and JNK1 on adiponectin-stimulated TCF/LEF-sensitive transcription in cementoblasts (**Figures 18A, B**). Consistent with the effect on β-Catenin accumulation, silencing JNK1 and P38α attenuated the TCF/LEF reporter transcription (**Figures 18A, B**). The effect of silencing RNA targeting AdipoR1 and AdipoR2 results in a slight inhibition of TCF/LEF transcription, indicating the involvement of adiponectin receptors in this process (**Figures 18A, B**).

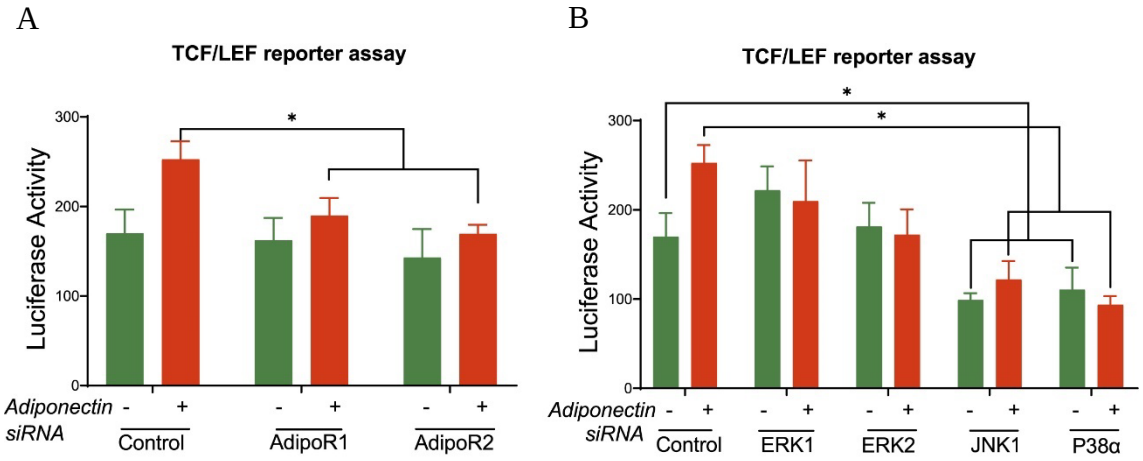

Figure 18. AdipoRs, P38α, JNK1, ERK1 and ERK2 are involved in the TCF/LEF transcription.

(A, B) OCCM-30 transfected with siRNA (AdipoR1, AdipoR2, P38α, JNK1, ERK1 and ERK2) as well as TCF/LEF luciferase reporter vector were subsequently treated with adiponectin for 1 hour.

Values are shown as means ± SD. Asterisks indicate significant differences compared to control cells (***$p < 0.001$, **$p < 0.01$, and *$p < 0.05$, ns = not significant).

7.2.7 Adiponectin modulates GSK-3β and β-Catenin by AdipoR1 commitment. P38α and JNK1 triggers β-Catenin activation in response to adiponectin addition.

To define the individual contribution of the adiponectin receptors as well as the MAPK isoforms stimulated with adiponectin on β-Catenin regulation, I silenced the mRNA expression of AdipoR1, AdipoR2, ERK1 (MAPK3), ERK2 (MAPK1), JNK1 (MAPK8) and P38α (MAPK14) using siRNA transfection. The efficacy of the gene knock-down by siRNA transfections was analyzed by qRT-PCR. After a transfection period of 48 hours,

I could observe effective down-regulation of the target genes (**Figures 19A, B**).

Next, the cells were stimulated with adiponectin (100 ng/mL) and I observed that the group treated with siRNA against AdipoR2 showed significant increases of GSK-3β (*p < 0.05) and β-Catenin mRNA levels (*p < 0.05), whereas mock treatment did not alter either GSK-3β or β-Catenin mRNA levels significantly. Conversely, the group treated with siRNA against AdipoR1 did not show significant differences in the expression of GSK-3β or β-Catenin (**Figure 20A**).

After 48 hours incubation with siRNA against ERK1, ERK2, JNK1 and P38α mRNA or mock treatment in the presence or absence of adiponectin, RT-PCR was performed to analyze GSK-3β or β-Catenin mRNA expression. Adiponectin treatment in JNK1 and P38α siRNA groups down-regulated the GSK-3β mRNA expression. The silencing of ERK2 but not of ERK1 caused GSK-3β mRNA upregulation after adiponectin addition (**p < 0.01). The knockdown of JNK1 or P38α alone resulted in the reduction of β-Catenin mRNA expression. This downregulation was reversed after adiponectin addition (100 ng/mL) (**Figure 20B**).

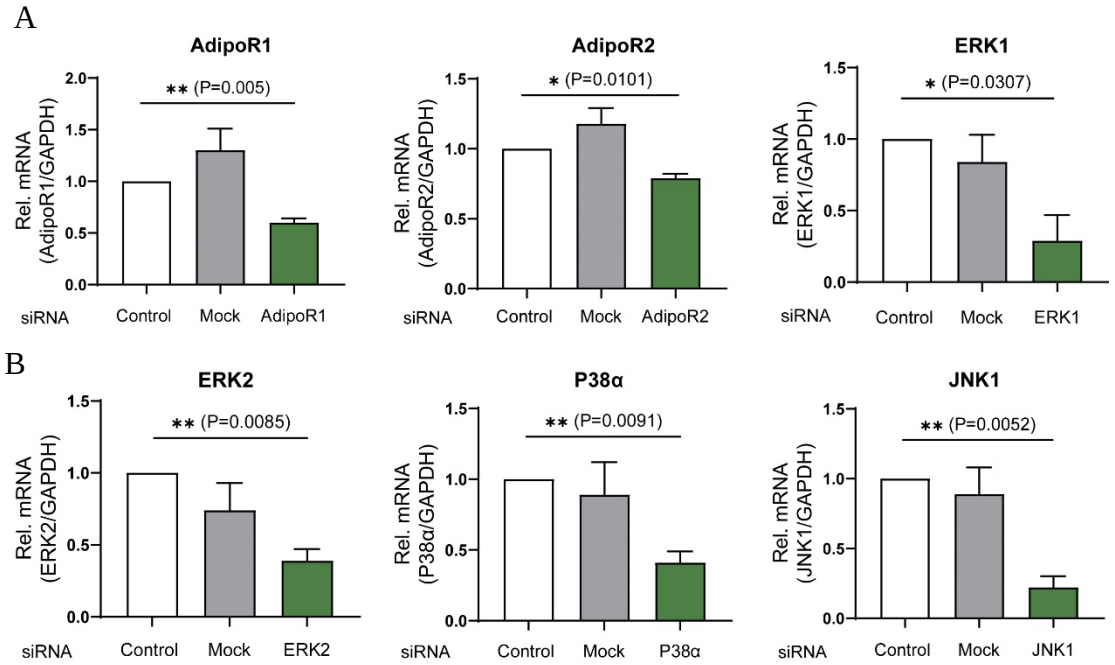

Figure 19. The efficacy of siRNA transfections.

(A, B) Values are shown as means ± SD. Asterisks indicate statistical significance (***p < 0.001, **p < 0.01, and *p < 0.05, ns = not significant).

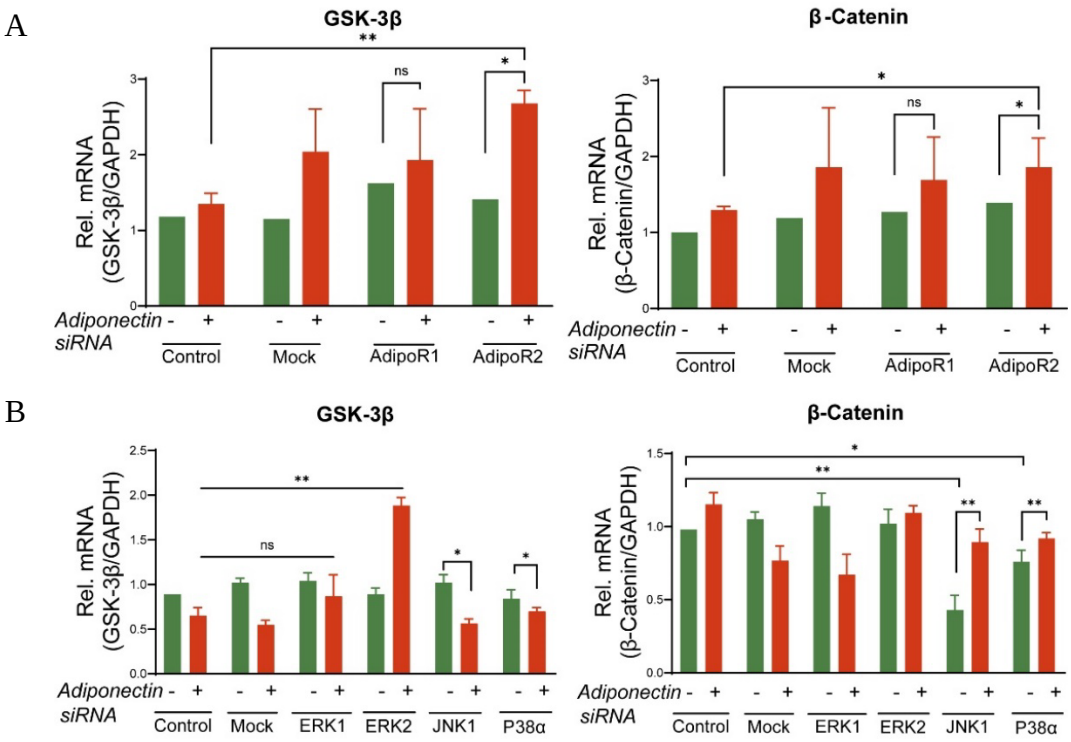

Figure 20. AdipoR1/P38α/JNK1 participate in the regulation of GSK-3β and β-Catenin expression.

(A) Single knocking down of AdipoR2 in the presence of adiponectin induced up-regulation of GSK-3β gene expression and significantly increased β-Catenin expression (*p < 0.05).

(B) The silencing of ERK2 alone causes increased gene expression of GSK-3β after adiponectin treatment (**p < 0.01). Silencing of P38α and JNK1 slightly up-regulated GSK-3β gene expression. After addition of adiponectin, its expression was significantly down-regulated (*p < 0.05). Suppression of P38α or JNK1 alone significantly decreased β-Catenin expression (**p < 0.01 and *p < 0.05, respectively). This effect was reversed after adiponectin addition in both groups.

Values are shown as means ± SD. Asterisks indicate significant differences compared to control cells (***p < 0.001, **p < 0.01, and *p < 0.05, ns = not significant).

7.2.8 Adiponectin/AdipoR1/P38α pathways are involved in the modulation of cementogenesis-related marker expression on cementoblasts.

After cementogenesis induction, knockdown of AdipoR1 or AdipoR2 decreased OCN and OPG mRNA expression at varying degrees (*p < 0.05) (**Figures 21A, B**). In the presence of adiponectin, the silencing of P38α alone, but not that of ERK1, ERK2 or JNK1 significantly decreased OCN and OPG expression (**Figures 21A, B**). The results indicate that the adiponectin/AdipoR1/P38α cascade is particularly involved in adiponectin induced cementogenesis (**p < 0.01) (**Figure 22**).

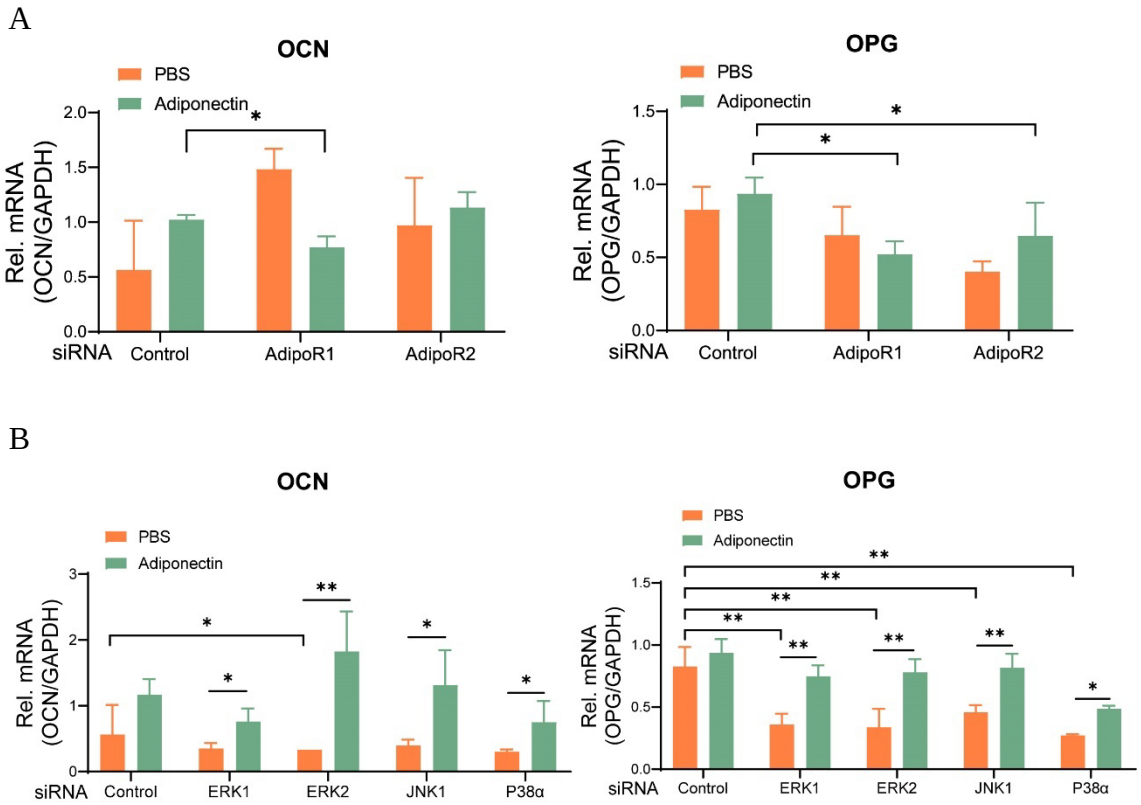

Figure 21. Adiponectin/AdipoR1/P38α cascade is particularly involved in adiponectin-induced cementogenesis marker expression.

(A, B) Knocking down of AdipoR1 or AdipoR2 alone did not down-regulate OCN (*p < 0.05) and OPG (**p < 0.01) mRNA expression. The silencing of P38α alone induced a significant downregulation of OCN (*p < 0.05) and OPG gene expression upon stimulation with adiponectin (100 ng/mL) (**p < 0.01). These effects were not observed after suppression of ERK1, ERK2 and JNK1 alone.

Values are shown as means ± SD. Asterisks indicate significant differences compared to control cells (***p < 0.001, **p < 0.01, and *p < 0.05, ns = not significant).

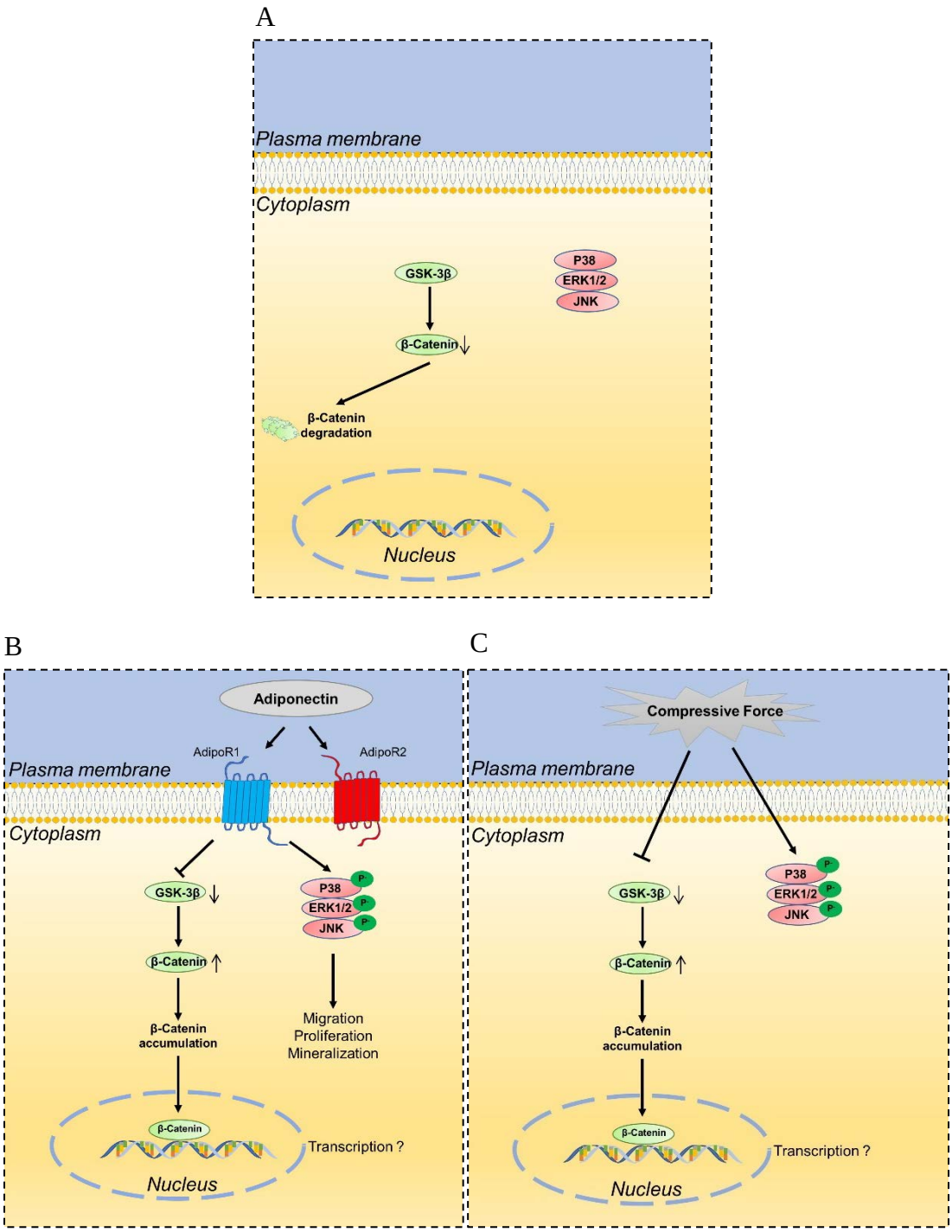
A
Plasma membrane
Cytoplasm
GSK-3β
P38
ERK1/2
JNK
β-Catenin
β-Catenin degradation
Nucleus
B
Adiponectin
AdipoR1
AdipoR2
Plasma membrane
Cytoplasm
GSK-3β
P38
ERK1/2
JNK
β-Catenin
β-Catenin accumulation
Migration
Proliferation
Mineralization
β-Catenin
Transcription ?
Nucleus
C
Compressive Force
Plasma membrane
Cytoplasm
GSK-3β
P38
ERK1/2
JNK
β-Catenin
β-Catenin accumulation
β-Catenin
Transcription ?
Nucleus

D E

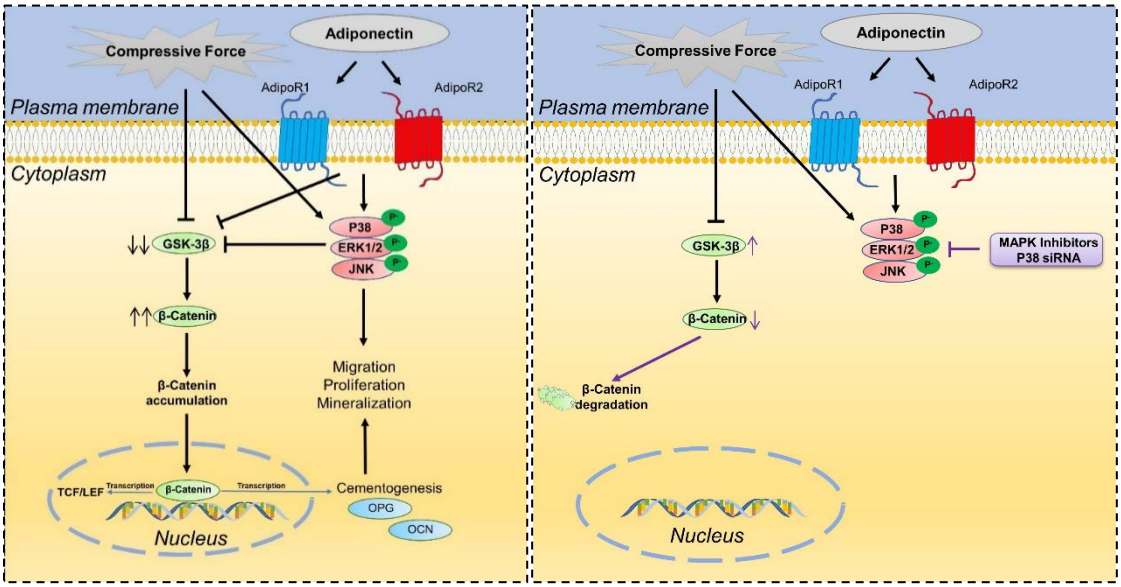

Figure 22. Scheme

(A-E) Schemic representation of the role of adiponectin (B), compressive force (C) and their combination (D) in the activation of MAPK signaling pathways and β-Catenin in OCCM-30 cementoblasts. The negative control (A) refers to non-stimulation of OCCM-30 cells. (E) Proposed molecular interactions between MAPK signaling pathways and β-Catenin on OCCM-30 cementoblasts cultivated with MAPK chemical inhibitors or siRNA. The arrow symbols represent the activation (←) or inhibition (⊢—) of the signaling pathways.

8. Discussion

In the present study, I demonstrated that OCCM-30 cementoblasts express adiponectin receptors and that their activation facilitates cell migration, proliferation and mineralization. These effects are partially orchestrated via activation of the MAPK signaling pathway. Moreover, adiponectin in combination with compressive forces enhance the activation of MAPK and β-Catenin pathways in cementoblasts. Through a cross link mechanism, compression as well as adiponectin induce β-Catenin accumulation in OCCM-30 cells by MAPK pathway commitment principally via AdipoR1. This effect involves multiple mediators including JNK1 and P38α that are key players in this process. Such deeper insights into the mechanisms underlying the OIIRR in response to compressive force may provide the clinician with important clues on potential prevention strategy and improve the orthodontic treatment strategy of obese patients.

In recent decades, clinical trials have reported that the normal salivary adiponectin levels are around 10.92 (3.22 - 28.71) ng/mL and the normal serum adiponectin levels are around 12.27 (8.15 - 14.70) μg/mL [89]. These values drastically decrease in case of obesity [49]. Moreover, reduced levels of adiponectin and AdipoRs are also detectable in patients with severe periodontitis compared to healthy subjects, a fact that suggests impaired adiponectin function to be associated with disease severity [19, 54]. In my experiments, I focused on the effects normal salivary adiponectin levels (20 ng/mL) and increased adiponectin concentrations exert *in vitro* on OCCM-30 cementoblasts.

8.1 Increased migration, proliferation and mineralization with higher concentration of adiponectin addition.

Several reports have revealed that adiponectin exerts favorable effects *in vitro* on the proliferation of human osteoblasts via the MAPK signaling pathway [90-92]. In the present study, I observed over a period of 24 hours, that the number of viable cementoblasts was significantly increased in presence of higher concentrations of adiponectin compared to unstimulated cells. Similar results were also obtained by Berner

et al. (2004) showing that supplementation of cell culture medium with recombinant adiponectin enhances the proliferation of murine osteoblasts [91]. In contrast to the study performed by Kanazawa et al. (2007) which reported that even low concentrations of adiponectin stimulate the proliferation of the MC3T3-E1 osteoblast cell line [92], I observed that lower concentrations of adiponectin did not significantly stimulate cementoblast proliferation.

Recent studies suggest that adiponectin enhances bone mineral density *in viv*o and osteogenesis *in vitro* [90, 93]. I could observe that adiponectin strongly promotes mineralization in OCCM-30 cells. The findings described in this thesis that upregulation of cementogenesis occurs in response to stimulation with higher adiponectin concentrations appear especially meaningful since the lower adiponectin levels in obese patients may be one of the critical factors for increased OIIRR and less repair during OTM. The present results provide first evidence that adiponectin increases mineralization in the cementogenesis process of cementoblasts. In concordance with these results, Wang et al. (2017) demonstrated the osteogenic capacity of adiponectin *in vitro* using rat mesenchymal stem cells [94]. Another study showed that adiponectin enhanced the mineralization of osteoblasts [93]. Iwayama et al. (2012) also observed that adiponectin promotes AP and Runx-2 mRNA expression as well as up-regulates the AP enzymatic activity of HPDL cells [95]. However, in the latter study, extremely high concentrations (5 to 10 μg/mL) of adiponectin were used to observe these effects [95]. In the present experiment, I used ranges of adiponectin concentrations of up to 100 ng/mL, demonstrating that murine cementoblasts require lower concentrations of this adipokine to achieve the same results. However, these concentrations still exceed the biologic concentrations of adiponectin in saliva or in crevicular fluid [89].

8.2 Adiponectin facilitates cementogenesis-related gene expression in cementoblasts.

Treatment of OCCM-30 cells with adiponectin for 14 days induced increased mineralization. To further examine the kinetic effect of adiponectin in cementoblasts, the cementogenesis-related markers were checked.

It was demonstrated, that the gene expression of Runx-2, an essential transcription factor for osteoblast differentiation, mineralization and migration [96, 97] as well as for cementogenesis [98], was strongly up-regulated in OCCM-30 cells in response to high concentrations of adiponectin. Adiponectin-induced Runx-2 upregulation in cementoblasts may occur in the course of wound healing and cementum repair and regeneration, since Runx-2 exerts a regulatory role in cementum formation [99]. F-Spondin, a cementoblast specific gene that orchestrates cementoblast differentiation [61], was also up-regulated by adiponectin.

Likewise, the OCCM-30 cells presented up-regulated mRNA expression of AP, BSP, OCN and OPG after adipokine stimulation. Our *in vitro* results are consistent with previous data supporting the fact that adiponectin can enhance the osteogenic differentiation of osteoblasts [100] as well as promote osteoblastogenesis of HPDL cells [95]. Alkaline phosphatase (AP) is essential for cementoblast [98] function and is up-regulated during cementogenesis, thus, it is generally considered as an early marker for cementoblasts [101]. It is well known that AP regulates the formation of cementum and is involved more in the formation of acellular than cellular cementum [60]. Here I could observe that adiponectin strongly increases mRNA expression of AP as well as AP enzymatic activity in cementoblasts. Bone sialoprotein (BSP, or integrin binding sialoprotein) is found to be present in both acellular and cellular cementum [102]. It is strongly expressed by cementoblasts. It was suggested that this protein might contribute to cementum formation and mineralization [103]. Foster et al. (2013) suggested that BSP is essential for acellular cementum formation and likely to be involved in the initiating of mineralization on the root surface [104]. Osteocalcin (OCN) is a non-collagenous protein that plays a regulatory role during the mineralization process [105, 106]. Its expression is restricted to cells with mineralizing capacity, including osteoblasts, odontoblasts as well as cementoblasts [107, 108]. In my results, the up-regulation of BSP and OCN after adiponectin stimulation clearly indicates that this adipokine favorably induces cementogenesis. Thus, adiponectin could enhance the cementogenesis process and it could promote cementum mineralization

8.3 Activation of MAPK signaling pathways in adiponectin treated cementoblasts.

The present results indicate that in OCCM-30 cells, adiponectin addition induces activation of ERK1/2, JNK and P38 MAPK pathways. Moreover, the data show that activation of MAPK pathway is essential for adiponectin-stimulated OCCM-30 proliferation and migration as these effects were partially counteracted upon application of SB203580, FR180204 and SP600125, three highly selective inhibitors of the MAP kinase cascade. These results are in accordance with previous studies showing that long-term inhibition of the MAPK signaling pathway promotes early mineralization as well as the increase of AP activity in preosteoblastic cells [109].

Several *in vitro* studies have shown that adiponectin plays a role as regulator of the MAP kinase pathways in cell homeostasis [90, 110, 111]. I have shown that MAPK signaling is partially involved in the homeostasis regulation of adiponectin on cementoblasts. The results are congruent with several other studies that were performed with different cell lines. For example, Miyazaki et al. (2005) showed that adiponectin activates the P38 and JNK pathways in myocytes [110]. In osteoarthritis, adiponectin induces P38-MAPK to promote osteophyte formation [111]. Interesting, Luo et al. (2005) showed that adiponectin can activate P38 and JNK but not ERK1/2 on primary osteoblasts and that suppression of AdipoR1 abolished adiponectin induced cell proliferation, suggesting that cell proliferation is regulated by AdipoR/JNK signaling whereas differentiation is mediated via the AdipoR/P38 cascade [90]. On the contrary, Kono et al. (2007) noted that activation of ERK pathways strongly down-regulate the matrix mineralization of osteoblasts, while its suppression promoted the process [112]. This is in agreement with the interesting observation from my work that inhibition of P38 and ERK1/2 significantly enhances the mineralization rate of cementoblasts. This effect could partially be counteracted by adiponectin addition.

However, very few studies have investigated the association between adiponectin and the Catenin signaling pathway, one of the most important pathways in osteogenesis, with respect to the regulation of bone formation.

8.4 Co-stimulation of adiponectin combined with compression regulates the MAPK and β-Catenin signaling in OCCM-30 cells.

Wang et al. (2017) reported *in vivo* and *in vitro* that adiponectin could facilitate bone mesenchymal stem cell (BMSC) osteogenic differentiation and osteogenesis by the WNT/β-Catenin pathway [94]. I observed that adiponectin may interact with cementoblasts and influence their biological response to compressive forces promoting the expression of p-P38, p-ERK1/2 and p-JNK. Interestingly, I further observed a longer up-regulation period of p-P38 and p-ERK1/2 by co-stimulation of adiponectin combined with compression, while the expression levels of p-JNK altered after co-stimulation and reached an expression peak later. This indicates that compressive forces additionally trigger the MAP kinase pathway.

In the current study, it was also verified that compression forces activate β-Catenin signaling in OCCM-30 cells. This finding is in accordance with the results of Shuqin et al. (2015) describing that the effect of mechanical forces on OCCM-30 cells regulate β-Catenin expression [113]. Recently, Sindhavajiva et al. (2018) showed that compression induces human mandibular-derived osteoblast differentiation via WNT/β-Catenin signaling [76]. However, Korb et al. (2016) demonstrated the compression induced apoptosis of human primary cementoblasts by upregulation of the pro-apoptotic gene AXUD1 via a JNK-dependent pathway [114]. The present study showed that the inhibition of β-Catenin due to MAPK inhibition was restored by the application of compressive forces on cementoblasts. Based on this observation, the current study reveals a novel finding that MAPK activation is the bridge factor between compression application and β-Catenin signaling activation. The proposed scheme (**Figure 22**) depicts the relation between MAPK and β-Catenin signaling when non-stimulated (A) and stimulated with adiponectin (**Figure 22B**), compressive force (**Figure 22C**) or their combination (**Figure 22D**). As illustrated in the scheme, adiponectin binding to AdipoRs increased the expression of phosphorylated MAPK signaling and affected the homeostatic maintenance in cementoblasts (**Figure 22B**). Compression forces induced an accumulation of β-Catenin (**Figure 22C**). The precise mechanism revealed that

adiponectin activates β-Catenin through the MAPK pathway (**Figure 22D**). This process could be interacted by MAPK inhibition especially through P38α and is responsible for TCF/LEF-dependent transcription (**Figure 22E**).

An important observation that is cause for discussion is that adiponectin addition combined with compression of OCCM-30 cells did not significantly affect β-Catenin expression, even under the inhibition of MAPKs. This fact suggests that adiponectin addition exerts a multistep process leading to β-Catenin modulation that needs to be further investigated. However, all present results imply that MAPK signaling participates in the process of β-Catenin signaling on cementoblasts.

8.5 Cooperative interaction between the MAPK and β-Catenin signaling.

The cooperative interaction between the β-Catenin and MAPK signaling pathways has been reported in previous studies [78-80, 115]. On MC3T3-E1 cells, MEKK2 activation, a kinase with the ability to activate downstream MAPK pathways, could promote bone formation by rescuing β-Catenin degradation [116]. Chen et al. (2010) reported that blockade of P38 phosphorylation eliminates activation of WNT signaling in preosteoblasts, indicating that osteoblast differentiation triggered by P38 MAPK/β-Catenin promotes bone growth in female Sprague-Dawley rats [117]. Decreased phosphorylated P38 and increased ERK protein levels facilitate the β-Catenin pathway through enhancement of the expression of β-Catenin in MC3T3-E1 cells [118]. TGF-β activated kinase 1 was reported to promote the phosphorylation of P38, JNK and β-Catenin, at the same time it down regulated GSK-3β expression in mesenchymal stem cells [119]. In contrast, Wang et al. (2012) showed that pretreatment with P38 inhibitor (SB203580) on primary osteoblasts did not affect β-Catenin protein expression [120].

In the present study, I observed that JNK, ERK1/2 as well as P38 chemical inhibition reduced β-Catenin expression on OCCM-30 cells. Further, the single gene silencing of ERK1 and ERK2 as well as P38α and JNK1 showed that adiponectin-induced β-Catenin activation on OCCM-30 cementoblasts was especially sensitive to P38α and JNK1 knock out. JNK1 and P38α silencing negatively regulated β-Catenin, whereas ERK1 had a

significant up-regulation effect on GSK-3β expression. Furthermore, β-Catenin expression was up-regulated after adiponectin addition. In these contexts, the present results revealed the role of both molecules in triggering adiponectin-MAPK and β-Catenin signaling interactions. Our data are consistent with previous studies performed with other cell types [80, 121]. Thornton et al. (2008) showed that P38 MAPK inactivates GSK-3β and this inactivation leads to an accumulation of β-Catenin in the brain and thymocytes [80]. Sakisaka et al. (2016) showed that P38 MAPK modulates β-Catenin transcriptional activity, but have no effects on the phosphorylated of GSK-3β as well as β-Catenin expression in dental follicle cells [121]. However, the present results do not clarify the relationship between the expression of GSK-3β and the phosphorylated status of MAPK signaling mediators (P38, JNK, ERK1/2). Therefore, future studies should be performed to elucidate this mechanism in detail.

8.6 Adiponectin/AdipoR1 pathway is involved in the crosstalk between MAPK and β-Catenin signaling in the cellular responses of cementoblasts under adiponectin and compression forces.

In the present experiment, knockout of AdipoR2 in OCCM-30 cells induced β-Catenin up-regulation after adiponectin addition. Furthermore, together with my findings showing that the up-regulation of GSK-3β mRNA expression occurred after adiponectin addition in AdipoR2 silenced group, strongly suggest that the modulatory effect that adiponectin exerts on β-Catenin expression is mostly mediated by AdipoR1. These data provide evidence that adiponectin in turn up-regulates β-Catenin through the adiponectin/AdipoR1 pathway. There also appears to be a certain different functional specialization between AdipoR1 and AdipoR2, with the former being more tightly coupled to MAPK activation and the crosstalk with β-Catenin signaling.

The mRNA expression of cementogenesis biomarkers OCN and OPG [122] decreased after P38α knock-down in the presence of adiponectin. Hence, OCN and OPG appear to be altered by the interplays between MAPK and β-Catenin signaling in the cellular responses of cementoblasts under adiponectin and compression forces. Nemoto et al.

(2009) indicated that inhibition of GSK-3β on cementoblasts suppresses AP activity and the gene expression of AP, BSP and OCN [77]. Thus, the present results implicate P38α as the key mediator in adiponectin/AdipoR1 mediated cementogenesis and homeostasis.

8.7 Limitations of the present experiments.

In clinical practice, it was pointed out that the answer to the question of the optimal force is still far away [123]. Moreover, there is a large interindividual variation regarding the applied forces in both human experiments and animal research [123]. Even with standardized, constant, and equal forces, the speed of OTM may vary substantially among and within individuals [124]. As demonstrated with an *in vivo* study, Taddei et al. (2012) identified the ideal force of 0.35 N for OTM in mice because this force level promoted optimal OTM and osteoclast recruitment without root resorption [125]. In different *in vitro* studies, the OCCM-30 was subjected to different compressive forces by different methods such as hydrostatic pressure (threshold level of compression between 27 to 68 gf/cm^2) [126], micro-gravity [127], centrifugation [128, 129] and direct weight application [85, 127]. For instance, Kenji et al. (2016) loaded the human cementoblast cell line by mounting coverslips at 0.25 gf/cm^2 to reach a light compressive force [130]. Other researchers used cover glasses cylinders which exerted a static force of 1.0, 1.5, 2.0 gf/cm^2 to press on OCCM-30 cell monolayer [130-132]. However, Diercke et al. (2012) compressed the OCCM-30 cells at 30.3 gf/cm^2 using centrifugation. In the same manner, Korb et al. (2016) applied the compressive loading at 5.0, 20, and 30 gf/cm^2 to human primary cementoblasts via centrifugation [114]. Shi et al. (2019) subjected the compressive force of 47.5 gf/cm^2 and 73.7 gf/cm^2 to human PDL-derived fibroblasts by centrifugation [129].

In the present study, the compressive forces of 1.2, 2.4 and 3.6 gf/cm^2 that were applied to the mono-cultured OCCM-30 cells are within the range of established orthodontic force preciously used for OTM [131, 133]. The present results showed that 2.4 gf/cm^2 could trigger the cellular response with more pronounced AdipoRs expression and induce relevant signaling activation such as MAPK and β-Catenin pathway. Thus, the value 2.4

gf/cm^2 was chosen to further analyze the signaling interaction between MAPK and β-Catenin pathway in the present study. In contrast to other studies using higher magnitude compressive forces [114, 129], a limitation in the present study is that the experimental applied forces are not adequate to show the cellular response when stimulated with higher magnitude mechanical force such as 30 gf/cm^2. Therefore, much-higher compressive forces should be considered for experiments OCCM-30 cells in the experiments in further studies.

When it comes to the speed of OTM, Saloom et al. (2017) conducted a prospective clinical cohort study aiming to establish the connection between obesity and the speed of induced OTM [9], but it could not significantly reveal any direct association. At 1-week, initial tooth displacement was significantly increased in the obese group and obese patients had a significantly higher speed of tooth movement compared with normal-weight patients over the period of alignment [9]. Despite being identified during the first week, differences could not be explained and treatment time remained unchanged. In spite of the lack of studies about the connection between obesity and the speed of OTM, there are no changed protocols provided for the clinician nor were significant differences between normal-weight and obese individuals presumed [12]. My results provide new evidence at molecular levels during OTM to determine the exact biological effects of adiponectin in cementoblasts. However, the adiponectin-deficient mice underlying OTM would further serve as the animal model to study the cementum reaction toward orthodontic forces.

It should also be noted, that murine cementoblasts are probably not fully comparable to human primary cementoblasts, so that investigations on primary human material are mandatory before patient studies.

8.8 Further work.

The present results indicated the need for further animal and clinical experiments.

Clinical studies have described that the level of adiponectin is reduced in the serum of obese individuals [38]. In this context, obese patients undergoing orthodontic treatment may be influenced by these lower levels of circulating adiponectin. Since constant or

intermittent mechanical compression is present on the stress-side of the tooth root surface, it can be assumed that less expression of adiponectin-MAPK signaling in this area may lead to less activation of β-Catenin. The possible clinical implication of this study may be that depressed adiponectin levels in obese subjects during orthodontic tooth movement may negatively affect the process of OIIRR in response to mechanical stimulation by decreasing β-Catenin, which is capable of inhibiting mediators such as OPG and OCN that form extracellular matrices in OCCM-30 cells [134]. Thus, a deeper analysis of how adiponectin affects biologic cell responses should be identified using *in vitro* rat models. Clinically, the outcomes of the thesis highlight potential implications of adiponectin for orthodontic treatment in obese patients. Additional studies should be conducted to compare the influence of adiponectin on orthodontic tooth movement during orthodontic treatment in obese and normal weight patients.

9. Conclusions

In conclusion, the present study demonstrated the expression of adiponectin receptors on OCCM-30 cells and revealed that adiponectin influences *in vitro* the migration, proliferation and cementogenesis of OCCM-30 cells partly through the MAPK signaling pathway.

Moreover, it was shown that adiponectin as well as compressive forces stimulate both the MAPK and β-Catenin signaling pathways in cementoblasts. The inhibition of P38, JNK and ERK1/2 differentially regulate β-Catenin expression as well as TCF/LEF transcription. Furthermore, adiponectin regulates the compression induced β-Catenin signaling via cross-interacting with the MAPK signaling pathway.

10. Summary

In obese patients, current clinical evidences suggest that changes in levels of circulating adipokines such as adiponectin can influence the speed of orthodontically induced tooth movement due to their capacity to regulate peripheral bone formation.

Here, qRT-PCR and Western blots were performed to verify the mRNA and protein levels of adiponectin receptors (AdipoRs) of OCCM-30 cells. Alizarin Red S staining revealed that adiponectin increased mineralized nodule formation and quantitative AP activity in a dose-dependent manner. Adiponectin up-regulates the mRNA levels of AP, BSP, OCN, OPG, Runx-2 as well as F-Spondin. Adiponectin also increases the migration and proliferation of OCCM-30 cells. Moreover, Adiponectin induces a transient activation of JNK, P38 and ERK1/2. The activation of adiponectin-mediated migration and proliferation was attenuated after pharmacological inhibition of P38, ERK1/2 and JNK in different degrees, whereas mineralization was facilitated by MAPK inhibition in varying degrees. Based on our results, I showed that adiponectin could favorably affect cementoblast migration, proliferation as well as cementogenesis partly through the activation of MAPK signaling pathways.

Furthermore, siRNAs targeting P38α, JNK1, ERK1, ERK2 and AdipoRs were performed. It was found that compressive forces increased the expression of AdipoRs. Western blots showed that co-stimuli of adiponectin and compression activated MAPK and β-Catenin signaling pathways. The MAPK inhibition alters the compression-induced β-Catenin activation. The siRNAs targeting AdipoR1, P38α and JNK1 showed the interaction of single MAPK molecules and β-Catenin signaling in response to compression and/or adiponectin. Silencing by a dominant negative-version of P38α and JNK1 attenuated adiponectin-induced TCF/LEF reporter activation. P38α is a key connector between β-Catenin, TCF/LEF transcription and MAPK signaling pathway.

In conclusion, compressive forces activate β-Catenin and MAPK signaling pathways. Adiponectin regulates β-Catenin signaling principally by inactivating GSK-3β kinase activity. β-Catenin expression was partially inhibited by MAPK blockade indicating that

MAPK plays a crucial role regulating β-Catenin during cementogenesis. Moreover, adiponectin modulates GSK-3β and β-Catenin mostly through AdipoR1.

11. Zusammenfassung

Für übergewichtige Patienten deuten aktuelle klinische Ergebnisse darauf hin, dass Veränderungen das Spiegels zirkulierender Adipokine wie Adiponektin die Geschwindigkeit kieferorthopädisch induzierter Zahnbewegungen auf der Basis ihrer Fähigkeit zur Regulierung der peripheren Knochenbildung beeinflussen können.

Im Rahmen dieser Arbeit wurden RT-PCR und Western Blots durchgeführt, um die mRNA- und Proteinspiegel von Adiponektin-Rezeptoren (AdipoRs) von OCCM-30-Zellen zu quantifizieren. Färbungen mit Alizarin Red S zeigten, dass Adiponektin die Bildung von Mineralisationsknoten und die quantitative AP-Aktivität dosisabhängig erhöht. Adiponektin hoch regulierte die mRNA-Level von AP, BSP, OCN, OPG, Runx-2 sowie F-Spondin. Adiponektin erhöhte weiterhin das Ausmaß der Migration und Proliferation von OCCM-30-Zellen. Darüber hinaus induzierte Adiponektin eine vorübergehende Aktivierung von JNK, P38 und ERK1/2. Die Aktivierung der Adiponektin-vermittelten Migration und Proliferation wurde nach pharmakologischer Hemmung von P38, ERK1/2 und JNK in unterschiedlichem Ausmaß abgeschwächt, während die Mineralisierung durch MAPK-Hemmung in unterschiedlichem Ausmaß erleichtert wurde. Basierend auf Ergebnissen konnten gezeigt werden, dass Adiponektin die Zementoblasten den vorliegenden-migration, und -proliferation sowie die Zementogenese teilweise durch die Aktivierung von MAPK-Signalwegen günstig beeinflussen könnte.

Darüber hinaus wurden siRNAs gegen P38α, JNK1, ERK1, ERK2 und AdipoRs eingesetzt. Es zeigte sich, dass Druckkräfte die Expression von AdipoRs erhöhen. Western Blots zeigten, dass Co-Stimuli von Adiponektin und Kompression die MAPK- und β-Catenin-Signalwege aktivierten. Die MAPK-Hemmung veränderte die kompressionsinduzierte β-Catenin-Aktivierung. Die siRNAs, die auf AdipoR1, P38α und JNK1 abzielen, zeigten die Interaktion einzelner MAPK-Moleküle und β-Catenin-Signalgebung als Reaktion auf Kompression und/oder Adiponektin. Silencing durch eine dominante Negativversion von P38α und JNK1 schwächte die Adiponektin-induzierte

TCF/LEF-Reporteraktivierung ab. P38α ist ein Schlüsselverbinder zwischen β-Catenin, der TCF/LEF-Transkription und dem MAPK-Signalweg.

Zusammenfassend aktivieren leichte Druckkräfte die β-Catenin- und MAPK-Signalwege. Adiponektin reguliert die β-Catenin-Signalgebung hauptsächlich durch Inaktivierung der GSK-3β-Kinase-Aktivität. Die β-Catenin-Expression wurde teilweise durch die MAPK-Blockade gehemmt, was darauf hindeutet, dass MAPK eine entscheidende Rolle bei der Regulierung von β-Catenin während der Zementogenese spielt. Darüber hinaus moduliert Adiponektin GSK-3β und β-Catenin hauptsächlich über AdipoR1.

12. References

1. Obesity: preventing and managing the global epidemic. Report of a WHO consultation. World Health Organ Tech Rep Ser. 2000;894:i-xii, 1-253.

2. Zhang Y, Proenca R, Maffei M, Barone M, Leopold L, Friedman JM. Positional cloning of the mouse obese gene and its human homologue. Nature. 1994;372(6505):425-32. doi: 10.1038/372425a0.

3. Kershaw EE, Flier JS. Adipose tissue as an endocrine organ. J Clin Endocrinol Metab. 2004;89(6):2548-56. doi: 10.1210/jc.2004-0395.

4. Leal Vde O, Mafra D. Adipokines in obesity. Clin Chim Acta. 2013;419:87-94. doi: 10.1016/j.cca.2013.02.003.

5. Fasshauer M, Bluher M. Adipokines in health and disease. Trends Pharmacol Sci. 2015;36(7):461-70. doi: 10.1016/j.tips.2015.04.014.

6. von Bremen J, Lorenz N, Ludwig B, Ruf S. Increased BMI in children-an indicator for less compliance during orthodontic treatment with removable appliances. Eur J Orthod. 2018;40(4):350-5. doi: 10.1093/ejo/cjy007.

7. von Bremen J, Lorenz N, Ruf S. Impact of body mass index on oral health during orthodontic treatment: an explorative pilot study. Eur J Orthod. 2016;38(4):386-92. doi: 10.1093/ejo/cjv074.

8. Lopez-Gomez JJ, Perez Castrillon JL, de Luis Roman DA. Impact of obesity on bone metabolism. Endocrinol Nutr. 2016;63(10):551-9. doi: 10.1016/j.endonu.2016.08.005.

9. Saloom HF, Papageorgiou SN, Carpenter GH, Cobourne MT. Impact of Obesity on Orthodontic Tooth Movement in Adolescents: A Prospective Clinical Cohort Study. J Dent Res. 2017;96(5):547-54. doi: 10.1177/0022034516688448.

10. Azamar-Llamas D, Hernandez-Molina G, Ramos-Avalos B, Furuzawa-Carballeda J. Adipokine Contribution to the Pathogenesis of Osteoarthritis. Mediators Inflamm. 2017;2017:5468023. doi: 10.1155/2017/5468023.

11. Neeley WW, 2nd, Gonzales DA. Obesity in adolescence: implications in orthodontic treatment. Am J Orthod Dentofacial Orthop. 2007;131(5):581-8. doi:

10.1016/j.ajodo.2006.03.028.

12. Consolaro A. Obesity and orthodontic treatment: is there any direct relationship? Dental Press J Orthod. 2017;22(3):21-5. doi: 10.1590/2177-6709.22.3.021-025.oin.

13. Kadowaki T, Yamauchi T. Adiponectin and adiponectin receptors. Endocr Rev. 2005;26(3):439-51. doi: 10.1210/er.2005-0005.

14. Saloom HF, Papageorgiou SN, Carpenter GH, Cobourne MT. The effect of obesity on orofacial pain during early orthodontic treatment with fixed appliances: a prospective cohort study. Eur J Orthod. 2018;40(4):343-9. doi: 10.1093/ejo/cjx064.

15. Dilsiz A, Kilic N, Aydin T, Ates FN, Zihni M, Bulut C. Leptin levels in gingival crevicular fluid during orthodontic tooth movement. Angle Orthod. 2010;80(3):504-8. doi: 10.2319/072109-402.1.

16. Li W, Zhu W, Hou J, Huang B, Liu K, Meng H. Leptin and its receptor expression in dental and periodontal tissues of primates. Cell Tissue Res. 2014;355(1):181-8. doi: 10.1007/s00441-013-1729-0.

17. Ruiz-Heiland G, Yong JW, von Bremen J, Ruf S. Leptin reduces in vitro cementoblast mineralization and survival as well as induces PGE2 release by ERK1/2 commitment. Clin Oral Investig. 2020. doi: 10.1007/s00784-020-03501-3.

18. Berner HS, Lyngstadaas SP, Spahr A, Monjo M, Thommesen L, Drevon CA, et al. Adiponectin and its receptors are expressed in bone-forming cells. Bone. 2004;35(4):842-9. doi: 10.1016/j.bone.2004.06.008.

19. Yamaguchi N, Hamachi T, Kamio N, Akifusa S, Masuda K, Nakamura Y, et al. Expression levels of adiponectin receptors and periodontitis. J Periodontal Res. 2010;45(2):296-300. doi: 10.1111/j.1600-0765.2009.01222.x.

20. Funahashi T, Nakamura T, Shimomura I, Maeda K, Kuriyama H, Takahashi M, et al. Role of adipocytokines on the pathogenesis of atherosclerosis in visceral obesity. Intern Med. 1999;38(2):202-6. doi: 10.2169/internalmedicine.38.202.

21. Haugen S, Aasarod KM, Stunes AK, Mosti MP, Franzen T, Vandevska-Radunovic V, et al. Adiponectin prevents orthodontic tooth movement in rats. Arch Oral Biol. 2017;83:304-11. doi: 10.1016/j.archoralbio.2017.08.009.

22. Scherer PE, Williams S, Fogliano M, Baldini G, Lodish HF. A novel serum protein similar to C1q, produced exclusively in adipocytes. J Biol Chem. 1995;270(45):26746-9. doi: 10.1074/jbc.270.45.26746.

23. Hu E, Liang P, Spiegelman BM. AdipoQ is a novel adipose-specific gene dysregulated in obesity. J Biol Chem. 1996;271(18):10697-703. doi: 10.1074/jbc.271.18.10697.

24. Maeda K, Okubo K, Shimomura I, Funahashi T, Matsuzawa Y, Matsubara K. cDNA cloning and expression of a novel adipose specific collagen-like factor, apM1 (AdiPose Most abundant Gene transcript 1). Biochem Biophys Res Commun. 1996;221(2):286-9. doi: 10.1006/bbrc.1996.0587.

25. Nakano Y, Tobe T, Choi-Miura NH, Mazda T, Tomita M. Isolation and characterization of GBP28, a novel gelatin-binding protein purified from human plasma. J Biochem. 1996;120(4):803-12. doi: 10.1093/oxfordjournals.jbchem.a021483.

26. Siitonen N, Pulkkinen L, Lindstrom J, Kolehmainen M, Eriksson JG, Venojarvi M, et al. Association of ADIPOQ gene variants with body weight, type 2 diabetes and serum adiponectin concentrations: the Finnish Diabetes Prevention Study. BMC Med Genet. 2011;12:5. doi: 10.1186/1471-2350-12-5.

27. Katsiougiannis S, Kapsogeorgou EK, Manoussakis MN, Skopouli FN. Salivary gland epithelial cells: a new source of the immunoregulatory hormone adiponectin. Arthritis Rheum. 2006;54(7):2295-9. doi: 10.1002/art.21944.

28. Min X, Lemon B, Tang J, Liu Q, Zhang R, Walker N, et al. Crystal structure of a single-chain trimer of human adiponectin globular domain. Febs Lett. 2012;586(6):912-7. doi: 10.1016/j.febslet.2012.02.024.

29. Pajvani UB, Du X, Combs TP, Berg AH, Rajala MW, Schulthess T, et al. Structure-function studies of the adipocyte-secreted hormone Acrp30/adiponectin. Implications fpr metabolic regulation and bioactivity. J Biol Chem. 2003;278(11):9073-85. doi: 10.1074/jbc.M207198200.

30. Tilg H, Moschen AR. Adipocytokines: mediators linking adipose tissue, inflammation and immunity. Nat Rev Immunol. 2006;6(10):772-83. doi: 10.1038/nri1937.

31. Ghoshal K, Bhattacharyya M. Adiponectin: Probe of the molecular paradigm

associating diabetes and obesity. World J Diabetes. 2015;6(1):151-66. doi: 10.4239/wjd.v6.i1.151.

32. Achari AE, Jain SK. Adiponectin, a Therapeutic Target for Obesity, Diabetes, and Endothelial Dysfunction. Int J Mol Sci. 2017;18(6). doi: 10.3390/ijms18061321.

33. Tsao TS, Tomas E, Murrey HE, Hug C, Lee DH, Ruderman NB, et al. Role of disulfide bonds in Acrp30/adiponectin structure and signaling specificity. Different oligomers activate different signal transduction pathways. J Biol Chem. 2003;278(50):50810-7. doi: 10.1074/jbc.M309469200.

34. Hirose H, Yamamoto Y, Seino-Yoshihara Y, Kawabe H, Saito I. Serum high-molecular-weight adiponectin as a marker for the evaluation and care of subjects with metabolic syndrome and related disorders. J Atheroscler Thromb. 2010;17(12):1201-11. doi: 10.5551/jat.6106.

35. Yamauchi T, Kamon J, Ito Y, Tsuchida A, Yokomizo T, Kita S, et al. Cloning of adiponectin receptors that mediate antidiabetic metabolic effects. Nature. 2003;423(6941):762-9. doi: 10.1038/nature01705.

36. Khoramipour K, Chamari K, Hekmatikar AA, Ziyaiyan A, Taherkhani S, Elguindy NM, et al. Adiponectin: Structure, Physiological Functions, Role in Diseases, and Effects of Nutrition. Nutrients. 2021;13(4). doi: 10.3390/nu13041180.

37. Yamauchi N, Takazawa Y, Maeda D, Hibiya T, Tanaka M, Iwabu M, et al. Expression levels of adiponectin receptors are decreased in human endometrial adenocarcinoma tissues. Int J Gynecol Pathol. 2012;31(4):352-7. doi: 10.1097/PGP.0b013e3182469583.

38. Hug C, Wang J, Ahmad NS, Bogan JS, Tsao TS, Lodish HF. T-cadherin is a receptor for hexameric and high-molecular-weight forms of Acrp30/adiponectin. Proc Natl Acad Sci U S A. 2004;101(28):10308-13. doi: 10.1073/pnas.0403382101.

39. Denzel MS, Scimia MC, Zumstein PM, Walsh K, Ruiz-Lozano P, Ranscht B. T-cadherin is critical for adiponectin-mediated cardioprotection in mice. J Clin Invest. 2010;120(12):4342-52. doi: 10.1172/JCI43464.

40. Lin YY, Chen CY, Chuang TY, Lin Y, Liu HY, Mersmann HJ, et al. Adiponectin receptor 1 regulates bone formation and osteoblast differentiation by GSK-3beta/beta-

catenin signaling in mice. Bone. 2014;64:147-54. doi: 10.1016/j.bone.2014.03.051.

41. Sun Y, Chen X. Effect of adiponectin on apoptosis: proapoptosis or antiapoptosis? Biofactors. 2010;36(3):179-86. doi: 10.1002/biof.83.

42. Tilg H, Wolf AM. Adiponectin: a key fat-derived molecule regulating inflammation. Expert Opin Ther Targets. 2005;9(2):245-51. doi: 10.1517/14728222.9.2.245.

43. Buechler C, Wanninger J, Neumeier M. Adiponectin receptor binding proteins - recent advances in elucidating adiponectin signalling pathways. Febs Lett. 2010;584(20):4280-6. doi: 10.1016/j.febslet.2010.09.035.

44. Yamauchi T, Kamon J, Terauchi Y, Froguel P, Tobe K, Nagai R, et al. Cloning of receptors for adiponectin that mediates anti-diabetic and anti-atherogenic effeccts. Circulation. 2003;108(17):113-.

45. Ding QR, Wang ZZ, Chen Y. Endocytosis of adiponectin receptor 1 through a clathrin- and Rab5-dependent pathway. Cell Res. 2009;19(3):317-27. doi: 10.1038/cr.2008.299.

46. Swarbrick MM, Havel PJ. Physiological, pharmacological, and nutritional regulation of circulating adiponectin concentrations in humans. Metab Syndr Relat Disord. 2008;6(2):87-102. doi: 10.1089/met.2007.0029.

47. Toda M, Morimoto K. Comparison of saliva sampling methods for measurement of salivary adiponectin levels. Scand J Clin Lab Invest. 2008;68(8):823-5. doi: 10.1080/00365510802147006.

48. Naot D, Musson DS, Cornish J. The Activity of Adiponectin in Bone. Calcif Tissue Int. 2017;100(5):486-99. doi: 10.1007/s00223-016-0216-5.

49. Carbone F, La Rocca C, Matarese G. Immunological functions of leptin and adiponectin. Biochimie. 2012;94(10):2082-8. doi: 10.1016/j.biochi.2012.05.018.

50. Kopp HP, Krzyzanowska K, Mohlig M, Spranger J, Pfeiffer AF, Schernthaner G. Effects of marked weight loss on plasma levels of adiponectin, markers of chronic subclinical inflammation and insulin resistance in morbidly obese women. Int J Obes (Lond). 2005;29(7):766-71. doi: 10.1038/sj.ijo.0802983.

51. de Carvalho PM, Gaviao MB, Carpenter GH. Altered autophagy and sympathetic innervation in salivary glands from high-fat diet mice. Arch Oral Biol. 2017;75:107-13.

doi: 10.1016/j.archoralbio.2016.10.033.

52. Benedix F, Westphal S, Patschke R, Granowski D, Luley C, Lippert H, et al. Weight loss and changes in salivary ghrelin and adiponectin: comparison between sleeve gastrectomy and Roux-en-Y gastric bypass and gastric banding. Obes Surg. 2011;21(5):616-24. doi: 10.1007/s11695-011-0374-5.

53. Cao Z, Li J, Luo L, Li X, Liu M, Gao M, et al. Molecular cloning and expression analysis of adiponectin and its receptors (AdipoR1 and AdipoR2) in the hypothalamus of the Huoyan goose during different stages of the egg-laying cycle. Reprod Biol Endocrinol. 2015;13:87. doi: 10.1186/s12958-015-0085-1.

54. Saito T, Yamaguchi N, Shimazaki Y, Hayashida H, Yonemoto K, Doi Y, et al. Serum levels of resistin and adiponectin in women with periodontitis: the Hisayama study. J Dent Res. 2008;87(4):319-22. doi: 10.1177/154405910808700416.

55. Seo BM, Miura M, Gronthos S, Bartold PM, Batouli S, Brahim J, et al. Investigation of multipotent postnatal stem cells from human periodontal ligament. Lancet. 2004;364(9429):149-55. doi: 10.1016/S0140-6736(04)16627-0.

56. Park CH, Oh JH, Jung HM, Choi Y, Rahman SU, Kim S, et al. Effects of the incorporation of epsilon-aminocaproic acid/chitosan particles to fibrin on cementoblast differentiation and cementum regeneration. Acta Biomater. 2017;61:134-43. doi: 10.1016/j.actbio.2017.07.039.

57. Caverzasio J, Manen D. Essential role of Wnt3a-mediated activation of mitogen-activated protein kinase p38 for the stimulation of alkaline phosphatase activity and matrix mineralization in C3H10T1/2 mesenchymal cells. Endocrinology. 2007;148(11):5323-30. doi: 10.1210/en.2007-0520.

58. Nanci A, Bosshardt DD. Structure of periodontal tissues in health and disease. Periodontol 2000. 2006;40:11-28. doi: 10.1111/j.1600-0757.2005.00141.x.

59. Arzate H, Zeichner-David M, Mercado-Celis G. Cementum proteins: role in cementogenesis, biomineralization, periodontium formation and regeneration. Periodontol 2000. 2015;67(1):211-33. doi: 10.1111/prd.12062.

60. Saygin NE, Giannobile WV, Somerman MJ. Molecular and cell biology of cementum.

Periodontol 2000. 2000;24:73-98. doi: 10.1034/j.1600-0757.2000.2240105.x.

61. Kitagawa M, Ao M, Miyauchi M, Abiko Y, Takata T. F-spondin regulates the differentiation of human cementoblast-like (HCEM) cells via BMP7 expression. Biochem Biophys Res Commun. 2012;418(2):229-33. doi: 10.1016/j.bbrc.2011.12.155.

62. Matthews BG, Roguljic H, Franceschetti T, Roeder E, Matic I, Vidovic I, et al. Gene-expression analysis of cementoblasts and osteoblasts. J Periodontal Res. 2016;51(3):304-12. doi: 10.1111/jre.12309.

63. Matalová E, Lungova V, Sharpe P. Development of Tooth and Associated Structures. 2015. p. 335-46.

64. Diekwisch TG. The developmental biology of cementum. Int J Dev Biol. 2001;45(5-6):695-706.

65. Bosshardt DD, Stadlinger B, Terheyden H. Cell-to-cell communication--periodontal regeneration. Clin Oral Implants Res. 2015;26(3):229-39. doi: 10.1111/clr.12543.

66. Liu J, Ruan J, Weir MD, Ren K, Schneider A, Wang P, et al. Periodontal Bone-Ligament-Cementum Regeneration via Scaffolds and Stem Cells. Cells. 2019;8(6). doi: 10.3390/cells8060537.

67. Li Y, Jacox LA, Little SH, Ko CC. Orthodontic tooth movement: The biology and clinical implications. Kaohsiung J Med Sci. 2018;34(4):207-14. doi: 10.1016/j.kjms.2018.01.007.

68. King JS. Mechanical stress meets autophagy: potential implications for physiology and pathology. Trends Mol Med. 2012;18(10):583-8. doi: 10.1016/j.molmed.2012.08.002.

69. Krishnan V, Davidovitch Z. On a path to unfolding the biological mechanisms of orthodontic tooth movement. J Dent Res. 2009;88(7):597-608. doi: 10.1177/0022034509338914.

70. Yassir YA, McIntyre GT, Bearn DR. Orthodontic treatment and root resorption: an overview of systematic reviews. Eur J Orthod. 2020. doi: 10.1093/ejo/cjaa058.

71. Kanas RJ, Kanas SJ. Dental root resorption: a review of the literature and a proposed new classification. Compend Contin Educ Dent. 2011;32(3):e38-52.

72. Brezniak N, Wasserstein A. Orthodontically induced inflammatory root resorption.

Part I: The basic science aspects. Angle Orthod. 2002;72(2):175-9. doi: 10.1043/0003-3219(2002)072<0175:OIIRRP>2.0.CO;2.

73. Consolaro A. The four mechanisms of dental resorption initiation. Dental Press J Orthod. 2013;18(3):7-9. doi: 10.1590/s2176-94512013000300004.

74. Diercke K, Kohl A, Lux CJ, Erber R. Compression of human primary cementoblasts leads to apoptosis: A possible cause of dental root resorption? J Orofac Orthop. 2014;75(6):430-45. doi: 10.1007/s00056-014-0237-5.

75. Lim WH, Liu B, Hunter DJ, Cheng D, Mah SJ, Helms JA. Downregulation of Wnt causes root resorption. Am J Orthod Dentofacial Orthop. 2014;146(3):337-45. doi: 10.1016/j.ajodo.2014.05.027.

76. Sindhavajiva PR, Sastravaha P, Arksornnukit M, Pavasant P. Intermittent compressive force induces human mandibular-derived osteoblast differentiation via WNT/beta-catenin signaling. J Cell Biochem. 2018;119(4):3474-85. doi: 10.1002/jcb.26519.

77. Nemoto E, Koshikawa Y, Kanaya S, Tsuchiya M, Tamura M, Somerman MJ, et al. Wnt signaling inhibits cementoblast differentiation and promotes proliferation. Bone. 2009;44(5):805-12. doi: 10.1016/j.bone.2008.12.029.

78. Bikkavilli RK, Malbon CC. Mitogen-activated protein kinases and Wnt/beta-catenin signaling: Molecular conversations among signaling pathways. Commun Integr Biol. 2009;2(1):46-9. doi: 10.4161/cib.2.1.7503.

79. Bikkavilli RK, Feigin ME, Malbon CC. p38 mitogen-activated protein kinase regulates canonical Wnt-beta-catenin signaling by inactivation of GSK3beta. J Cell Sci. 2008;121(Pt 21):3598-607. doi: 10.1242/jcs.032854.

80. Thornton TM, Pedraza-Alva G, Deng B, Wood CD, Aronshtam A, Clements JL, et al. Phosphorylation by p38 MAPK as an alternative pathway for GSK3beta inactivation. Science. 2008;320(5876):667-70. doi: 10.1126/science.1156037.

81. Sanchavanakit N, Saengtong W, Manokawinchoke J, Pavasant P. TNF-alpha stimulates MMP-3 production via PGE2 signalling through the NF-kB and p38 MAPK pathway in a murine cementoblast cell line. Arch Oral Biol. 2015;60(7):1066-74. doi: 10.1016/j.archoralbio.2015.04.001.

82. Chen X, Lu J, Bao J, Guo J, Shi J, Wang Y. Adiponectin: a biomarker for rheumatoid arthritis? Cytokine Growth Factor Rev. 2013;24(1):83-9. doi: 10.1016/j.cytogfr.2012.07.004.

83. D'Errico JA, Berry JE, Ouyang H, Strayhorn CL, Windle JJ, Somerman MJ. Employing a transgenic animal model to obtain cementoblasts in vitro. J Periodontol. 2000;71(1):63-72. doi: 10.1902/jop.2000.71.1.63.

84. Cadena-Herrera D, Esparza-De Lara JE, Ramirez-Ibanez ND, Lopez-Morales CA, Perez NO, Flores-Ortiz LF, et al. Validation of three viable-cell counting methods: Manual, semi-automated, and automated. Biotechnol Rep (Amst). 2015;7:9-16. doi: 10.1016/j.btre.2015.04.004.

85. Kanzaki H, Chiba M, Shimizu Y, Mitani H. Periodontal ligament cells under mechanical stress induce osteoclastogenesis by receptor activator of nuclear factor kappaB ligand up-regulation via prostaglandin E2 synthesis. J Bone Miner Res. 2002;17(2):210-20. doi: 10.1359/jbmr.2002.17.2.210.

86. Proff P, Reicheneder C, Faltermeier A, Kubein-Meesenburg D, Romer P. Effects of mechanical and bacterial stressors on cytokine and growth-factor expression in periodontal ligament cells. J Orofac Orthop. 2014;75(3):191-202. doi: 10.1007/s00056-014-0212-1.

87. Livak KJ, Schmittgen TD. Analysis of relative gene expression data using real-time quantitative PCR and the 2(-Delta Delta C(T)) Method. Methods. 2001;25(4):402-8. doi: 10.1006/meth.2001.1262.

88. Cortes-Rios J, Zarate AM, Figueroa JD, Medina J, Fuentes-Lemus E, Rodriguez-Fernandez M, et al. Protein quantification by bicinchoninic acid (BCA) assay follows complex kinetics and can be performed at short incubation times. Anal Biochem. 2020;608:113904. doi: 10.1016/j.ab.2020.113904.

89. Mamali I, Roupas ND, Armeni AK, Theodoropoulou A, Markou KB, Georgopoulos NA. Measurement of salivary resistin, visfatin and adiponectin levels. Peptides. 2012;33(1):120-4. doi: 10.1016/j.peptides.2011.11.007.

90. Luo XH, Guo LJ, Yuan LQ, Xie H, Zhou HD, Wu XP, et al. Adiponectin stimulates

human osteoblasts proliferation and differentiation via the MAPK signaling pathway. Exp Cell Res. 2005;309(1):99-109. doi: 10.1016/j.yexcr.2005.05.021.

91. Berner HS, Lyngstadaas SP, Spahr A, Monjo M, Thommesen L, Drevon CA, et al. Adiponectin and its receptors are expressed in bone-forming cells. Bone. 2004;35(4):842-9. doi: 10.1016/j.bone.2004.06.008.

92. Kanazawa I, Yamaguchi T, Yano S, Yamauchi M, Yamamoto M, Sugimoto T. Adiponectin and AMP kinase activator stimulate proliferation, differentiation, and mineralization of osteoblastic MC3T3-E1 cells. BMC Cell Biol. 2007;8:51. doi: 10.1186/1471-2121-8-51.

93. Oshima K, Nampei A, Matsuda M, Iwaki M, Fukuhara A, Hashimoto J, et al. Adiponectin increases bone mass by suppressing osteoclast and activating osteoblast. Bone. 2006;38(3):S29-S. doi: 10.1016/j.bone.2006.01.119.

94. Wang Y, Zhang X, Shao J, Liu H, Liu X, Luo E. Adiponectin regulates BMSC osteogenic differentiation and osteogenesis through the Wnt/beta-catenin pathway. Sci Rep. 2017;7(1):3652. doi: 10.1038/s41598-017-03899-z.

95. Iwayama T, Yanagita M, Mori K, Sawada K, Ozasa M, Kubota M, et al. Adiponectin regulates functions of gingival fibroblasts and periodontal ligament cells. J Periodontal Res. 2012;47(5):563-71. doi: 10.1111/j.1600-0765.2012.01467.x.

96. Bosshardt DD. Are cementoblasts a subpopulation of osteoblasts or a unique phenotype? J Dent Res. 2005;84(5):390-406. doi: 10.1177/154405910508400501.

97. Liu TM, Lee EH. Transcriptional regulatory cascades in Runx2-dependent bone development. Tissue Eng Part B Rev. 2013;19(3):254-63. doi: 10.1089/ten.TEB.2012.0527.

98. Hakki SS, Bozkurt SB, Turkay E, Dard M, Purali N, Gotz W. Recombinant amelogenin regulates the bioactivity of mouse cementoblasts in vitro. Int J Oral Sci. 2018;10(2):15. doi: 10.1038/s41368-018-0010-5.

99. Kimura A, Kunimatsu R, Yoshimi Y, Tsuka Y, Awada T, Horie K, et al. Baicalin Promotes Osteogenic Differentiation of Human Cementoblast Lineage Cells Via the Wnt/beta Catenin Signaling Pathway. Curr Pharm Des. 2018;24(33):3980-7. doi:

10.2174/138161282466618111610351 4.

100. Lee HW, Kim SY, Kim AY, Lee EJ, Choi JY, Kim JB. Adiponectin stimulates osteoblast differentiation through induction of COX2 in mesenchymal progenitor cells. Stem Cells. 2009;27(9):2254-62. doi: 10.1002/stem.144.

101. Carvalho SM, Oliveira AA, Jardim CA, Melo CB, Gomes DA, de Fatima Leite M, et al. Characterization and induction of cementoblast cell proliferation by bioactive glass nanoparticles. J Tissue Eng Regen Med. 2012;6(10):813-21. doi: 10.1002/term.488.

102. McKee MD, Zalzal S, Nanci A. Extracellular matrix in tooth cementum and mantle dentin: localization of osteopontin and other noncollagenous proteins, plasma proteins, and glycoconjugates by electron microscopy. Anat Rec. 1996;245(2):293-312. doi: 10.1002/(sici)1097-0185(199606)245:2<293::Aid-ar13>3.0.Co;2-k.

103. MacNeil RL, Berry J, D'Errico J, Strayhorn C, Piotrowski B, Somerman MJ. Role of two mineral-associated adhesion molecules, osteopontin and bone sialoprotein, during cementogenesis. Connect Tissue Res. 1995;33(1-3):1-7. doi: 10.3109/03008209509016974.

104. Foster BL, Soenjaya Y, Nociti FH, Jr., Holm E, Zerfas PM, Wimer HF, et al. Deficiency in acellular cementum and periodontal attachment in bsp null mice. J Dent Res. 2013;92(2):166-72. doi: 10.1177/0022034512469026.

105. Tokiyasu Y, Takata T, Saygin E, Somerman M. Enamel factors regulate expression of genes associated with cementoblasts. J Periodontol. 2000;71(12):1829-39. doi: 10.1902/jop.2000.71.12.1829.

106. Thomson TS, Berry JE, Somerman MJ, Kirkwood KL. Cementoblasts maintain expression of osteocalcin in the presence of mineral trioxide aggregate. J Endod. 2003;29(6):407-12. doi: 10.1097/00004770-200306000-00007.

107. McKee MD, Nanci A. Osteopontin at mineralized tissue interfaces in bone, teeth, and osseointegrated implants: ultrastructural distribution and implications for mineralized tissue formation, turnover, and repair. Microsc Res Tech. 1996;33(2):141-64. doi: 10.1002/(SICI)1097-0029(19960201)33:2<141::AID-JEMT5>3.0.CO;2-W.

108. Saygin NE, Giannobile WV, Somerman MJ. Molecular and cell biology of

cementum. Periodontol 2000. 2000;24:73-98.

109. Higuchi C, Myoui A, Hashimoto N, Kuriyama K, Yoshioka K, Yoshikawa H, et al. Continuous inhibition of MAPK signaling promotes the early osteoblastic differentiation and mineralization of the extracellular matrix. J Bone Miner Res. 2002;17(10):1785-94. doi: 10.1359/jbmr.2002.17.10.1785.

110. Miyazaki T, Bub JD, Uzuki M, Iwamoto Y. Adiponectin activates c-Jun NH2-terminal kinase and inhibits signal transducer and activator of transcription 3. Biochem Biophys Res Commun. 2005;333(1):79-87. doi: 10.1016/j.bbrc.2005.05.076.

111. Junker S, Frommer KW, Krumbholz G, Tsiklauri L, Gerstberger R, Rehart S, et al. Expression of adipokines in osteoarthritis osteophytes and their effect on osteoblasts. Matrix Biol. 2017;62:75-91. doi: 10.1016/j.matbio.2016.11.005.

112. Kono SJ, Oshima Y, Hoshi K, Bonewald LF, Oda H, Nakamura K, et al. Erk pathways negatively regulate matrix mineralization. Bone. 2007;40(1):68-74. doi: 10.1016/j.bone.2006.07.024.

113. Shuqin L, Shan Y, Aishu R, Hongwei D. [Investigation of Wnt/beta-catenin signaling pathway on regulation of Runx2 in cementoblasts under mechanical stress in vitro]. Hua Xi Kou Qiang Yi Xue Za Zhi. 2015;33(1):35-9.

114. Korb K, Katsikogianni E, Zingler S, Daum E, Lux CJ, Hohenstein A, et al. Inhibition of AXUD1 attenuates compression-dependent apoptosis of cementoblasts. Clin Oral Investig. 2016;20(9):2333-41. doi: 10.1007/s00784-016-1740-4.

115. Osaki LH, Gama P. MAPKs and signal transduction in the control of gastrointestinal epithelial cell proliferation and differentiation. Int J Mol Sci. 2013;14(5):10143-61. doi: 10.3390/ijms140510143.

116. Greenblatt MB, Shin DY, Oh H, Lee KY, Zhai B, Gygi SP, et al. MEKK2 mediates an alternative β-catenin pathway that promotes bone formation. Proc Natl Acad Sci U S A. 2016;113(9):E1226-35. doi: 10.1073/pnas.1600813113.

117. Chen JR, Lazarenko OP, Wu X, Kang J, Blackburn ML, Shankar K, et al. Dietary-induced serum phenolic acids promote bone growth via p38 MAPK/β-catenin canonical Wnt signaling. J Bone Miner Res. 2010;25(11):2399-411. doi: 10.1002/jbmr.137.

118. Guo C, Yang RJ, Jang K, Zhou XL, Liu YZ. Protective Effects of Pretreatment with Quercetin Against Lipopolysaccharide-Induced Apoptosis and the Inhibition of Osteoblast Differentiation via the MAPK and Wnt/β-Catenin Pathways in MC3T3-E1 Cells. Cell Physiol Biochem. 2017;43(4):1547-61. doi: 10.1159/000481978.

119. Yang H, Guo Y, Wang D, Yang X, Ha C. Effect of TAK1 on osteogenic differentiation of mesenchymal stem cells by regulating BMP-2 via Wnt/β-catenin and MAPK pathway. Organogenesis. 2018;14(1):36-45. doi: 10.1080/15476278.2018.1455010.

120. Wang PP, Zhu XF, Yang L, Liang H, Feng SW, Zhang RH. Puerarin stimulates osteoblasts differentiation and bone formation through estrogen receptor, p38 MAPK, and Wnt/β-catenin pathways. J Asian Nat Prod Res. 2012;14(9):897-905. doi: 10.1080/10286020.2012.702757.

121. Sakisaka Y, Kanaya S, Nakamura T, Tamura M, Shimauchi H, Nemoto E. p38 MAP kinase is required for Wnt3a-mediated osterix expression independently of Wnt-LRP5/6-GSK3beta signaling axis in dental follicle cells. Biochem Biophys Res Commun. 2016;478(2):527-32. doi: 10.1016/j.bbrc.2016.07.076.

122. d'Apuzzo F, Cappabianca S, Ciavarella D, Monsurro A, Silvestrini-Biavati A, Perillo L. Biomarkers of periodontal tissue remodeling during orthodontic tooth movement in mice and men: overview and clinical relevance. ScientificWorldJournal. 2013;2013:105873. doi: 10.1155/2013/105873.

123. Ren Y, Maltha JC, Kuijpers-Jagtman AM. Optimum force magnitude for orthodontic tooth movement: a systematic literature review. Angle Orthod. 2003;73(1):86-92. doi: 10.1043/0003-3219(2003)073<0086:OFMFOT>2.0.CO;2.

124. Pilon JJ, Kuijpers-Jagtman AM, Maltha JC. Magnitude of orthodontic forces and rate of bodily tooth movement. An experimental study. American Journal of Orthodontics and Dentofacial Orthopedics. 1996;110(1):16-23.

125. Taddei SR, Moura AP, Andrade I, Jr., Garlet GP, Garlet TP, Teixeira MM, et al. Experimental model of tooth movement in mice: a standardized protocol for studying bone remodeling under compression and tensile strains. J Biomech. 2012;45(16):2729-35. doi: 10.1016/j.jbiomech.2012.09.006.

126. Nakago-Matsuo C, Matsuo T, Nakago T. Intracellular calcium response to hydraulic pressure in human periodontal ligament fibroblasts. Am J Orthod Dentofacial Orthop. 1996;109(3):244-8. doi: 10.1016/s0889-5406(96)70147-6.

127. Carmeliet G, Nys G, Stockmans I, Bouillon R. Gene expression related to the differentiation of osteoblastic cells is altered by microgravity. Bone. 1998;22(5 Suppl):139S-43S. doi: 10.1016/s8756-3282(98)00007-6.

128. Inoue H, Nakamura O, Duan Y, Hiraki Y, Sakuda M. Effect of centrifugal force on growth of mouse osteoblastic MC3T3-E1 cells in vitro. J Dent Res. 1993;72(9):1351-5. doi: 10.1177/00220345930720091601.

129. Shi J, Folwaczny M, Wichelhaus A, Baumert U. Differences in RUNX2 and P2RX7 gene expression between mono- and coculture of human periodontal ligament cells and human osteoblasts under compressive force application. Orthod Craniofac Res. 2019;22(3):168-76. doi: 10.1111/ocr.12307.

130. Matsunaga K, Ito C, Nakakogawa K, Sugiuchi A, Sako R, Furusawa M, et al. Response to light compressive force in human cementoblasts in vitro. Biomed Res. 2016;37(5):293-8. doi: 10.2220/biomedres.37.293.

131. Yang Y, Huang Y, Liu H, Zheng Y, Jia L, Li W. Compressive force regulates cementoblast migration via downregulation of autophagy. J Periodontol. 2021. doi: 10.1002/JPER.20-0806.

132. Liu H, Huang Y, Zhang Y, Han Y, Zhang Y, Jia L, et al. Long noncoding RNA expression profile of mouse cementoblasts under compressive force. Angle Orthod. 2019;89(3):455-63. doi: 10.2319/061118-438.1.

133. Premaraj S, Souza I, Premaraj T. Mechanical loading activates beta-catenin signaling in periodontal ligament cells. Angle Orthod. 2011;81(4):592-9. doi: 10.2319/090310-519.1.

134. Qiao LJ, Kang KL, Heo JS. Simvastatin promotes osteogenic differentiation of mouse embryonic stem cells via canonical Wnt/beta-catenin signaling. Mol Cells. 2011;32(5):437-44. doi: 10.1007/s10059-011-0107-6.

13. PUBLICATIONS

June 2019	**Leptin reduces in vitro cementoblast mineralization and survival as well as induces PGE_2 release by ERK1/2 commitment.** Ruiz-Heiland G, **Yong JW**, von Bremen J and Ruf S ***Clin Oral Invest***. doi: 10.1007/s00784-020-03501-3
April 2020	**Adiponectin Interacts In-Vitro with Cementoblasts Influencing Cell Migration, Proliferation and Cementogenesis Partly Through the MAPK Signaling Pathway.** **Yong JW**, von Bremen J, Ruiz-Heiland G and Ruf S ***Front Pharmaco.*** doi: 10.3389/fphar.2020.585346
March 2021	**Adiponectin as Well as Compressive Forces Regulate in vitro β-Catenin Expression on Cementoblasts via Mitogen-Activated Protein Kinase Signaling Activation.** **Yong JW**, von Bremen J, Ruiz-Heiland G and Ruf S ***Front Cell Dev Bio.*** doi: 10.3389/fcell.2021.645005
August 2021	**Hypoxia-inducible factor 1-alpha acts as a bridge factor for crosstalk between ERK1/2 and caspases in hypoxia-induced apoptosis of cementoblasts** **Yong JW**, von Bremen J, Groeger S, Ruiz-Heiland G and Ruf S ***J Cell Mol Med.*** doi: 10.1111/jcmm.16920

14. Declaration

“I declare that I have completed this dissertation single-handedly without the unauthorized help of a second party and only with the assistance acknowledged therein. I have appropriately acknowledged and referenced all text passages that are derived literally from or are based on the content of published or unpublished work of others, and all information that relates to verbal communications. I have abided by the principles of good scientific conduct laid down in the charter of the Justus Liebig University of Giessen in carry out the investigations described in the dissertation.”

Giessen 2022 Jiawen Yong

15. Acknowledgement

I would like to express my sincere gratitude to my supervisor Prof. Dr. Sabine Ruf for allowing me to pursue Ph.D. study in the department of orthodontics, for her encouragement and strongly support during my Ph.D. research work in the laboratory.

I sincerely thank Prof. J. Deschner and Dr. M. Nokhbehsaim (Department of Periodontology, University of Bonn, Germany) to facilitate the sending of OCCM-30 cells and Dr. P. Roemer (Department of Orthodontics, University of Regensburg, Germany) for his help in the establishment of the cell culture compression method in our laboratory.

I also would like to express my special thanks to Dr. Dr. Gisela Ruiz-Heiland, Dr. Sabine Groeger, Dr. Julia von Bremen for scientific instruction during my study and contributions to the manuscript correction.

I also send acknowledgements to all my colleagues and friends that I have worked with over the years who offered great help. Of note, Dr. Niko Christian Bock, Dr. Katharina Klaus, Mrs. Anja Krämer, Mr. Hartmut Meyer.

I also thank the China Scholarship Council (CSC) for Ph.D. life financial support.

Der Lebenslauf wurde aus der elektronischen Version der Arbeit entfernt.

The curriculum vitae was removed from the electronic version of the paper.